

SALAL UNDERSTORY REMOVAL EFFECTS ON THE
SOIL WATER REGIME AND TREE TRANSPIRATION RATES
IN A DOUGLAS-FIR FOREST

by

FRANCIS MAURICE KELLIHER

A.A.S., Paul Smith's College, 1975

B.S., State University of New York,
College of Environmental Science and Forestry, 1977

M.S., Oklahoma State University, 1979

A THESIS SUBMITTED IN PARTIAL FULFILLMENT OF
THE REQUIREMENTS FOR THE DEGREE OF
DOCTOR OF PHILOSOPHY

in

THE FACULTY OF GRADUATE STUDIES

Department of Soil Science

We accept this thesis as conforming to the required standard

22

THE UNIVERSITY OF BRITISH COLUMBIA

June 1985

© Francis Maurice Kelliher, 1985

In presenting this thesis in partial fulfilment of the requirements for an advanced degree at the University of British Columbia, I agree that the Library shall make it freely available for reference and study. I further agree that permission for extensive copying of this thesis for scholarly purposes may be granted by the head of my department or by his or her representatives. It is understood that copying or publication of this thesis for financial gain shall not be allowed without my written permission.

Department of Soil Science

The University of British Columbia
1956 Main Mall
Vancouver, Canada
V6T 1Y3

Date July 3, 1985

ABSTRACT

Salal (Gaultheria shallon Pursh.) understory in a 800 tree/ha 31-year-old Douglas-fir (Pseudotsuga menziesii (Mirb.) Franco) stand was cut and removed from around one of each of four pairs of adjacent trees, the root zones of which were isolated using plastic sheeting buried to bedrock. The differences in the courses of the average root zone soil water content (θ) during the growing season were small (maximum difference = $0.03 \text{ m}^3 \text{ m}^{-3}$) because total evapotranspiration was only slightly higher where salal was present than where it had been removed. Porometer and lysimeter measurements on selected days indicated that salal transpiration was $0.5\text{-}1 \text{ mm d}^{-1}$ greater than forest floor evaporation in cut subplots and that Douglas-fir transpiration was $0.2\text{-}0.5 \text{ mm d}^{-1}$ higher where salal had been removed. The slight increase in θ where salal had been removed corresponded to significantly higher soil water potential and Douglas-fir pre-dawn twig xylem water potential at low values of θ , owing to the steepness of the water retention curve for the gravelly sandy loam soil. This resulted in significantly greater tree diameter growth where salal had been removed than where it remained.

Shuttleworth's development of the Penman-Monteith equation for multilayer, partially wet forest canopies was modified for use in the hypostomatous canopies of Douglas-fir and salal. This evapotranspiration theory was combined with standard hourly micrometeorological measurements, transfer resistance functions and canopy and root zone water balance equations to provide calculations of forest evapotranspiration (E) over

extended growing season periods. There was generally good agreement between calculated values of E and values determined using Bowen ratio/energy balance, water balance and porometer measurements. The slightly higher values of θ resulting from understory removal corresponded to significantly higher tree transpiration rates calculated over early (June) and late (August) growing season periods. Most of the difference in calculated tree transpiration occurred during the final one-half of these periods when at low values of θ slightly lower θ corresponded to significantly lower Ψ_s where salal remained, leading to a reduction in Douglas-fir transpiration due to stomatal closure. The increase in calculated tree transpiration as a result of understory removal was greatest where understory leaf area index was highest and trees were largest.

TABLE OF CONTENTS

	Page
ABSTRACT	ii
TABLE OF CONTENTS	iv
LIST OF TABLES	vii
LIST OF FIGURES	ix
NOTATION	xiv
ACKNOWLEDGEMENTS	xxi
INTRODUCTION	1
CHAPTER 1 - EFFECTS OF SALAL UNDERSTORY REMOVAL ON THE SOIL WATER REGIME AND GROWTH OF DOUGLAS-FIR TREES	3
1. INTRODUCTION	4
2. METHODS	5
1. Site Description	5
2. Experimental Design	6
3. Measurements	7
1. Growing Season Weather Observations	7
2. Root Zone Soil Water Content and Evapotranspiration Rate	8
3. Soil Water Potential and Tree Pre-dawn Twig Xylem Water Potential	10
4. Forest Floor Evaporation Rate	12
5. Transpiration of Understory and Trees	13
6. Tree Diameter Growth	14
3. RESULTS AND DISCUSSION	15
1. Growing Season Weather Observations	15
2. Root Zone Soil Water Content	18

3.	Soil Water Potential and Tree Pre-dawn Twig Xylem Water Potential	26
4.	Evapotranspiration Rates Calculated from the Soil Water Balance	26
5.	Partitioning Evapotranspiration Between Douglas-fir and Salal Transpiration and Forest Floor Evaporation	34
6.	Tree Diameter Growth	36
4.	CONCLUSIONS	36
5.	REFERENCES	40
CHAPTER 2 - APPLICATION OF AN EVAPOTRANSPIRATION MODEL TO ESTIMATING SALAL UNDERSTORY REMOVAL EFFECTS IN A DOUGLAS-FIR FOREST		43
1.	INTRODUCTION	44
2.	THEORY	45
3.	METHODS	47
1.	Site and Experimental Design	47
2.	Micrometeorological Measurements	48
3.	Canopy Resistance Functions	49
4.	Root Zone Water Balance Equation	54
5.	Testing the Evapotranspiration and Root Zone Water Balance Equations	54
4.	RESULTS AND DISCUSSION	56
1.	Measured and Calculated Courses of E	56
2.	Forest Floor Evaporation After Salal Removal	56
3.	Measured and Calculated Courses of θ	62
1.	Using Equations (1) to (4)	62
2.	Effect of Assuming $r_{A1} = 0$ in Equations (1) to (4)	62

	Page
4. Partitioning of Evapotranspiration in Cut and Uncut Subplots	68
5. CONCLUSIONS	72
6. REFERENCES	73
CONCLUSIONS	76
APPENDIX I - DERIVATION OF EQUATION (1) IN CHAPTER 2	81
APPENDIX II - DERIVATION OF THE EQUATION FOR r_c SHOWING DEPENDENCE ON THE FRACTION OF WET LEAF AREA	85
APPENDIX III - RELATIONSHIP BETWEEN STOMATAL RESISTANCES OF AMPHISTOMATOUS AND HYPOSTOMATOUS LEAVES THAT RESULTS IN EQUAL TRANSPIRATION RATES	91
APPENDIX IV - DERIVATION OF EQUATION (5) IN CHAPTER 2	94
APPENDIX V - ELECTRICAL ANALOGS OF THE LATENT AND SENSIBLE HEAT FLUXES IN UNCUT AND CUT SUBPLOTS	96
APPENDIX VI - UNDERSTORY REMOVAL EFFECTS ON THE BELOW-TREE- CANOPY RADIATION REGIME	100
APPENDIX VII - MEASUREMENTS OF r_s in DOUGLAS-FIR AND SALAL	118
APPENDIX VIII - SOIL WATER RETENTION CURVE	121

LIST OF TABLES

Table		Page
1.1	Measured average depth (mm) to bedrock (\pm one standard deviation) in the eight subplots. Also shown are the four plot average values (\pm one standard deviation). . . .	19
1.2	Depth (mm) to base of the neutron probe access tubes placed in the eight subplots.	20
1.3	Minimum measured values of average root zone water content ($m^3 m^{-3}$) in the eight subplots.	25
1.4	Douglas-fir pre-dawn total twig xylem water potential (MPa) in the eight subplots.	30
1.5	Average evapotranspiration rates ($mm d^{-1}$) in the eight subplots in August 1981 as calculated from $-(\Delta\theta/\Delta t)\zeta + P$ assuming drainage was negligible. On August 24, 9 mm of rain fell while during the other three periods there was no rain. For July 30-August 19 and August 19-27, standard deviations were typically 0.5 and 0.3 $mm d^{-1}$ respectively.	31
1.6	Average evapotranspiration rates ($mm d^{-1}$) in the eight subplots in May and June 1982 as calculated from $-(\Delta\theta/\Delta t)\zeta + P$ assuming drainage was negligible. During the period April 19-May 27, 12 mm of rain fell while during the other three periods there was no rain. Standard deviations were typically 0.3 $mm d^{-1}$	32
1.7	Measured rates ($mm d^{-1}$) of Douglas-fir and salal transpiration (E_T), forest floor evaporation (E_o) and total evapotranspiration (E) in plot 2 using porometry and equations (2) and (3) and small weighing lysimeters. The root mean square errors for Douglas-fir and salal E_T were typically 0.1-0.2 $mm d^{-1}$. These errors were determined by differentiation of (2) and (3). For (2), a 30% error was assumed for a_s and r_b and a 20% error for $e_l^* - e_a$ while the standard deviation of the r_s measurements was used as the error in r_s . For (3), a 30% error was assumed for $A_{t\ell}$ and a 10% error for D while the standard deviation of the r_s measurements was used as the error in r_s . For E_o , standard deviations were typically 0.1 $mm d^{-1}$	35
1.8	Diameter (including bark), at the 1.37 m height, of the four pairs of adjacent trees using a tape with a 1 mm (in diameter) resolution.	38

Table	Page
1.9 Basal area increment ($\text{mm}^2 \text{ tree}^{-1} \text{ year}^{-1}$) for the four pairs of adjacent trees calculated using Table 1.8.	39
2.1 Values of the empirical constants λ , μ , ν , ξ and o in the stomatal resistance (r_s) characteristics function $r_s \text{ (s m}^{-1}\text{)} = \exp[\lambda - \mu(\Psi_s + \nu) + (\xi + o(\Psi_s + \nu))D^2]$ where Ψ_s is average root zone soil water potential (MPa) and D is vapour pressure deficit (kPa).	50
2.2 Daily total net radiation flux density above the forest (R_{na}) ($\text{MJ m}^{-2} \text{ d}^{-1}$) and daily measured and calculated values of evapotranspiration rate (E) (mm d^{-1}) following initialization of calculations on August 20, 1982 when measured θ was $0.16 \text{ m}^3 \text{ m}^{-3}$ ($\Psi_s = -0.3 \text{ MPa}$).	57
2.3 Average values of the minimum measured and calculated average root zone water content ($\text{m}^3 \text{ m}^{-3}$) on the same day in the cut (C) and uncut (U) subplots.	65
2.4 Average calculated values (mm) of total evapotranspiration (E), transpiration (E_T'), evaporation of intercepted water (E_I') and forest floor evaporation (E_O) in the cut (C) and uncut (U) subplots for the periods July 24-September 3, 1981 and May 27-July 1, 1982.	69
AVI.1 Sky view factors (S.V.F.) determined from photographs taken with a fish eye lens in each of the four plots and along the path traversed by the tram.	112
AVI.2 Daily total values of the ratio of below to above tree canopy net radiation flux density (R_{nb}/R_{na}) and solar irradiance ($K\downarrow_b/K\downarrow_a$) for the cut and uncut portions of the tram's path for seven days in 1982. Also shown is the solar irradiance and net radiation flux density above the forest ($K\downarrow_a$ and R_{na}) for the same days.	113

LIST OF FIGURES

Figure		Page
1.1	Courses of five day average daily values of rainfall rate (P), maximum and minimum forest canopy air temperature (T_{air}) and solar irradiance above the forest ($K_{\downarrow a}$) for the experimental site from April 1 - October 31, 1981. Measurements of P and T_{air} are from the Campbell River airport (13 km north of the site) from April 1 - May 14 and October 15-31. For the same periods, $K_{\downarrow a}$ measurements are from Nanaimo Departure Bay (130 km south of the site).	16
1.2	Same as for Fig. 1.1. except for 1982 and April 1 - May 19 and September 15 - October 31.	17
1.3	Courses of average root zone soil water content (θ) in the cut (O) and uncut (O) subplots of plot 1 from May 27 - October 22, 1981 and from April 29 - October 6, 1982. Also shown is the daily rainfall rate (P). Root zone depth was 731 mm.	21
1.4	Same as for Fig. 1.3 except for plot 2 and 667 mm.	22
1.5	Same as for Fig. 1.3 except for plot 3 and 618 mm.	23
1.6	Same as for Fig. 1.3 except for plot 4 and 613 mm.	24
1.7	Profiles of soil water content (θ) on selected days in 1982 in the cut (top half of graph) and uncut (bottom half of graph) subplots of plot 2.	27
1.8	Courses of average root zone soil water potential (Ψ_s) in the cut (O) and uncut (O) subplots of plot 2 from July 24 - September 1, 1981.	28
1.9	Same as for Fig. 1.8 except for June 9 - 25, 1982.	29
1.10	Courses of Douglas-fir basal area in the cut (O) and uncut (O) subplots of plot 2 from June 4 - September 23, 1981 and April 29 - September 14, 1982.	37
2.1	Relationship between daily throughfall (above the salal) and rainfall rates at the experimental site in 1978. A line of unit slope along the upper limit of the data is also shown. The negative intercept of this line (0.6 mm d^{-1}) gives the maximum water storage of the Douglas-fir subcanopy following Rutter <u>et al.</u> (1971).	53

2.2 Courses of net radiation flux density and vapour pressure deficit above the forest (R_{na} (—) and D (- - -)) and measured (—) and calculated (- - -) forest evapotranspiration rate (E) (with understory) on August 25, 1982, a clear day when average root zone soil water potential (Ψ_s) was about -0.7 MPa. Errors in measured E were approximately 0.02-0.04 mm h⁻¹ (Spittlehouse and Black 1980). Root mean square errors in calculated E were 0.04-0.06 mm h⁻¹ as determined by differentiation of (1) applied to two layers and soil. A 10% error was assumed for D_i , a 20% error for (R_{ni} - G) and a 30% error for the transfer resistances (r_{si} , r_{bi} , and r_{ai}), LE_o and R_{no} 58

2.3 Relationship between forest floor diffusive resistance (r_{co}) and average root zone soil water content (θ) in the cut subplot of plot 2 for ten days in July and August 1981. For θ less than 0.185, r_{co} (s m⁻¹) = -83000 θ + 16100 ($R^2 = 0.96$) as shown by the solid line. For θ greater than 0.185, r_{co} was 800 s m⁻¹, on average, as shown by the dashed line. 59

2.4 Courses of net radiation flux density and vapour pressure deficit above the forest floor (R_{no} (—) and D_o (- - -)) and measured (—) and calculated (- - -) forest floor evaporation rate (E_o) in the cut subplot of plot 2 on July 24-25, 1981, two clear days when average root zone soil water potential (Ψ_s) was about -0.05 MPa. Standard deviations for measured E_o values were typically 0.004 mm h⁻¹ at night and 0.015 mm h⁻¹ during the daytime. Root mean square errors for calculated E_o values were similar. These errors were determined by differentiation of (1) with $\delta_o = 0$. A 20% error was assumed for (R_{no} - G) and r_{co} , a 10% error for D_o and a 30% error for r_{Ao} 61

2.5 Courses of measured (symbols) and calculated (lines) average root zone soil water content (θ) and soil water potential (Ψ_s) in the cut (Δ and - - -) and uncut (Δ and —) subplots of plot 2 for the period July 24 - September 3, 1981. Also shown is the daily rainfall rate (P). 63

2.6 Same as for Fig. 2.5 except for May 27 - July 1, 1982 and \circ and \bullet 64

Figure	Page	
2.7	Courses of measured (symbols) and calculated (lines) average root zone soil water content (θ) in the cut (O) and uncut (●) subplots of plot 2 for the period July 30 - August 18, 1981. Calculated values with and without the aerodynamic and boundary-layer transfer resistances for the Douglas-fir and salal subcanopies are shown by the solid and dashed lines, respectively. Error bars are one standard deviation.	67
2.8	Courses of calculated tree transpiration rates in the cut (- - -) and uncut (—) subplots of plot 2 for the period July 24 - September 3, 1981. Also shown is the daily rainfall rate (P).	70
2.9	Same as for Fig. 2.8 except for May 27 - July 1, 1982. . . .	71
C.1	Relationship between salal leaf area index and Douglas-fir stand basal area in 31-36 year old stands close to and including the one at the experimental site. The curve indicates salal leaf area index = 288 (Douglas-fir stand basal area ($\text{m}^2 \text{ ha}^{-1}$)) ^{-1.57} ($R^2 = 0.89$).	79
C.2	Relationship between the average area of salal leaves and Douglas-fir stand basal area in 31-36 year old stands close to and including the one at the experimental site. The line indicates average area of salal leaves ($\text{mm}^2 \text{ leaf}^{-1}$) = 0.41 (Douglas-fir stand basal area ($\text{m}^2 \text{ ha}^{-1}$)) + 16 ($R^2 = 0.41$).	80
AI.1	Electrical analog depicting the transfer of latent and sensible heat fluxes for a single canopy layer 1 (LE_1 and H_1) where T_{S1}^e is the "effective" surface temperature of the layer (i.e. wet and dry portions) and other symbols have been previously defined. The depiction shows the identical leaf, single source limit of the Penman-Monteith equation described by Shuttleworth (1979).	83
AV.1	Electrical analog depicting the transfer of latent and sensible heat fluxes in an uncut subplot.	98
AV.2	Same as for Fig. AV.1 except for cut subplot.	99

Figure	Page
AVI.1 Construction of a hemisphere of radius r_0 over a small area of forest floor (dA_1). The angle ϕ between the normal to dA_1 and the straight line connecting dA_1 and a small area on the hemisphere (dA_2) is $\pi/4$ radians. Using the azimuthal angle α and the derived geometric relationships shown in this figure, $dA_2 = r_0 \sin \phi \, d\alpha \, r_0 \, d\phi$. The partial obscuration of dA_2 indicates the forest canopy.	105
AVI.2 Grid used for analyses of fish eye lens photographs of radius r_0 . The $0-r_0/3$ annulus of the grid was divided into nine equal size sectors while the $r_0/3 - 2r_0/3$ and $2r_0/3 - r_0$ annuli were each divided into eighteen equal size sectors.	108
AVI.3 Fish eye lens photograph taken at about the 300 mm height from the 1981 location of the net radiometer (below the tree canopy) in the cut subplot of plot 2 on November 23, 1983. The forest floor-sky view factor for this location was 0.28.	109
AVI.4 Courses of solar irradiance (top line) and net radiation flux density above the forest (K^+_a and R_{na}) for the period July 31 - September 1, 1981. Also shown are the courses of the ratio of below to above tree canopy solar irradiance (K^+_b/K^+_a) for the cut subplot of plot 2 and the ratio of below to above tree canopy net radiation flux density (R_{nb}/R_{na}) for the cut (- - -) and uncut (—) subplots of plot 2 during the same period.	111
AVI.5 Courses of net radiation flux density above the forest (R_{na}) and the ratio of below to above tree canopy net radiation flux density (R_{nb}/R_{na}) for the cut (- - -) and uncut (—) portions of the tram path on July 30, 1982.	115
AVI.6 Same as for AVI.5 except for August 18, 1982.	116
AVI.7 Same as for AVI.5 except for September 1, 1982 and R_{nb}/R_{na} for the cut portion of the tram path measured using a single stationary net radiometer (• • •).	117

Figure		Page
AVII.1	Relationship between stomatal resistance (r_s) and vapour pressure deficit (D) in Douglas-fir and salal adjacent to the four plots at the experimental site for June-August 1980 (O) and 1981 (O) when average root zone soil water potential (Ψ_s) was greater than -0.3 MPa and photon flux density was greater than 2.5 and 1.0 $\text{mol m}^{-2} \text{s}^{-1}$ for Douglas-fir and salal respectively. Curves show characteristic r_s values for $\Psi_s = -0.01$ (lower curve) and -0.3 MPa (upper curve) (see Table 2.1).	120
AVIII.1	Relationship between average root zone soil water potential (Ψ_s) and water content (θ) in plot 2. The soil water retention curve shown is $\Psi_s \text{ (MPa)} = -0.005 (\theta/0.3)^{-6.5}$	123

NOTATION

$A_{t\ell}$	tree leaf area on a one-sided basis ($m^2 \text{ tree}^{-1}$)
A_1	area on the forest floor (m^2)
A_2	area on a hemisphere constructed over a small area on the forest floor (dA_1) (m^2)
BAI	basal area increment ($mm^2 \text{ tree}^{-1} \text{ period}^{-1}$)
C	canopy water storage (mm)
D	vapour pressure deficit (kPa)
D_i	vapour pressure deficit just above layer i (kPa)
D_{i-1}	vapour pressure deficit just above layer $i-1$ (and within layer i) (kPa)
D_0	vapour pressure deficit within the canopy (i.e. at the effective source height) (kPa)
E	evapotranspiration rate above a forest consisting of a number of layers (eg. trees, understory and soil) ($mm \text{ period}^{-1}$)
E_i	evapotranspiration rate above layer i ($mm \text{ period}^{-1}$)
E'_i	evapotranspiration rate from layer i (i.e. $E_i - E_{i-1}$) where i is 2 for trees, 1 for understory and 0 for forest floor ($mm \text{ period}^{-1}$)
E'_I	rate of evaporation of intercepted water from tree or understory subcanopy ($mm \text{ period}^{-1}$)
E'_{Ii}	rate of evaporation of intercepted water from layer i ($mm \text{ period}^{-1}$)
E_T	transpiration rate ($mm \text{ period}^{-1}$)
E'_T	transpiration rate from tree or understory subcanopy ($mm \text{ period}^{-1}$)
F	root zone drainage rate ($mm \text{ period}^{-1}$)
G	soil heat flux density ($W \text{ m}^{-2}$)
H	sensible heat flux density ($W \text{ m}^{-2}$)
H_i	sensible heat flux density above layer i ($W \text{ m}^{-2}$)
I	radiance ($W \text{ m}^{-2}$)

$K_{\uparrow a}$	solar irradiance above the forest ($W m^{-2}$)
$K_{\uparrow b}$	solar irradiance below the tree canopy ($W m^{-2}$)
$K_{\uparrow b}$	solar irradiance below the tree subcanopy which is reflected from the understory subcanopy or forest floor surface ($W m^{-2}$)
L	latent heat of vaporization of water ($J kg^{-1}$)
LE	latent heat flux density ($W m^{-2}$)
LE _i	latent heat flux density above layer i ($W m^{-2}$)
M	forest canopy heat storage rate ($W m^{-2}$)
O _d	porosity of the dry forest floor (and soil) surface layer (dimensionless)
P	rainfall rate ($mm period^{-1}$)
Q	subcanopy drainage rate ($mm (15 min.)^{-1}$)
R ²	coefficient of determination in a linear regression analysis (dimensionless)
R _n	net radiation flux density ($W m^{-2}$)
R _{na}	net radiation flux density above the forest ($W m^{-2}$)
R _{nb}	net radiation flux density below the tree canopy ($W m^{-2}$)
R _{ni}	net radiation flux density above layer i ($W m^{-2}$)
S	maximum water storage of a subcanopy (mm)
T _{air}	air temperature ($^{\circ}C$)
T _i	air temperature just above layer i ($^{\circ}C$)
T _{si}	surface temperature of layer i ($^{\circ}C$)
T _{si} ^d	surface temperature of the dry portion of layer i ($^{\circ}C$)
T _{si} ^e	"effective" surface temperature of layer i including wet and dry portions ($^{\circ}C$)
T _{si} ^w	surface temperature of the wet portion of layer i ($^{\circ}C$)
V ₁₂	fraction of view by area 1 that is occupied by area 2 (dimensionless)

V_{fc}	forest floor-canopy view factor (dimensionless)
V_{fs}	forest floor-sky view factor (dimensionless)
W_i	fraction of leaf area in layer i that is completely wet (dimensionless)
a	leaf area index on a one-sided basis ($m^2 m^{-2}$)
a_i	leaf area index on a one-sided basis for layer i ($m^2 m^{-2}$)
a_s	salal leaf area index on a one-sided basis ($m^2 m^{-2}$)
c	30 second count when neutron probe is in soil (s)
c_p	specific heat of moist air ($J kg^{-1} °C^{-1}$)
c_s	30 second count when neutron probe is withdrawn into the shield (i.e. standard count) (s)
d	day
d_l	leaf diameter (mm)
e_a	vapour pressure of the air (kPa)
e_i	vapour pressure of the air above layer i (kPa)
e_l^*	saturated vapour pressure of the stomatal cavities (kPa)
$e^*(T_{s1})$	saturated vapour pressure of the air just above layer i at the surface temperature of layer i (kPa)
$f(\phi, \alpha)$	fraction of a small area on a hemisphere constructed over a small area of forest floor which is not obscured by the forest canopy (dimensionless)
$\bar{f}(\phi)$	average non-obscuration fraction for a small annulus on a hemisphere constructed over a small area of forest floor (dimensionless)
$\bar{f}'(r_1)$	average non-obscuration fraction for the annulus r_1 , of width Δr_1 , on the projection of a hemisphere constructed over a small area of forest floor (eg. fish eye photograph) (dimensionless)
l_d	thickness of the dry forest floor (and soil) surface layer (m)

p	free throughfall coefficient (dimensionless)
q_{12}	flux emitted by area 1 toward area 2 (W)
r	distance from the center of a projection of a hemisphere constructed over a small area of forest floor to the projection of an object on the hemisphere (m)
r_i	annulus on a projection of a hemisphere constructed over a small area of forest floor (dimensionless)
r_o	radius of a hemisphere constructed over a small area of forest floor (m)
r_{ai}	eddy diffusive resistance above layer i assuming the similarity of eddy diffusive resistances to sensible heat and water vapour transfer ($s\ m^{-1}$)
r_{aHi}	eddy diffusive resistance to sensible heat transfer above layer i ($s\ m^{-1}$)
r_{aVi}	eddy diffusive resistance to water vapour transfer above layer i ($s\ m^{-1}$)
r_{Ai}	total aerodynamic resistance for layer i assuming the similarity of total aerodynamic resistances to sensible heat and water vapour transfer ($s\ m^{-1}$)
r_{AHi}	total aerodynamic resistance to sensible heat transfer for layer i ($s\ m^{-1}$)
r_{AVi}	total aerodynamic resistance to water vapour transfer for layer i ($s\ m^{-1}$)
r_b	boundary-layer resistance assuming the similarity of boundary-layer resistances to sensible heat and water vapour transfer ($s\ m^{-1}$)
r_{bi}	boundary-layer resistance for layer i assuming the similarity of boundary-layer resistances to sensible heat and water vapour transfer ($s\ m^{-1}$)
r_{ci}	canopy resistance for layer i ($s\ m^{-1}$)
r_H	boundary-layer resistance to sensible heat transfer ($s\ m^{-1}$)
r_{Ha}	total boundary-layer resistance of a leaf to sensible heat transfer on a one-sided leaf area basis divided by the leaf area index on a one-sided basis ($s\ m^{-1}$)

r_{HBOT}	boundary-layer resistance to sensible heat transfer on the bottom side of a leaf (s m^{-1})
r_{Hi}	boundary-layer resistance to sensible heat transfer on a one-sided leaf area basis for layer i (s m^{-1})
r_{HTOP}	boundary-layer resistance to sensible heat transfer of a leaf on the top side (s m^{-1})
r_{HTOT}	total boundary-layer resistance of a leaf to sensible heat transfer on a one-sided leaf area basis (s m^{-1})
r_{s}	stomatal resistance on a one-sided leaf area basis (s m^{-1})
r_{sa}	stomatal resistance on a one-sided leaf area basis for an amphistomatous leaf (s m^{-1})
r_{sBOT}	stomatal resistance on the bottom side of a leaf (s m^{-1})
r_{sh}	stomatal resistance on a one-sided leaf area basis for a hypostomatous leaf (s m^{-1})
r_{si}	stomatal resistance on a one-sided leaf area basis for layer i (s m^{-1})
r_{sTOP}	stomatal resistance on the top of a leaf (s m^{-1})
r_{V}	boundary-layer resistance to water vapour transfer on one side of a leaf assuming the boundary-layer resistance to water vapour transfer is identical on the top and bottom sides of the leaf (s m^{-1})
r_{Va}	total boundary-layer resistance of a leaf to water vapour transfer on a one-sided leaf area basis divided by the leaf area index on a one-sided basis (s m^{-1})
r_{VBOT}	boundary-layer resistance to water vapour transfer on a bottom side of a leaf (s m^{-1})
r_{Vi}	boundary-layer resistance to water vapour transfer on a one-sided leaf area basis for layer i (s m^{-1})
r_{Vsa}	total resistance to water vapour transfer of a leaf on a one-sided leaf area basis divided by the leaf area index on a one-sided basis (s m^{-1})
r_{VTOP}	boundary-layer resistance to water vapour transfer on the top side of a leaf (s m^{-1})
r_{VTOT}	total resistance of a leaf to water vapour transfer on a one-sided leaf area basis (s m^{-1})

r'_{VTOT}	total boundary-layer resistance of a leaf to water vapour transfer on a one-sided leaf area basis ($s\ m^{-1}$)
s	slope of the saturated vapour pressure curve ($kPa\ ^\circ C^{-1}$)
t	time period (15 min., 1 hour or 1 day)
u	wind speed ($m\ s^{-1}$)
u_{15m}	wind speed at the 15 m height (i.e. 1 m above the forest) ($m\ s^{-1}$)
Ω_t	"tortuosity" factor for the dry forest floor (and soil) surface layer (dimensionless)
α	azimuthal angle (radians)
β	Bowen ratio (dimensionless)
γ	psychrometric constant ($kPa\ ^\circ C^{-1}$)
δ_i	term in (1) of chapter 2 to account for the net radiation and latent heat flux densities below layer 1 in determining the evapotranspiration rate from layer 1 (kPa)
δ'_i	term in (A1.6) to account for the net radiation and latent heat flux densities below layer 1 in determining the evapotranspiration rate above layer 1 (kPa)
ϵ_1	emittance of area 1 ($W\ m^{-2}$)
ζ	root zone depth (mm)
η	ratio of the radius of a hemisphere constructed over a small area of forest floor to the constant width of an annuli on a projection of the hemisphere (dimensionless)
θ	volumetric soil water content ($m^3\ m^{-3}$)
$\bar{\theta}$	average volumetric root zone water content ($m^3\ m^{-3}$)
θ_d	volumetric water content of the dry forest floor (and soil) surface layer ($m^3\ m^{-3}$)
κ_d	diffusivity for water vapour of the dry forest floor (and soil) surface layer ($m^2\ s^{-1}$)
$\lambda, \mu, \nu, \xi, \sigma$	constants for the empirical stomatal resistance characteristics functions (dimensionless)
ρ	density of moist air ($kg\ m^{-3}$)

- ϕ angle between the normal to a small area on the forest floor (dA_1) and the straight line connecting dA_1 and a small area (dA_2) on a hemisphere constructed over dA_1 (radians)
- Ψ_s soil water potential (MPa)
- Ψ_{Ttx} total twig xylem water potential (MPa)
- ω solid angle (steradians)

ACKNOWLEDGEMENTS

I am most grateful to my family Leslie, Anna and Alex for their loving support and encouragement.

I wish to thank the faculty and staff of the Department of Soil Science for their help. In particular, the contribution of my supervisor, Dr. Andy Black, is greatly appreciated.

I could not have completed my field work without the friendship and assistance of Ralph Adams, Alan Barr, Doug Beames, Ron Emerson and Dave Price. Fran Dixon and the staff of the Oyster River Farm and John Harwijne and Dave McBride of Crown Forest Industries Ltd. also provided essential support in the field.

Bob Stathers gave me necessary help in writing the computer programs for Chapter 2 and Appendix VI. Dave Spittlehouse generously supplied his neutron probe data analysis program as well as valuable soil physics, throughfall and rainfall data.

My stipend was provided by contracts from the B.C. Ministry of Forests, a U.B.C. Graduate Fellowship and a contract from Crown Forest Industries Ltd. Funds for the research project were provided by contracts from the B.C. Ministry of Forests and a grant from the Natural Science and Engineering Research Council.

I've saved a special thanks for Lila Harter who provided the typing wizardry.

INTRODUCTION

Where forest soils have low water storage capacity and rainfall rates during the growing season are low, it is common silvicultural practice to reduce or eliminate competing vegetation when planting valuable conifer seedlings. In pine stands of the southern United States, this practice is often extended until tree canopy closure by controlled burning of the forests. However, relatively few studies have dealt with the effects of understory vegetation on tree water use and growth. Competition for soil water by salal understory in young Douglas-fir stands on dry sites on the eastern coast of Vancouver Island is considered to be a major reason for the often observed poor tree growth response to thinning.

This problem led to the conduction of a two year salal understory removal experiment in a 31-year-old, thinned Douglas-fir stand near Courtenay, British Columbia. To minimize the effects of soil and tree variability in the stand, four plots 7 m in diameter were selected so that each contained two very similar trees not more than four metres apart. Each plot was divided into two semicircular subplots, each containing one of the two similar trees. All understory was cut close to the ground and removed from one subplot of each plot at the start of the experiment. The root zone of each of the eight trees was isolated using plastic sheeting buried to bedrock. The results of this study form the basis of the two chapters comprising this thesis, which has been written in paper format.

In Chapter 1, the effects of understory removal on root zone water content, soil water potential, pre-dawn twig xylem water potential and tree diameter growth are reported. A simple root zone water balance analysis is used to compare the evapotranspiration rates of adjacent subplots with and without understory present. Measurements of forest floor evaporation and stomatal resistance of understory and trees on selected days are used to estimate the amount of additional water which understory removal provided to the trees during summer drying periods.

In Chapter 2, Shuttleworth's development of the Penman-Monteith evapotranspiration equation for multilayer, partially wet forests is modified for use in hypostomatous canopies. This evapotranspiration theory is combined with standard hourly micrometeorological measurements, transfer resistance functions and canopy and root zone water balance equations to give calculations of forest evapotranspiration over extended periods during the growing season. Calculations are tested using Bowen ratio/energy balance, water balance, porometer and lysimeter measurements. The calculations are then applied to explain the effects of salal understory removal on Douglas-fir transpiration rates during the growing season.

In Appendices I-IV, derivations of the equations from Shuttleworth's evapotranspiration theory as modified for use in hypostomatous canopies are given. Appendix V shows electrical analogs of the latent and sensible heat fluxes in subplots with and without understory present. Appendix VI reports the measurements of the below tree canopy radiation regime and sky view factors are derived from fish-eye lens photographs. Appendix VII reports stomatal resistance measurements made in 1980 and 1981 adjacent to the four plots at the experimental site. Appendix VIII reports the soil water retention curve measurements.

CHAPTER 1

EFFECTS OF SALAL UNDERSTORY REMOVAL ON THE SOIL WATER REGIME
AND GROWTH OF DOUGLAS-FIR TREES

CHAPTER 1

EFFECTS OF SALAL UNDERSTORY REMOVAL ON THE SOIL WATER REGIME AND GROWTH OF DOUGLAS-FIR TREES

1. INTRODUCTION

Competition for soil water by salal (Gaultheria shallon Pursh.) understory in young Douglas-fir (Pseudotsuga menziesii (Mirb.) Franco) stands on dry sites on the eastern coast of Vancouver Island is considered to be a major reason for the observed poor tree growth response to thinning (Black et al. 1980). Following thinning, salal understory in a Douglas-fir stand near Courtenay, British Columbia used up to 50% of the total soil water over a 30-day summer drying period (Black et al. 1980). In the U.K., Roberts et al. (1980) found that, during warm dry periods, bracken (Pteridium aquilinum L.) understory accounted for more than 50% of the evapotranspiration in a 50-year-old Scots pine (Pinus sylvestris L.) stand. In the U.S., workers have found significant increases in tree growth of loblolly (Pinus taeda L.) and shortleaf (Pinus echinata Mill.) pine (Grano 1970; Balmer et al. 1978) and ponderosa pine (Pinus ponderosa Laws.) (Oliver 1979) resulting from understory removal. Zahner (1958), also working in the U.S., found summertime root zone water storage was up to 50 mm greater (0.04 m³ m⁻³ greater) in upland loblolly and shortleaf pine stands with understory removed than with it present. He concluded that the understory competed significantly for soil water. Where forest soils have low water storage capacity and rainfall rates during the growing season are low, silvicultural

practices that reduce or eliminate understory vegetation can result in more efficient tree water use and growth (Barrett and Youngberg 1965; Black and Spittlehouse 1981).

The objective of this chapter is to report the effects of salal understory removal in a Douglas-fir stand on (i) root zone water content, (ii) soil water potential and pre-dawn twig xylem water potential, and (iii) tree diameter growth over two successive growing seasons. A root zone water balance analysis will be used to compare the evapotranspiration rates of plots with and without understory present. Measurements of forest floor evaporation and stomatal resistance of understory and trees on selected days will be used to determine how much additional water salal understory removal provides to the trees during summer drying periods.

2. METHODS

1. Site Description

The field experiment was conducted in a thinned Douglas-fir stand approximately 27 km northwest of Courtenay on the eastern coast of Vancouver Island (49° 50'N, 125° 14'W, 150 m above sea level). The trees were planted as 2-0 stock of unknown provenance in 1952 (J. Harwijne, Crown Forest Industries Ltd., personal communication) and thinned from about 1500 to about 800 trees ha⁻¹ in 1974. The stand was fertilized once (February 28, 1981), with urea applied aerially at a rate of 200 kg (nitrogen) ha⁻¹. At the end of the 1982 growing season, stand (excluding understory) basal area was 16 m² ha⁻¹ and average tree height was 14 m. Average tree leaf area index on a one-sided leaf area basis, was about 6 in 1982 as calculated from dbh (diameter, including bark, at the 1.37 m height (breast height)) measurements and a relationship between dbh and tree leaf area index for

this site (Spittlehouse 1981). Salal leaf area index on a one-sided leaf area basis, obtained from measurements made on eight 1 m² plots, was about 3 in 1982. The soil, an Orthic Humo Ferric Podzol (Anonymous 1978), is a gravelly sandy loam of variable depth (0.3 - 1.0 m) and volumetric coarse fragment (>2 mm diameter) content (0.10 - 0.45) over sandstone bedrock. The site is on a slight slope of less than 10%, with a northeast aspect.

Further description of the site can be found in Nnyamah and Black (1977) and Spittlehouse and Black (1981).

2. Experimental Design

Four plots, each consisting of two subplots (one with understory to be removed and the other with it to be left in place), were selected in May 1981. To minimize the effects of soil and tree variability in the stand, plots 7 m in diameter were selected so that each one contained two very similar trees not more than four metres apart. Each plot was divided into semicircular subplots, each containing one of the two similar trees, by drawing a line bisecting at right angles the line joining the pair of trees. Each subplot contained two or three other trees. All understory was cut close to the soil surface using a gas-powered, rotary brush saw and removed from one subplot of each plot on May 21, 1981. In order to prevent possible lateral flow of water from a cut to an uncut subplot and water extraction from a cut subplot by the trees and salal in an uncut subplot, a 300 mm wide trench was excavated to bedrock between each pair of trees along the 7 m bisect line. A sheet of 0.15 mm thick polyethylene plastic was placed on both sides of the trench and the trench refilled with soil. A

layer of plastic was placed on the top of the trench to prevent rain from entering the soil between the sheets of plastic. The root zones of all eight experimental trees were isolated during the first two weeks of May 1982 by completing the trench (and plastic barrier) around each tree.

3. Measurements

1. Growing Season Weather Observations

In 1981 and 1982, standard forest micrometeorological measurements were made from May 15 until October 14, and May 20 until September 14, respectively. Solar irradiance was measured with a pyranometer (Kipp and Zonen, Delft, Holland) located on the top of a 15 m tall open lattice triangular tower adjacent to the four plots. A tipping bucket rain gauge (Sierra Misco, Inc., Berkeley, California, U.S.A.), with a 200 mm diameter orifice, was located on a horizontal bar extending 3 m from the tower at the 11 m height. A relative humidity sensor (Phys-Chemical Research Corporation, New York, NY, U.S.A.) coupled with a thermistor (Fenwal Electronics Corporation, Framingham, Massachusetts, U.S.A.) for measurement of air temperature was located at the 6 m height in a small Stevenson screen (450 mm by 300 mm by 300 mm) attached to the tower. The relative humidity sensor and thermistor were frequently checked in the field using an Assmann psychrometer. Windspeed was measured at the 15 m height using a sensitive Casella (C.F. Casella and Company, Ltd., London, England) cup anemometer. Based on 38 days of windspeed measurements (one hour averages) at the 1 m height in July and August 1980, the windspeed at this height was 13% of that at the 15 m height. Data were electronically logged as one hour averages or

totals using a Campbell Scientific model CR-21 data logger, stored on audio cassette tape and latter transferred to a microcomputer for processing.

2. Root Zone Soil Water Content and Evapotranspiration Rate

The average root zone depth of each subplot was determined by driving a 12 mm diameter steel rod vertically into the soil until it struck sandstone bedrock. There were about 20 samples per subplot (i.e. within the area enclosed by the plastic barrier) taken in a grid pattern. Roots were observed at all depths in the soil on faces of the trenches excavated around each of the eight subplots.

During the third week of May 1981, thin wall aluminum neutron moisture probe access tubes (48 mm inside diameter) were installed in the soil in all of the subplots. An access hole was obtained by driving a steel pipe (38 mm inside diameter, 51 mm outside diameter) vertically into the soil with a sledge hammer. The pipe was carefully withdrawn from the hole, at about 100 mm intervals, and the soil was removed from inside the pipe. This procedure continued until bedrock was reached. Three aluminum tubes were placed in each subplot of plots 1, 2 and 4, while four aluminum tubes were placed in each subplot of plot 3, for a total of 26 tubes.

A Campbell Pacific Nuclear hydroprobe (model CPN 503, Sacker Scientific Company, Edmonton, Alberta) was used to measure changes in soil water content (θ) using the neutron moderation technique. The neutron probe was lowered into each aluminum tube at 150 mm intervals beginning at a depth of 150 mm and continuing to bedrock. One 30 second reading was taken at each depth. In 1981 and 1982, measurements of θ were made from May 27 until

October 22, and April 29 until October 6 respectively, in one to two (and sometimes three week) intervals. During 1981 and 1982, the neutron probe was calibrated in the field using soil samples obtained with a heavy gauge open bucket-type auger (60 mm inside diameter) within 1.5 m of an aluminum tube, used for calibration, near the four plots. Soil samples were obtained at 100 mm intervals from the soil surface down to bedrock and placed in aluminum soil moisture sampling cans. The cans were later weighed, dried at 105°C for 48 hours, reweighed and θ was calculated using a bulk density and coarse fragment content obtained from an adjacent soil pit.

Calibration of the neutron probe was conducted in 1981 for values of θ ranging from 0.10 to 0.51 $\text{m}^3 \text{m}^{-3}$. A linear equation, $\theta = 0.224 (c/c_s) - 0.009$ (sample size = 44, $R^2 = 0.85$) where c is the neutron count per 30 seconds when the probe is in the soil and c_s is the neutron count per 30 seconds when the probe is withdrawn into the shield (i.e. the standard count), was found to describe the calibration data for all depths quite well. An independent calibration of the same neutron probe using the same procedure during the same measurement period and for similar soils at Mesachie Lake, B.C., by Giles (1983) resulted in a very similar equation ($\theta = 0.23 (c/c_s) - 0.021$). The same neutron probe was used in 1982 and calibration was then conducted for values of θ ranging from 0.09 to 0.46 $\text{m}^3 \text{m}^{-3}$. Since the 1982 calibration data lay along the 1981 calibration line, the 1981 calibration line was used for both 1981 and 1982.

Root zone water content and rainfall data were used to calculate average evapotranspiration rates (E) (mm d^{-1}) in cut and uncut subplots using the water balance equation written as

$$E = -(\Delta\bar{\theta}/\Delta t)\zeta + P \quad (1)$$

where $\Delta\bar{\theta}/\Delta t$ is the average rate of change in the average root zone water content ($\bar{\theta}$) over a 1-2 week period, ζ is the root zone depth and P is the average rainfall rate over the same period. Calculations were done for periods 2 or more days after rainfall and since the soil was a sandy loam, small decreases in θ corresponded to large decreases in unsaturated hydraulic conductivity so that root zone drainage could be neglected (Black and Spittlehouse, 1981).

3. Soil Water Potential and Tree Pre-dawn Twig Xylem Water Potential

On June 18, 1981 and June 8, 1982, thermocouple psychrometers (model PCT-55 measured using a model HR-33T dew-point microvoltmeter, Wescor Inc., Logan, Utah, U.S.A.) were installed in each subplot of plot 2. The thermocouple psychrometers were calibrated in the laboratory just prior to installation, using salt solutions of known osmotic potential (Nnyamah and Black 1977). A 150 mm by 300 mm hole was excavated to bedrock about 1 m from each of the two experimental trees in plot 2. Access holes were made by driving a 9 mm diameter steel rod about 150 mm horizontally into the soil on opposite sides of the large hole. Careful insertion of the thermocouple psychrometer to the end of the access hole assured that the porous ceramic cup was completely embedded in soil. The remainder of the access hole was

then refilled with stone-free soil which was lightly compacted. Most of the wire from the thermocouple psychrometer was wound about the perimeter of the large hole at the depth of installation. Only a length of the wire about 300 mm greater than the depth of installation remained to be led to the soil surface. This was done to minimize heat conduction down the wire to the thermocouple junction. Pairs of psychrometers were installed at about 150 mm depth intervals beginning at a depth of 150 mm and continuing to bedrock. Following installation, the large hole was refilled with the same soil (including stones) removed during excavation. The psychrometers were read in dew-point and psychrometer mode after being Peltier cooled for 5 seconds.

On June 18, 1981, tensiometers fabricated following van Bavel et al. (1968) were also installed in each subplot of Plot 2. The porous ceramic cups (Soil Moisture Equipment Corp., Santa Barbara, California, U.S.A.) had an air-entry value of 0.1 MPa, were 10 mm outside diameter and 25 mm long with 5 mm sealed in a length of 13 mm outside diameter clear acrylic tube. An access hole was obtained by driving a 12 mm diameter steel rod vertically into the soil to the desired depth. The tensiometer was inserted into the hole until the porous ceramic cup was completely embedded in the soil at the bottom of the hole. Tensiometers were installed at about 150 mm intervals beginning at a depth of 150 mm and continuing to bedrock. Tensiometers were not installed in 1982. In 1981 and 1982, measurements of soil water potential (Ψ_g) were made every two to seven days from July 4 until September 3, and June 9-25, respectively.

The pre-dawn total twig xylem water potential (Ψ_{Ttx}) of the eight measurement trees was measured using a pressure chamber, using the procedure described by Kelliher et al. (1984). In 1981, measurements were made on August 12 and 20 and October 23. In 1982, measurements were made on June 9, 17, 23 and 30.

4. Forest Floor Evaporation Rate

Forest floor evaporation rate was determined in 1981 using small weighing lysimeters. The lysimeters, 150 mm in diameter and 120 mm deep, were made by removing the top and bottom portions of a plastic jar (0.5 mm thick). Soil for the lysimeter was excavated from the cut subplot and trimmed so that the plastic tube could be snugly fitted over the undisturbed soil core. The top of the cylinder was temporarily covered and the core was placed on its side so that a plastic bottom could be taped in place. The lysimeter was then placed in the plastic sleeve of a hole excavated on the cut subplot, with the top flush with the soil surface. The sleeve prevented soil from adhering to the outside of the lysimeter which would have caused an increase in weight. Every one to two hours the lysimeter was carefully lifted out and carried to a nearby electric balance to determine weight loss. The resolution of the balance was equivalent to 0.001 mm depth of water. Four lysimeters were located in the cut subplot of plot 2, and one was situated beneath the salal in the uncut subplot of plot 2. Lysimeter soil cores were replaced every 1 to 2 days (Boast and Robertson 1982). Soil cores were generally obtained near the plastic sleeves, but on August 11 and 18, soil for the cut subplot lysimeters was obtained from cut subplots of plot 1 and 4 as well as plot 2.

5. Transpiration of Understory and Trees

The transpiration rate (E_T) of the understory ($\text{kg m}^{-2} \text{d}^{-1}$ or mm d^{-1}) was estimated using

$$E_T = a_s (\rho c_p / L \gamma) (e_l^* - e_a) / (r_s + r_b) \quad (2)$$

where a_s is the salal leaf area index, ρ is the density of moist air, c_p is the specific heat of moist air, L is the latent heat of vaporization of water, γ is the psychrometric constant, e_l^* is the saturated vapour pressure of the stomatal cavities, e_a is the vapour pressure of the air, r_s is the average stomatal resistance and r_b is the average boundary layer resistance of the leaves. The value of r_b was determined using the relationship between r_b and windspeed found for artificial salal leaves by Spittlehouse and Black (1982) and an estimated shelter factor of 2 (Thom 1971). This resulted in values of r_b of about 250 s m^{-1} . The vapour pressure was measured hourly using an Assmann psychrometer immediately above the salal canopy.

Stomatal resistance measurements of salal in the uncut subplot of plot 2 were made each hour from early morning until late afternoon on five days in 1981 from July 24 until Aug. 20, as well as Oct. 23. Measurements of abaxial r_s were made on at least ten leaves. A representative sample of leaves in both sun and shade was obtained each hour. A ventilated diffusion

porometer described by Turner et al. (1969) and modified by Tan and Black (1978) was used. Salal leaf temperature was measured in the shade and sun using a Barnes PRT-10 infrared thermometer (Barnes Engineering Company, Stamford, Connecticut, U.S.A.). Hourly estimates of the fraction of the subplot that was sunlit were used with the above measurements to calculate salal E_T .

The transpiration rate of the experimental trees ($\text{kg tree}^{-1} \text{ s}^{-1}$) was estimated using a simplified version of (2) in which $r_b \approx 0$ so that $e_{\ell}^* - e_a \approx D$, the vapour pressure deficit of the Douglas-fir canopy (Tan et al. 1978). This can be written as

$$E_T = A_{t\ell}(\rho c_p / L\gamma) D / r_s \quad (3)$$

where $A_{t\ell}$ is the projected leaf area of the tree and r_s is the average stomatal resistance of the tree. Conversion of E_T from a tree to a stand (mm d^{-1}) basis used a stocking density of 800 trees ha^{-1} .

Stomatal resistance measurements were made on the experimental trees of the cut and uncut subplots of plot 2 each hour from dawn until late afternoon on Aug. 12, Aug. 20, and Oct. 23, 1981 and June 9, 17, 23 and 30, 1982. Measurements were made using the ventilated porometer on at least two samples of four needles taken at the mid-crown level (approximately 7 m height) of each tree.

6. Tree Diameter Growth

The dbh of the eight experimental trees was measured using a diameter tape (with a resolution of 1 mm change in diameter) on June 4 and December 10, 1981, October 6, 1982 and November 28, 1983. Dendrometer bands,

fabricated following Liming (1957), were installed at the 1.37 m height on the experimental trees of plot 2 on July 3, 1981 and April 30, 1982 (additional dendrometer bands). The bands were made of 25 mm wide by 0.125 mm thick stainless steel with extension springs made of 0.625 mm diameter stainless steel wire into a 9 mm outside diameter by 63 mm long coil. Our verniers provided by Dr. H. Brix of the Canadian Forestry Service were pressure sensitive, silk screened aluminum labels with a resolution of 0.1 mm (change in diameter). In 1981 and 1982, measurements of dbh using dendrometer bands were made from July 3 until December 10, and April 30 until October 6 respectively, in one to two (and sometimes three to four) week intervals.

3. RESULTS AND DISCUSSION

1. Growing Season Weather Observations

The 1981 growing season was characterized by exceptionally high rainfall (total rainfall from April through October was 760 mm (Fig. 1.1)). The only extended dry period in 1981 occurred between July 30 and August 24 when daily maximum air temperature exceeded 25°C for fifteen consecutive days (August 5-19) and only two cloudy days (daily total solar irradiance < 12 MJ m⁻² day⁻¹) occurred (July 30 and August 3).

By contrast, total rainfall for the 1982 growing season was 540 mm, of which one-half fell during October (Fig. 1.2). An extended dry period occurred in 1982 between May 19 and June 26 when only 3 mm of rain fell, on June 2 (the only cloudy day during this period), and daily maximum air temperature exceeded 25°C for ten consecutive days (June 15-24).

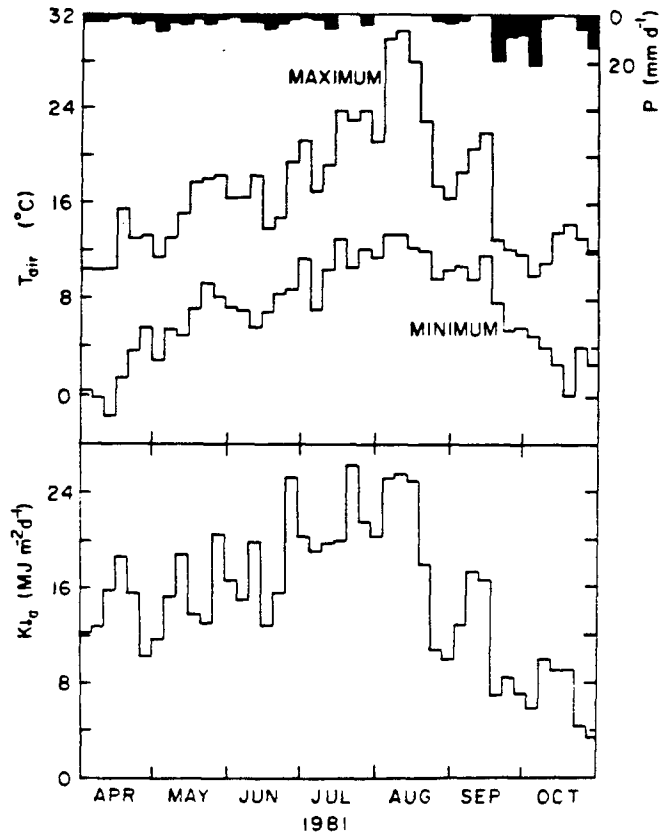


Figure 1.1 Courses of five day average daily values of rainfall rate (P), maximum and minimum forest canopy air temperature (T_{air}) and solar irradiance above the forest (K_{+a}) for the experimental site from April 1 - October 31, 1981. Measurements of P and T_{air} are from the Campbell River airport (13 km north of the site) from April 1 - May 14 and October 15-31. For the same periods, K_{+a} measurements are from Nanaimo Departure Bay (130 km south of the site).

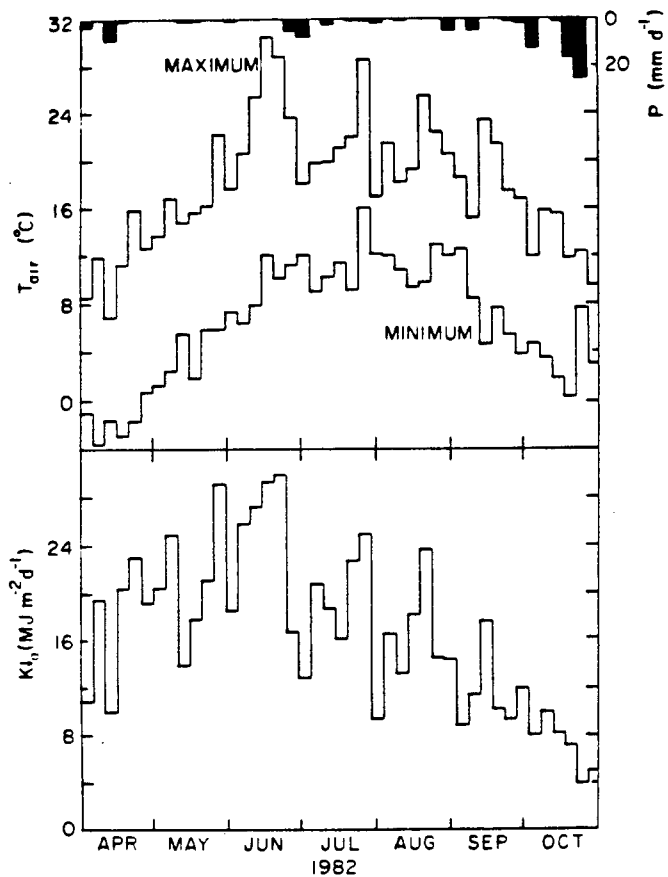


Figure 1.2

Same as for Fig. 1.1. except for 1982 and April 1 - May 19 and September 15 - October 31.

2. Root Zone Soil Water Content

Average depth to bedrock for adjacent subplots was not significantly different (Table 1.1). However, it was found that coarse fragments impeded penetration of the steel rod to bedrock in a 1 m² soil pit excavated to bedrock. Based on the relationship between soil depths obtained by the rod penetration and excavation methods, root zone depth for each plot was taken as the average of the adjacent subplot values plus one standard deviation based on all samples taken in the plot (Table 1.1). The neutron probe measurement made when the probe was at the bottom of the access tube (Table 1.2) was applied to the soil layer between the bottom of the access tube and the plot root zone depth.

There was little difference in the course of θ in adjacent subplots in the 1981 and 1982 growing seasons (Figs. 1.3-1.6). Except for plot 1 in 1981, minimum values of θ were slightly higher in the cut (0.15) than in the uncut (0.14) subplots (Figs. 1.3-1.6 and Table 1.3). Zahner (1958) and Barrett and Youngberg (1965) observed much higher minimum values of θ following understory removal from pine stands on silt loam, and pumice soils, respectively. For a sandy soil, Roberts et al. (1982) found that minimum values of θ were slightly higher in a pine stand without understory than in an adjacent pine stand with bracken understory.

Following considerable winter rainfall, which resulted in a uniformly wetted root zone, soil water content profiles during the 1982 springtime drying period were used to examine the effect of salal removal on water depletion patterns. As the drying period progressed, the soil profile dried uniformly with depth in adjacent subplots indicating equal depletion from

Table 1.1 Measured average depth (mm) to bedrock (\pm one standard deviation) in the eight subplots. Also shown are the four plot average values (\pm one standard deviation).

<u>Subplot</u>	<u>Uncut</u>	<u>Cut</u>	<u>Plot</u>
1	538 \pm 127	608 \pm 181	573 \pm 158
2	512 \pm 123	530 \pm 169	521 \pm 146
3	443 \pm 109	524 \pm 147	484 \pm 134
4	515 \pm 136	434 \pm 121	474 \pm 139

Table 1.2 Depth (mm) to base of the neutron probe access tubes placed in the eight subplots.

<u>Plot</u>	<u>Uncut</u>				<u>Cut</u>			
1	650	650	650	---	400	480	500	---
2	450	480	490	---	500	350	350	---
3	560	640	650	620	650	500	500	650
4	350	350	350	---	350	400	430	---

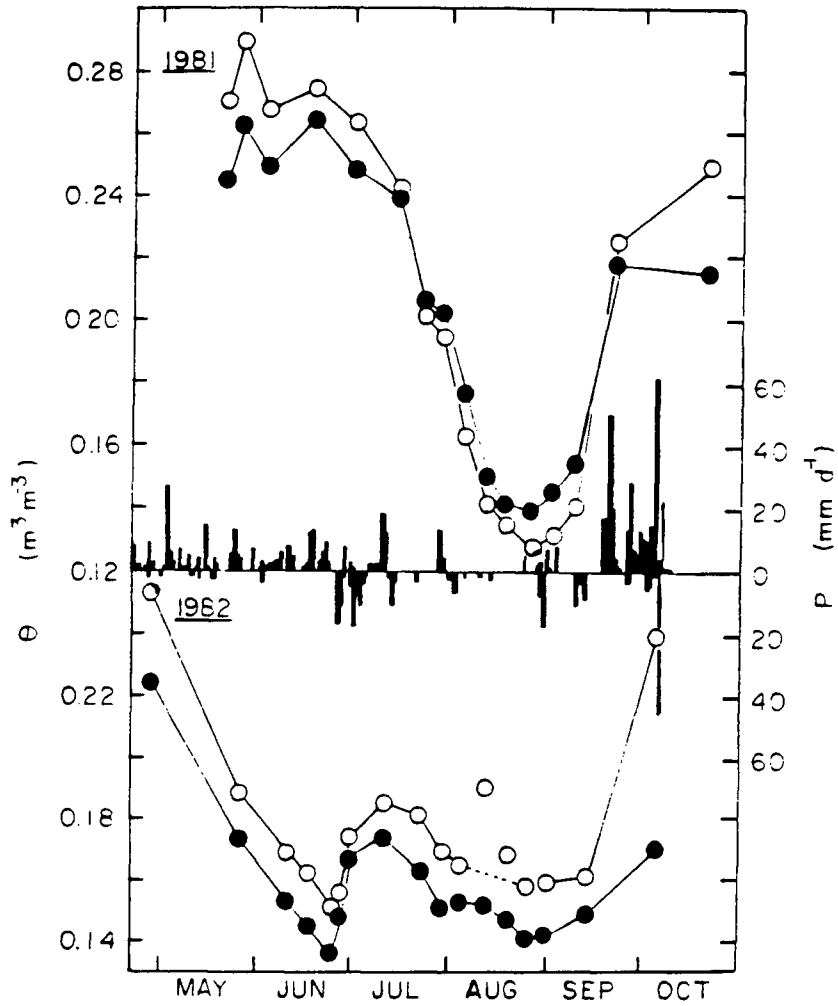


Figure 1.3 Courses of average root zone soil water content (θ) in the cut (O) and uncut (●) subplots of plot 1 from May 27 - October 22, 1981 and from April 29 - October 6, 1982. Also shown is the daily rainfall rate (P). Root zone depth was 731 mm.

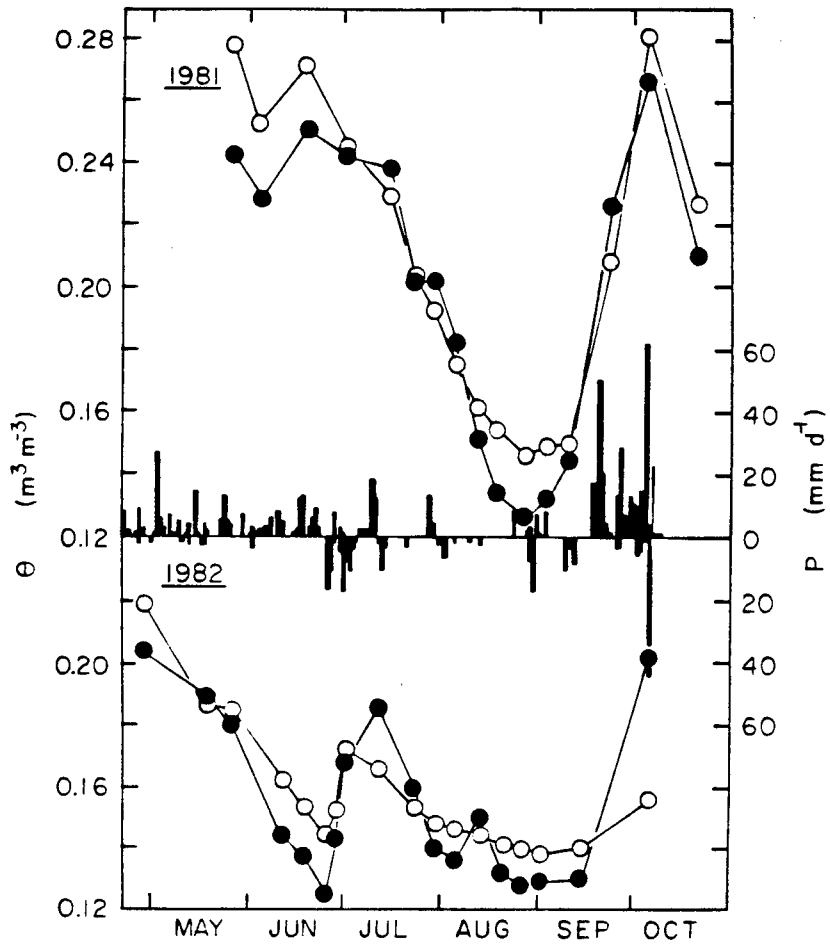


Figure 1.4 Same as for Fig. 1.3 except for plot 2 and 667 mm.

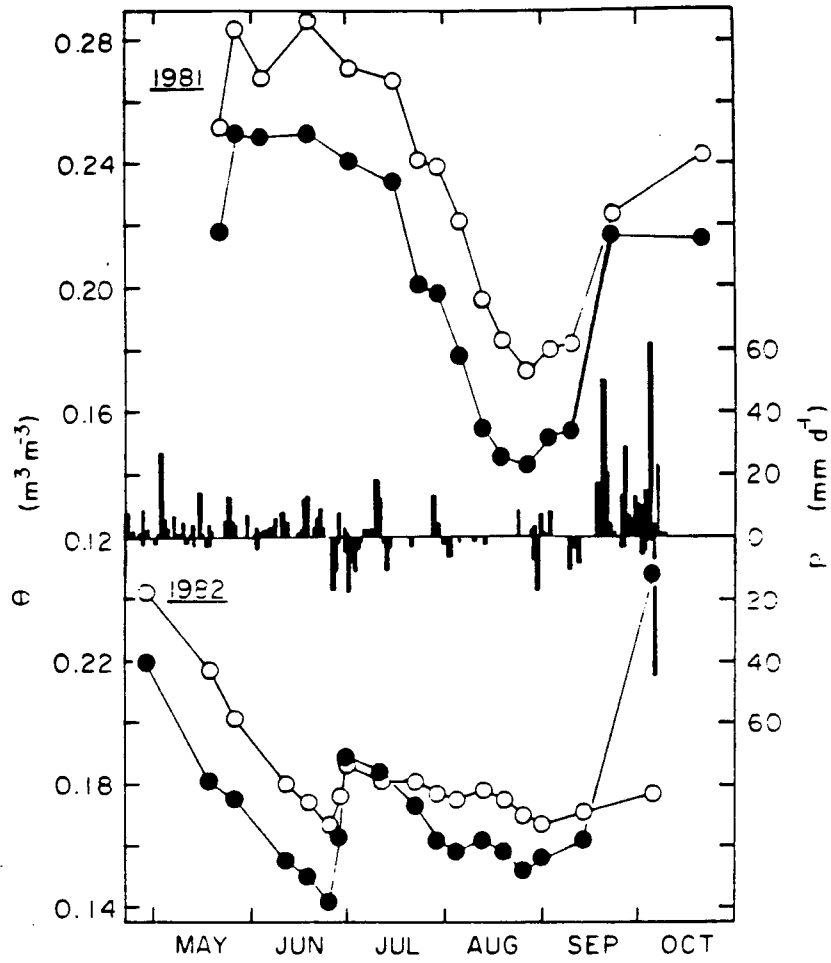


Figure 1.5 Same as for Fig. 1.3 except for plot 3 and 618 mm.

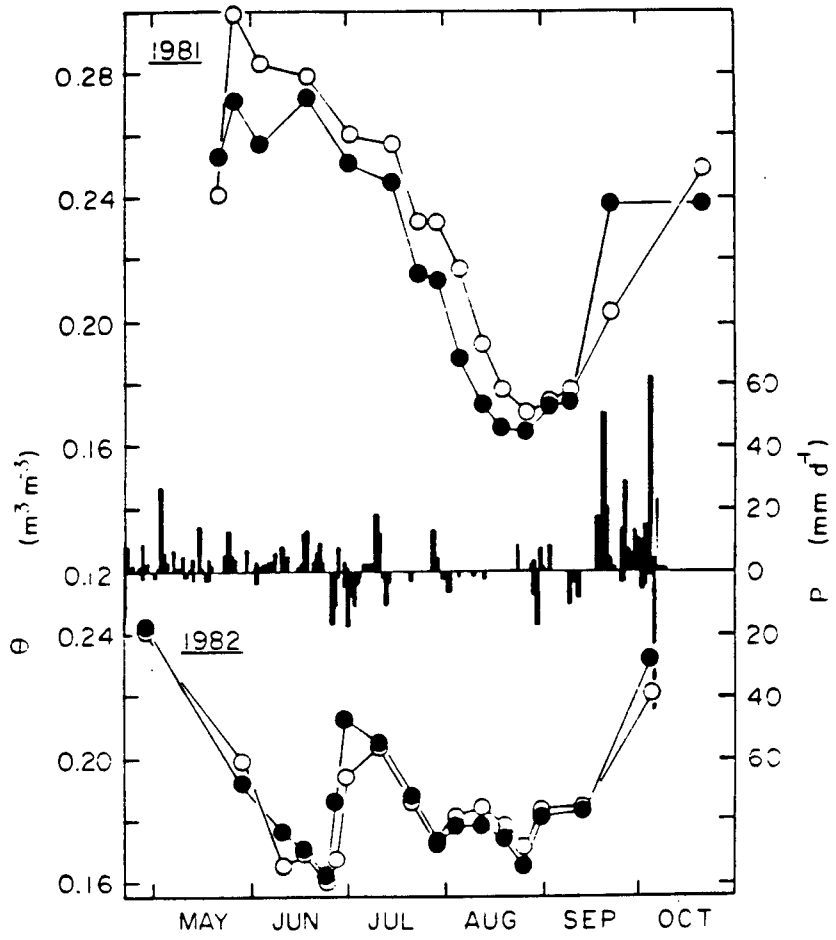


Figure 1.6 Same as for Fig. 1.3 except for plot 4 and 613 mm.

Table 1.3 Minimum measured values of average root zone water content ($\text{m}^3 \text{m}^{-3}$) in the eight subplots.

<u>Plot</u>	<u>Aug. 27, 1981</u>		<u>Jun. 25, 1982</u>	
	<u>Uncut</u>	<u>Cut</u>	<u>Uncut</u>	<u>Cut</u>
1	0.14	0.13	0.14	0.15
2	0.13	0.15	0.12	0.14
3	0.14	0.17	0.14	0.17
4	0.16	0.17	0.16	0.16
Ave.	0.14	0.16	0.14	0.16

the entire root zone (Fig. 1.7). Over the entire drying period similar quantities of water were lost from the top portion of the root zone (0.08 and 0.10 m³ m⁻³ for the cut and uncut subplot, respectively) as from the bottom portion (corresponding values were 0.09 and 0.08 m³ m⁻³).

3. Soil Water Potential and Tree Pre-Dawn Twig Xylem Water Potential

During drying periods in 1981 and 1982, Ψ_s was significantly higher as a result of salal removal in plot 2 (Figs. 1.8 and 1.9). In 1981, minimum values of Ψ_s were -0.9 and -1.2 MPa in the cut and uncut subplots, respectively, while in the 1982 the corresponding values were -1.0 and -1.5 MPa. As this gravelly sandy loam soil dried, small differences in θ corresponded to large difference in Ψ_s owing to the steepness of the (field determined) water retention curve described using an equation of the form proposed by Campbell (1974) (Ψ_s (MPa) = -0.005 ($\theta/0.3$)^{-6.5}).

Douglas-fir pre-dawn Ψ_{Ttx} was 0.1-0.2 MPa higher, during drying periods, as a result of salal removal (Table 1.4) except for plot 4 in 1982. Kelliher et al. (1984) showed that Douglas-fir pre-dawn Ψ_{Ttx} was generally similar to Ψ_s for $\Psi_s < -0.4$ MPa. For $\Psi_s > -0.4$ MPa, Douglas-fir pre-dawn Ψ_{Ttx} was about 0.4-0.5 MPa less than Ψ_s (eg. August 12 and October 23, 1981 and June 30, 1982).

4. Evapotranspiration Rates Calculated from the Soil Water Balance

When soil moisture was adequate (July 30 - August 13, 1981 and April 29 - May 27, 1982), E (Tables 1.5 and 1.6) was similar to those values determined by water balance analysis (Black et al. 1980) and weighing lysimeter (Fritschen et al. 1977) in similar well-watered Douglas-fir forests. For most of the 1981 and 1982 drying periods, E was generally slightly higher in the uncut subplots (Tables 1.5 and 1.6). This result and

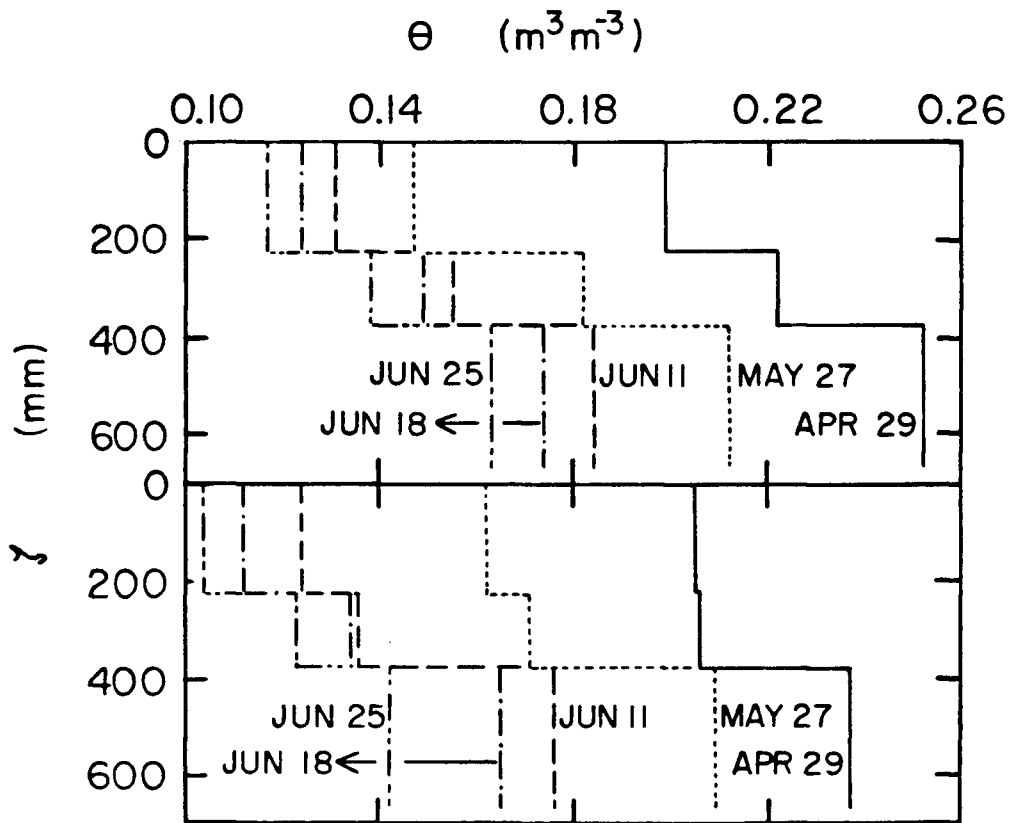


Figure 1.7 Profiles of soil water content (θ) on selected days in 1982 in the cut (top half of graph) and uncut (bottom half of graph) subplots of plot 2.

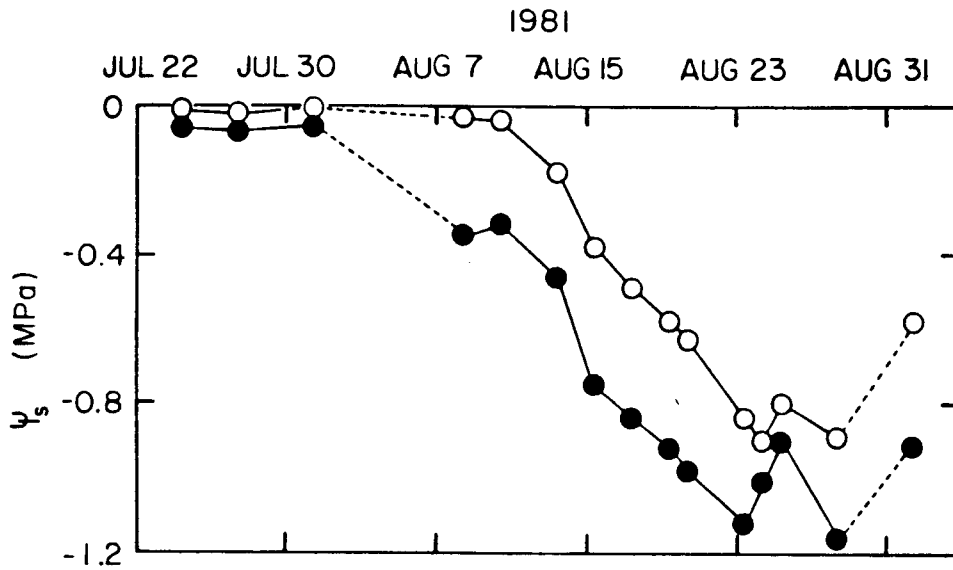


Figure 1.8 Courses of average root zone soil water potential (Ψ_s) in the cut (○) and uncut (●) subplots of plot 2 from July 24 - September 1, 1981.

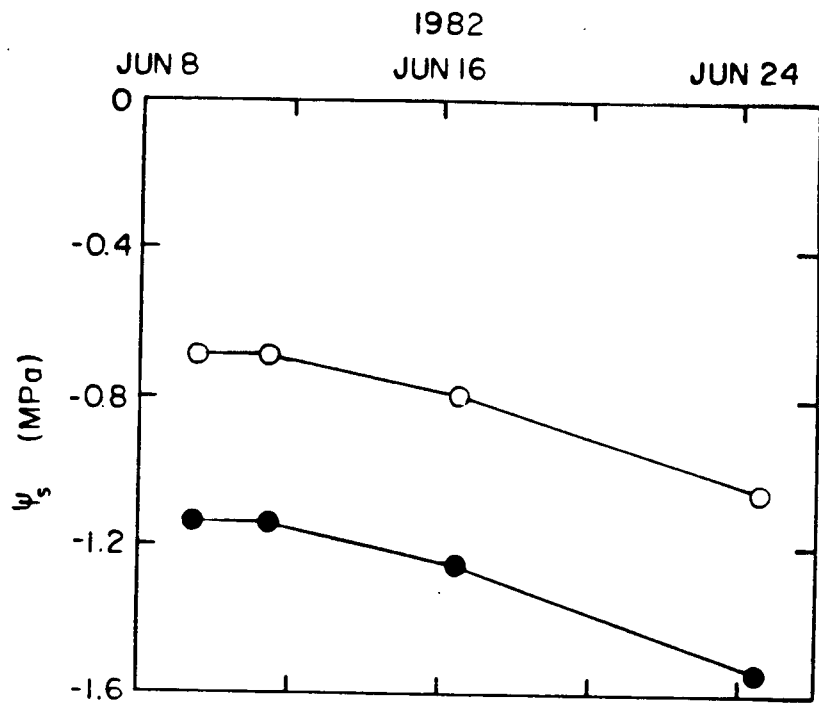


Figure 1.9 Same as for Fig. 1.8 except for June 9 - 25, 1982.

Table 1.4 Douglas-fir pre-dawn total twig xylem water potential (MPa) in the eight subplots.

<u>1981</u>	<u>August 12</u>		<u>August 20</u>		<u>October 23</u>			
<u>Plot</u>	<u>Uncut</u>	<u>Cut</u>	<u>Uncut</u>	<u>Cut</u>	<u>Uncut</u>	<u>Cut</u>		
1	--	--	-1.3	-1.1	-0.6	-0.6		
2	-0.5	-0.4	-0.9	-0.8	-0.6	-0.6		
3	--	--	-1.1	-0.6	-0.7	-0.6		
4	--	--	-0.9	-0.7	-0.6	-0.6		
Ave.	-0.5	-0.4	-1.0	-0.8	-0.6	-0.6		

<u>1982</u>	<u>June 9</u>		<u>June 17</u>		<u>June 23</u>		<u>June 30</u>	
<u>Plot</u>	<u>Uncut</u>	<u>Cut</u>	<u>Uncut</u>	<u>Cut</u>	<u>Uncut</u>	<u>Cut</u>	<u>Uncut</u>	<u>Cut</u>
1	-0.8	-0.7	-1.0	-0.7	-1.3	-0.9	-0.4	-0.6
2	-1.0	-0.7	-1.3	-0.8	-1.6	-1.1	-0.8	-0.6
3	-0.8	-0.7	-1.0	-0.8	-1.3	-1.0	-0.4	-0.5
4	-0.8	-0.9	-1.2	-1.4	-1.2	-1.6	-0.5	-0.8
Ave.	-0.8	-0.8	-1.1	-0.9	-1.4	-1.2	-0.5	-0.6

Table 1.5 Average evapotranspiration rates (mm d^{-1}) in the eight subplots in August 1981 as calculated from $-(\Delta\theta/\Delta t)\zeta + P$ assuming drainage was negligible. On August 24, 9 mm of rain fell while during the other three periods there was no rain. For July 30-August 19 and August 19-27, standard deviations were typically 0.5 and 0.3 mm d^{-1} respectively.

<u>Plot</u>	<u>July 30-Aug. 6</u>		<u>Aug. 6-13</u>	
	<u>Uncut</u>	<u>Cut</u>	<u>Uncut</u>	<u>Cut</u>
1	2.7	3.3	2.6	2.1
2	1.9	1.6	2.8	1.3
3	1.8	1.6	1.9	2.1
4	2.2	1.3	1.2	2.0
Ave.	2.2	2.0	2.1	1.9

<u>Plot</u>	<u>Aug. 13-19</u>		<u>Aug. 19-27</u>	
	<u>Uncut</u>	<u>Cut</u>	<u>Uncut</u>	<u>Cut</u>
1	1.1	0.9	1.2	1.6
2	1.9	0.8	1.7	1.7
3	0.9	1.3	1.3	1.8
4	0.7	1.5	1.1	1.6
Ave.	1.2	1.1	1.3	1.7

Table 1.6 Average evapotranspiration rates (mm d^{-1}) in the eight subplots in May and June 1982 as calculated from $-(\Delta\theta/\Delta t)\zeta + P$ assuming drainage was negligible. During the period April 19-May 27, 12 mm of rain fell while during the other three periods there was no rain. Standard deviations were typically 0.3 mm d^{-1} .

<u>Plot</u>	<u>Apr. 29-May 27</u>		<u>May 27-June 11</u>	
	<u>Uncut</u>	<u>Cut</u>	<u>Uncut</u>	<u>Cut</u>
1	1.8	2.1	1.0	0.9
2	1.5	1.5	1.6	1.0
3	1.4	1.4	0.8	0.9
4	1.5	1.3	0.7	0.8*
Ave.	1.6	1.6	1.0	0.9

<u>Plot</u>	<u>June 11-18</u>		<u>June 18-25</u>	
	<u>Uncut</u>	<u>Cut</u>	<u>Uncut</u>	<u>Cut</u>
1	0.8	0.7	0.9	1.1
2	0.7	0.9	1.1	0.9
3	0.4	0.5	0.7	0.6
4	0.5	0.8*	0.7	0.9
Ave.	0.6	0.7	0.8	0.9

*period was May 27 - June 18

the higher values of Ψ_s and tree pre-dawn Ψ_{Ttx} on cut subplots during these periods suggest that much of the soil water which would have been used by salal was immediately taken up by the tree in the cut subplot. This would not explain why E in the cut subplot of plots 3 and 4 during August 6-27, 1981 exceeded that in the adjacent uncut subplot. A possible explanation is as follows. Tree transpiration rate is equal to the tree rooting area (i.e. the effective ground area occupied by the tree's roots) multiplied by the rate of change in root zone water storage in this area due to water extraction by the tree $((\Delta\theta/\Delta t)\zeta)$. Now if one of two trees with the same transpiration rate has a 10% smaller rooting area than the other, then the former will have 10% larger values of $(\Delta\theta/\Delta t)\zeta$ than the latter. This suggests that in 1981 the tree in the cut subplot of plots 3 and 4 had a smaller rooting area than the tree in the adjacent uncut subplot. The fact that this was not the case in 1982 suggests that the completion of the isolation trench confined adjacent trees to an equal rooting area. For the period August 6-19, 1981, E in the uncut subplot of plot 2 was almost twice that in the cut subplot. This suggests an initial saving of soil water in the cut subplot for use later in the drying period.

During most of the 1982 drying period, E was much lower than during the 1981 drying period when similar values of θ existed. The 1982 drying period occurred during the emergence of new leaves for both Douglas-fir and salal so that E_T was estimated to be about 20% less than later in the growing season (eg. August) for the same soil moisture and meteorological conditions. For most of the 1982 drying period, vapour pressure deficits were higher than during the 1981 drying period. This suggests that r_s of both Douglas-fir and salal were higher in 1982 than in 1981. It would

appear that the increase in r_s was great enough that it offset the increase in $e_a^* - e_a$ in (2) and D in (3) so that E_T in 1982 was less than in 1981.

5. Partitioning Evapotranspiration Between Douglas-fir and Salal Transpiration and Forest Floor Evaporation

Comparison of daily total values of forest floor evaporation and salal transpiration for 5 days in the 1981 drying period in plot 2 indicated that the former was about $0.5-1 \text{ mm d}^{-1}$ less than the latter (Table 1.7). On August 12 and 20, 1981, Douglas-fir E_T was about 0.2 mm d^{-1} higher in the cut than the uncut subplot of 2. Similar results were obtained using the heat pulse technique described by Cohen et al. (1985) in the same plot on August 3 and 4, 1981 suggesting that these differences in Douglas-fir E_T were not a result of error in r_s measurements (Leverenz et al. 1982). On October 23, 1981, when the root zone was recharged with water, Douglas-fir E_T was very similar in the adjacent subplots indicating that earlier differences were due to differences in soil water stress between the two subplots. Daily total values of E on August 12 and 20, 1981, in Table 1.7 are similar to values for plot 2 in Table 1.5 in the corresponding periods. This suggests that the marked difference in water balance estimates of E between adjacent subplots in plot 2 (Table 1.5) was not a result of error in θ measurements and that, for some trees (eg. plot 2 and, to a lesser extent, plot 1), salal removal led to a reduction in E during part of the 1981 drying period.

In 1982, Douglas-fir E_T was lower than in 1981 since tree leaf area was lower as indicated earlier, early in the springtime of 1982 and vapour pressure deficits were much higher in 1982 (particularly on June 17, 1982).

Table 1.7 Measured rates (mm d^{-1}) of Douglas-fir and salal transpiration (E_T), forest floor evaporation (E_O) and total evapotranspiration (E) in plot 2 using porometry and equations (2) and (3) and small weighing lysimeters. The root mean square errors for Douglas-fir and salal E_T were typically $0.1\text{--}0.2 \text{ mm d}^{-1}$. These errors were determined by differentiation of (2) and (3). For (2), a 30% error was assumed for a_s and r_b and a 20% error for $e_l^* - e_a$ while the standard deviation of the r_s measurements was used as the error in r_s . For (3), a 30% error was assumed for A_{Tl} and a 10% error in D while the standard deviation of the r_s measurements was used as the error in r_s . For E_O , standard deviations were typically 0.1 mm d^{-1} .

Subplot	Uncut			Cut		
	E_T	E_O	E	E_T	E_O	E
	<u>Fir</u>	<u>Salal</u>		<u>Fir</u>		
1981						
July 24	---	1.5	---	---	0.6	---
July 31	---	1.5	---	---	0.5	---
Aug. 4	---	0.7	---	---	0.2	---
Aug. 12	1.1	1.6	0.1	2.8	1.4	0.3
Aug. 20	0.6	0.8	0.1	1.5	0.8	0.1
Oct. 23	1.7	0.9	---	---	1.8	---
1982						
June 9	0.3	---	---	---	0.8	---
June 17	0.4	---	---	---	0.4	---
June 23	0.5	---	---	---	0.7	---
June 30	0.4	---	---	---	0.5	---

Douglas-fir E_T was 0.2-0.5 mm d^{-1} higher as a result of salal removal in plot 2 during the 1982 drying period (except for June 17). Following 26 mm of rain from June 26-28, 1982, Douglas-fir E_T was similar in the adjacent subplots of plot 2 on June 30.

6. Tree Diameter Growth

There was close agreement between basal area increments (BAI) ($\text{mm}^2 \text{ tree}^{-1} \text{ year}^{-1}$) calculated from dendrometer band (Fig. 1.10) and diameter tape measurements (Tables 1.8 and 1.9). For three years following salal removal, BAI was higher in cut subplots except for plot 4. Increase in BAI as a result of salal removal was greatest in 1982 when the spring drying period limited tree growth where salal was present (Fig. 1.10). This shows the important effect of the higher values of Ψ_S on tree growth in the cut subplots during May and June 1982 when most of the BAI occurred. During the 1982 drying period, tree pre-dawn Ψ_{Ttx} was about 0.2-0.4 MPa higher in the uncut than the cut subplot of plot 4 (Table 1.4). Brix (1972) and Lassoie (1979) found that bole expansion of field-grown Douglas-fir trees ceased when Ψ_S was about -0.5 MPa. Values of Ψ_S were less than -0.5 MPa in plot 2 during the third week of August 1981 when BAI ceased. In 1982, BAI in plot 2 ceased (temporarily) during June when Ψ_S was again less than -0.5 MPa. However, during this period, BAI continued for an additional week in the cut subplot of plot 2.

4. CONCLUSIONS

Salal understory removal resulted in a slight increase in θ during growing season drying periods. This was a result of E being only slightly higher where salal was present than where it had been removed. Because

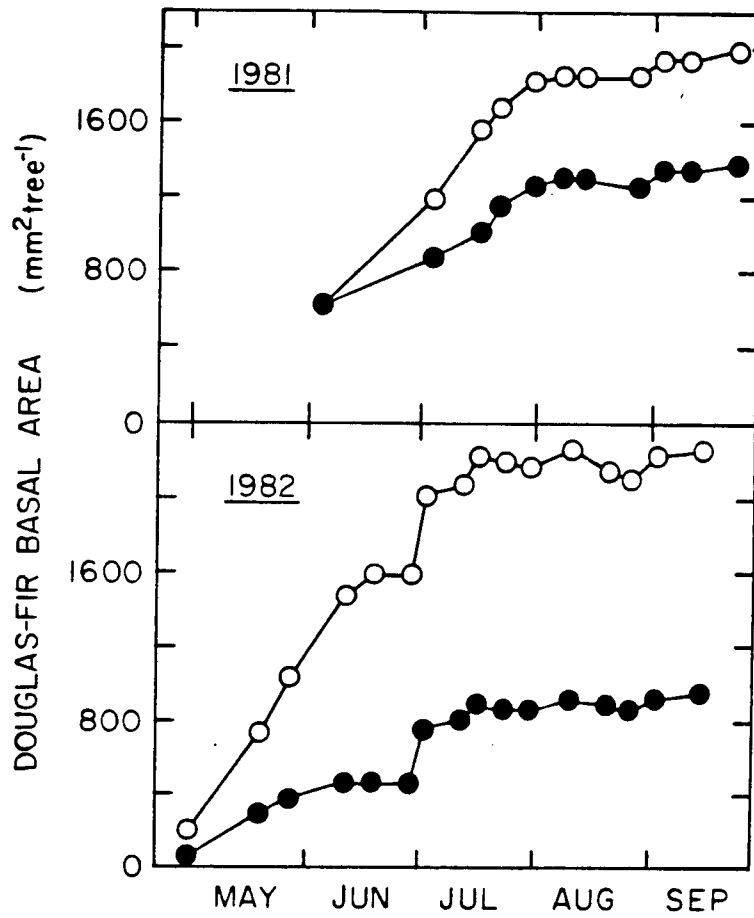


Figure 1.10 Courses of Douglas-fir basal area in the cut (O) and uncut (●) subplots of plot 2 from June 4 - September 23, 1981 and April 29 - September 14, 1982.

Table 1.8 Diameter (including bark), at the 1.37 m height, of the four pairs of adjacent trees using a tape with a 1 mm (in diameter) resolution.

<u>Subplot</u>	<u>June 4, 1981</u>	<u>Dec. 10, 1981</u>	<u>Oct. 6, 1982</u>	<u>Nov. 28, 1983</u>
1 Uncut	161	166	172	---
1 Cut	183	187	198	---
2 Uncut	179	182	185	188
2 Cut	180	185	192	198
3 Uncut	120	122	127	132
3 Cut	123	128	132	137
4 Uncut	112	117	123	130
4 Cut	102	105	109	116

Table 1.9 Basal area increment ($\text{mm}^2 \text{ tree}^{-1} \text{ year}^{-1}$) for the four pairs of adjacent trees calculated using Table 1.8.

<u>Plot</u>	<u>1981</u>		<u>1982</u>		<u>1983</u>	
	<u>Uncut</u>	<u>Cut</u>	<u>Uncut</u>	<u>Cut</u>	<u>Uncut</u>	<u>Cut</u>
1	1280	1160	1590	3330	----	----
2	850	1430	860	2070	880	1840
3	380	990	980	820	1020	1060
4	900	490	1130	670	1390	1240
Ave.	850	1020	1140	1720	1100	1380

salal transpiration was $0.5-1 \text{ mm d}^{-1}$ greater than forest floor evaporation in cut subplots, Douglas-fir transpiration was higher by 30 and 58%, on average, in 1981 and 1982 as a result of salal removal. The slight increase in θ corresponded to significantly higher values of Ψ_s and Douglas-fir pre-dawn Ψ_{Ttx} owing to the steepness of the soil water retention curve for this gravelly sandy loam soil at low values of θ . Douglas-fir BAI was increased significantly following salal removal as a result of increased Ψ_s in cut subplots during growing season drying periods. The results of this study suggest that in stands where consumption of water by understory is a growth limiting factor, understory control will result in more tree water use and growth.

5. REFERENCES

- Anonymous. 1978. The Canadian system of soil classification. Can. Soil Survey Com., Subcom. on Soil Classification, Can. Dept. of Agric. Publ. 1646, Supply and Services Can., Ottawa, Can.
- Barrett, J.W. and C.T. Youngberg. 1965. Effect of tree spacing and understory vegetation on water use in a pumice soil. Soil Sci. Soc. Am. Proc. 29: 472-475.
- Balmer, W.E., K.A. Utz and O.G. Langdon. 1978. Financial returns from cultural work in natural loblolly pine stands. South. J. Appl. For. 2: 111-117.
- Black, T.A., C.S. Tan and J.U. Nnyamah. 1980. Transpiration rate of Douglas-fir trees in thinned and unthinned stands. Can. J. Soil Sci. 60: 625-631.
- Black, T.A. and D.L. Spittlehouse. 1981. Modeling the water balance for watershed management. pp. 117-129. In: D.M. Baumgartner (ed.) Proc. Interior West Watershed Mgt. April 8-10, 1980. Spokane, WA, USA.
- Boast, C.W. and T.M. Robertson. 1982. A "micro-lysimeter" method for determining evaporation from bare soil: Description and laboratory evaluation. Soil Sci. Soc. Am. J. 46: 689-696.

- Brix, H. 1972. Nitrogen fertilization and water effects on photosynthesis and earlywood-latewood production in Douglas-fir. *Can. J. For. Res.* 2: 467-478.
- Campbell, G.S. 1974. A simple method of determining unsaturated conductivity from moisture retention data. *Soil Sci.* 117: 311-314.
- Cohen, Y., F.M. Kelliher and T.A. Black. 1985. Determination of sap flow in Douglas-fir trees using the heat pulse technique. *Can. J. For. Res.* 15: 422-428.
- Fritschen, L.J., J. Hsia and P. Doraiswamy. 1977. Evapotranspiration of a Douglas-fir determined with a weighing lysimeter. *Water Resour. Res.* 13: 145-148.
- Giles, D.G. 1983. Soil water regimes on a forested watershed. M.Sc. Thesis, Univ. of B.C., Vancouver, B.C.
- Grano, C.X. 1970. Small hardwoods reduce growth of pine overstory. USDA Forest Serv. South. Forest Exp. Sta. Res. Pap. SO-55.
- Kelliher, F.M., T.A. Black and A.G. Barr. 1984. Estimation of twig xylem water potential in young Douglas-fir trees. *Can. J. For. Res.* 14: 481-487.
- Lassoie, J.P. 1979. Stem dimensional fluctuations in Douglas-fir of different crown classes. *For. Sci.* 25: 132-144.
- Leverenz, J., J.D. Deans, E.D. Ford, P.G. Jarvis, R. Milne and D. Whitehead. 1982. Systematic spatial variation of stomatal conductance in a Sitka spruce plantation. *J. Appl. Ecol.* 19: 835-851.
- Liming, F.G. 1957. Homemade dendrometers. *J. For.* 55: 575-577.
- Oliver, W.W. 1979. Early response of ponderosa pine to spacing and brush: observations on a 12-year old plantation. USDA Forest Serv. Pac. Southwest For. and Range Exp. Sta. Res. Note PSW-341.
- Nnyamah, J.U. and T.A. Black. 1977. Field performance of the dewpoint hygrometer in studies of soil-root water relations. *Can. J. Soil Sci.* 57: 437-444.
- Roberts, J., C.F. Pymar, J.S. Wallace and R.M. Pitman. 1980. Seasonal changes in leaf area, stomatal conductance and transpiration from bracken below a forest canopy. *J. Appl. Ecol.* 17: 409-422.
- Roberts, J., R.M. Pitman and J.S. Wallace. 1982. A comparison of evaporation from stands of Scots pine and corsican pine in Thetford Chase, East Anglia. *J. Appl. Ecol.* 19: 859-872.
- Spittlehouse, D.L. 1981. Measuring and modelling evapotranspiration from Douglas-fir stands. Ph.D. Thesis, Univ. of B.C., Vancouver, B.C.

- Spittlehouse, D.L. and T.A. Black. 1981. A growing season water balance model applied to two Douglas-fir stands. *Water Resour. Res.* 17: 1651-1656.
- Spittlehouse, D.L. and T.A. Black. 1982. A growing season water balance model used to partition water use between trees and understory. pp. 195-214 In: *Proc. Can. Hydrol. Symp.* 82, Hydrol processes in for. areas. June 14-15, 1982, Fredericton, N.B.
- Tan, C.S. and T.A. Black. 1978. Evaluation of a ventilated diffusion porometer for the measurement of stomatal diffusion resistance of Douglas-fir needles. *Arch. Met. Geoph. Biokl., Ser. B.* 26: 257-273.
- Tan, C.S., T.A. Black and J.U. Nnyamah. 1978. A simple diffusion model of transpiration applied to a thinned Douglas-fir stand. *Ecol.* 59: 1221-1229.
- Thom, A.S. 1971. Momentum absorption by vegetation. *Quart. J. R. Met. Soc.* 97: 414-428.
- Turner, N.C., F.C.C. Pederson and W.H. Wright. 1969. An aspirated diffusion porometer for field use. *Conn. Agr. Sta. Special Soils Bull.* 29.
- van Bavel, C.H.M., G.B. Stirk and K.J. Brust. 1968. Hydraulic properties of a clay loam soil and the field measurement of water uptake by roots: I. Interpretation of water content and pressure profiles. *Soil Sci. Soc. Am. Proc.* 32: 310-317.
- Zahner, R. 1958. Hardwood understory depletes soil water in pine stands. *For. Sci.* 4: 178-184.

CHAPTER 2

APPLICATION OF AN EVAPOTRANSPIRATION MODEL TO
ESTIMATING SALAL UNDERSTORY REMOVAL EFFECTS IN A DOUGLAS-FIR FOREST

CHAPTER 2

APPLICATION OF AN EVAPOTRANSPIRATION MODEL TO ESTIMATING SALAL UNDERSTORY REMOVAL EFFECTS IN A DOUGLAS-FIR FOREST

1. INTRODUCTION

The Penman-Monteith equation (Monteith 1965) has provided useful insight into the physical and physiological factors affecting forest evapotranspiration (Stewart and Thom 1973; Tan and Black 1976). A further development of the equation for multilayer, partially wet forest canopies has provided a practical one-dimensional model (Shuttleworth 1978 and 1979) despite the simplifying assumptions regarding within canopy turbulent transfer (Jarvis et al. 1976; Raupach and Thom 1981; Finnegan 1985). With standard hourly micrometeorological measurements and stomatal resistance characteristics, the model can be combined with a root zone water balance model (e.g. Spittlehouse and Black 1982) to provide estimates of forest evapotranspiration over extended periods. This chapter (i) describes the evapotranspiration model as modified for use in hypostomatous canopies, (ii) tests the model using energy and water balance measurements and (iii) uses the model to explain the effects of salal (Gaultheria shallon Pursh.) understory removal on tree transpiration rates in a Douglas-fir (Pseudotsuga menziesii (Mirb.) Franco) forest.

2. THEORY

Using Shuttleworth's (1979) evapotranspiration theory and assuming the similarity of sensible heat and water vapour aerodynamic transfer resistances, it can be shown that the water vapour flux density from layer 1 (E'_1) with leaf area (one side) index (a_1) within a multilayer forest canopy of hypostomatous leaves can be expressed as (see Appendix I)

$$E'_1 = \frac{s(R_{ni} - G) + \rho c_p(D_i - \delta_i)/r_{Ai}}{L[s + \gamma(1 + r_{ci}/r_{Ai})]} \quad (1)$$

where E'_1 is the difference between the water vapour flux density above and below the layer (i.e. $E_1 - E_{i-1}$), R_{ni} and D_i are the net radiation flux density and vapour pressure deficit above layer 1 respectively, G is the soil heat flux density,

$$\delta_i = [s(R_{ni-1} - G)(r_{bi}/(2a_1)) + (s + \gamma)LE_{i-1}r_{ai}]/(\rho c_p), \quad (2)$$

r_{Ai} is the total aerodynamic resistance (Thom 1972) given by

$$r_{Ai} = r_{ai} + r_{bi}/(2a_1) \quad (3)$$

and r_{ci} is the canopy resistance of layer 1 expressed as (see Appendix II)

$$r_{ci} = \left[\frac{W_i}{(1 + s/\gamma)r_{bi}/(2a_1)} + \frac{1 - W_i}{r_{si}/a_1 + (2 + s/\gamma)r_{bi}/(2a_1)} \right]^{-1} - (1 + s/\gamma)r_{bi}/(2a_1) \quad (4)$$

where r_{ai} is the eddy diffusive resistance above layer i , r_{bi} and r_{si} are the boundary-layer and stomatal resistances of one side of the leaves in layer i respectively and W_i is the fraction of leaf area in layer i that is completely wet. The remaining symbols are as conventionally defined (see Notation). Stomatal resistances of hypostomatous leaves of Douglas-fir and salal on a one-sided basis have been related to light, leaf and soil water potential and D (Tan et al. 1977 and 1978).

Equation (1) is recognized as the Penman-Monteith equation with an additional term which accounts for the net radiation, latent and sensible heat flux densities below layer i . Black et al. (1970) used (1) as an evapotranspiration model for a dry snap bean canopy where $r_{bi} \ll r_{si}$ was assumed so that δ_i was equal to the soil evaporation rate multiplied by $r_{ai}(s + \gamma)/(\rho c_p)$. If r_{ai} is assumed to be zero, then (1) reduces to the Penman-Monteith equation applied to the layer (i.e. using the vapour pressure deficit and the available energy flux density ($R_{ni} - R_{ni-1}$) within the layer). Equation (4) gives the canopy resistance of a partially wet layer assuming that the individual leaves are either completely wet or completely dry so that the wet and dry leaves have different temperatures. Equation (4) differs slightly from Shuttleworth's (1978) equation (32) because his derivation was for amphistomatous leaves. When $W_i = 0$, $r_{ci} = r_{si}/a_i + r_{bi}/(2a_i)$ compared to $r_{ci} = r_{si}/(2a_i)$ for an amphistomatous leaf canopy as in (24) of Shuttleworth (1978) (see Appendix III). As expected when $W_i = 1$, $r_{ci} = 0$ in both hypostomatous and amphistomatous cases. Making use of Shuttleworth's (1978) theory, it can be shown that the

rate of evaporation of intercepted water from layer i (E'_{Ii}) is given by (see Appendix IV)

$$E'_{Ii} = \frac{E'_i W_i [(2 + s/\gamma)r_{bi} + 2r_{si}]}{(1 + s/\gamma)r_{bi} + W_i(r_{bi} + 2r_{si})} \quad (5)$$

The vapour flux density above layer i (E_i) is given by summing (1) from 0 to i , so that for a canopy of n layers the evapotranspiration rate is

$$E = \sum_{i=0}^n E'_i \quad (6)$$

where $E_0 = E'_0$ is the evaporation rate from the forest floor with $\delta_0 = 0$ and r_{c0} being the forest floor diffusive resistance. In this study, the forest canopy was divided into two layers ($n = 2$), where the Douglas-fir subcanopy was designated as layer 2 and the salal subcanopy as layer 1 (see Appendix V).

3. METHODS

1. Site and Experimental Design

The site and experimental design are described in detail in Chapter 1. Briefly, the site was a thinned 31-year-old Douglas-fir stand with salal understory over about 700 mm of gravelly sandy loam soil. The experimental design consisted of four circular plots about 7 m in diameter, each containing two subplots, one with salal understory present and the other with it cut and removed. Each subplot contained one tree about 14 m tall

and 160 mm in diameter (at the 1.37 m height) which was similar in size to the one in the adjacent subplot. The root zones of all eight trees were isolated by a trench and plastic barrier.

2. Micrometeorological Measurements

Standard hourly micrometeorological measurements of solar irradiance, air temperature (T_{air}), vapour pressure deficit, wind speed (u) and precipitation (P) above the forest are described in Chapter 1. In 1981, R_n above the forest (R_{na}) was measured using a Swissteco S-1 net radiometer. In 1981, R_n below the tree canopy (R_{nb}) was measured in one plot using one net radiometer above the salal canopy and another above the forest floor surface, where salal had been removed. In 1982, R_{na} was estimated, prior to August, from the solar irradiance measurements following Gates (1980) and Spittlehouse and Black (1981). During August 1982, R_{na} was measured using an S-1 net radiometer. In the same month, R_{nb} was measured using an S-1 net radiometer mounted on a tram travelling at the 1 m height along a 10 m path where salal along one half of the path had been removed. The tram travelled at 0.5 m min^{-1} and automatically reversed when it reached each end. The net radiometer output voltage was measured every 10 seconds (see Appendix VI). Prior to August 1982, R_{nb} was estimated to be approximately $0.16 R_{na}$ and $0.14 R_{na}$ for uncut and cut subplots, respectively (see Appendix VI). In 1981 and 1982, R_{no} below the salal canopy was estimated using $R_{no} = ((s + \gamma)/s)LE_o + G$ where LE_o was 2 W m^{-2} (measured using small weighing lysimeters (150 mm diameter by 120 mm deep) (see Chapter 1)). The soil heat flux density in each subplot of one plot at the 50 mm depth was measured using three soil heat flux plates (100 mm long

x 25 mm wide x 3 mm thick), similar to those described by Fuchs and Tanner (1968), connected in series and corrected for the rate of change of heat storage in the upper 50 mm of soil. In 1982 (prior to August), G was estimated to be $0.02 R_{na}$ and $0.03 R_{na}$ for uncut and cut subplots, respectively.

In 1981 and 1982, T_{air} and D were estimated below the tree canopy using hourly average values at the 6 m height with the relationships T_{air} ($^{\circ}C$) (0.5 m height) = $0.93T_{air}$ ($^{\circ}C$)(6 m height) + 1.2 and D (kPa) (0.5 m height) = $0.89 D$ (kPa) (6 m height) - 0.03 (based on 33 hourly average measurements of T_{air} and D at both heights on July 24 and 25, 1981). Hourly Assmann psychrometer measurements confirmed the validity of these relationships on several days in August 1981 and June 1982.

3. Canopy Resistance Functions

Stomatal resistances of Douglas-fir and salal were estimated using average root zone soil water potential (Ψ_s) and D for the layer following interpolation of the r_s characteristic functions in Tan et al. (1978) (Table 2.1)(see Appendix VII). When R_{na} was negative (i.e. 1900-0700 hours PST), r_s of both species was set to 10^5 s m^{-1} .

Boundary-layer resistances were estimated using a function for artificial leaves in Spittlehouse and Black (1982) and a shelter factor of two (Landsberg and Powell 1973; Jarvis et al. 1976) (r_b (s m^{-1}) = $2 \times 184 (d_l/u)^{0.5}$) where d_l is leaf diameter (1 mm for Douglas-fir and 60 mm for salal) and u is the windspeed near the leaf ($0.5 u_{15m}$ for Douglas-fir and $0.1 u_{15m}$ for salal where u_{15m} is the windspeed at the 15 m height (i.e. 1 m above the forest)). In 1982 (prior to August), u_{15m} was estimated to

Table 2.1 Values of the empirical constants λ , μ , ν , ξ and o in the stomatal resistance (r_s) characteristics function r_s ($s\ m^{-1}$) = $\exp[\lambda - \mu(\Psi_s + \nu) + (\xi + o(\Psi_s + \nu))D^2]$ where Ψ_s is average root zone soil water potential (MPa) and D is vapour pressure deficit (kPa).

Species	Ψ_s	λ	μ	ν	ξ	o
Salal	≥ -0.10	0.40	7.0	0.01	0.19	0.10
Salal	≥ -0.35 to < -0.10	1.05	1.5	0.10	0.20	0.10
Salal	≥ -0.95 to < -0.35	1.40	1.0	0.35	0.24	0.02
Salal	≥ -1.10 to < -0.95	1.95	1.8	0.95	0.27	0.02
Salal	< -1.10	2.20	0.5	1.10	0.27	0.02
Douglas-fir	≥ -0.10	1.10	5.0	0.01	0.37	0.20
Douglas-fir	≥ -0.35 to < -0.10	1.60	0.6	0.10	0.38	0.10
Douglas-fir	≥ -0.95 to < -0.35	1.80	1.4	0.35	0.40	0.20
Douglas-fir	≥ -1.10 to < -0.95	2.60	1.5	0.95	0.54	0.10
Douglas-fir	< -1.10	2.85	0.5	1.10	0.56	0.10

be 3 m s^{-1} for 1100-2000 h PST and 1.5 m s^{-1} for the rest of the day. Dividing these values by $2a_1$ gave mean boundary-layer resistances similar to those estimated following the relationships given by Garratt and Hicks (1973). The eddy diffusive resistance above the Douglas-fir subcanopy was estimated assuming a logarithmic wind profile (Jarvis et al. 1976) with a zero plane displacement height of 8.5 m (Szeicz et al. 1969) and a roughness length of 1.5 m (Stanhill 1969), while that above the salal subcanopy was estimated assuming an exponential eddy diffusivity profile from the top of the trees to the salal subcanopy (Thom 1975) with an attenuation coefficient of 2. This value was based on the ratio of the above to below tree canopy windspeeds being about 0.13. Daytime eddy diffusive resistances above the salal subcanopy were calculated to be about 40 s m^{-1} compared to 20 s m^{-1} for the 600 trees ha^{-1} Thetford (Shuttleworth 1979; Roberts et al. 1980) and the 400 trees ha^{-1} Jadraas (Lindroth 1984) forests. For the forest floor, values of r_{ai} estimated for the salal subcanopy were used. Forest floor diffusive resistances for ten days in July and August 1981 were determined by choosing a value which resulted in agreement between daily total values of measured and calculated E_0 on each day. These values were linearly related to average root zone water content for calculations of forest floor diffusive resistances on other days.

For each Douglas-fir tree, leaf area was estimated from the diameter at the 1.37 m height using a function in Spittlehouse (1981). Ground area occupied by the tree was estimated using a tree location map and the "polygon of occupancy" (Santantonio et al. 1977). Tree leaf area divided by the polygon of occupancy was taken as the value of a for Douglas-fir in each subplot. For salal, a was estimated from 1 m^2 sample measurements made in each of the cut subplots on May 21, 1981.

The leaf wetness variable for each subcanopy was estimated using the ratio of the subcanopy water storage (C) to the maximum water storage of the subcanopy (S). The value of S for the Douglas-fir subcanopy was determined by plotting 24 hour throughfall (above the salal) against the corresponding rainfall using data of Spittlehouse (1981) for 1978 (Fig. 2.1). Rutter et al. (1971) showed that the negative intercept of the line of unit slope along the upper limit of the throughfall data gives the value of S. This was found to be 0.6 mm d^{-1} . Since a of the Douglas-fir in 1978 was 5, the average depth of water on the leaves was 0.12 mm. This was very close to the depth of water after drainage on a foliated Douglas-fir branch sprayed in the laboratory (Spittlehouse and Black 1982). The value of S for the salal subcanopy was approximated by multiplying salal a by 0.12.

The value of C was calculated for each time j using the following water balance equation for each subcanopy

$$C_j = C_{j-1} + [(1-p)P_j - E'_{Ij} - Q_j] \Delta t \quad (7)$$

where Δt is 15 minutes and Q_j is the drainage of intercepted water for the interval between $j-1$ and j . The free throughfall coefficient p was calculated by taking the average of the ratio of 24 hour throughfall (above salal) to rainfall for 5 days from Spittlehouse (1981) where $P < S$ (Rutter et al. 1971). It was found to be 0.6. Drainage was assumed to be zero until C_j exceeded S . At this point drainage was calculated as the amount by which $(1-p) P_j - E'_{Ij}$ exceeded the remaining water storage capacity of the leaves ($S - C_j$).

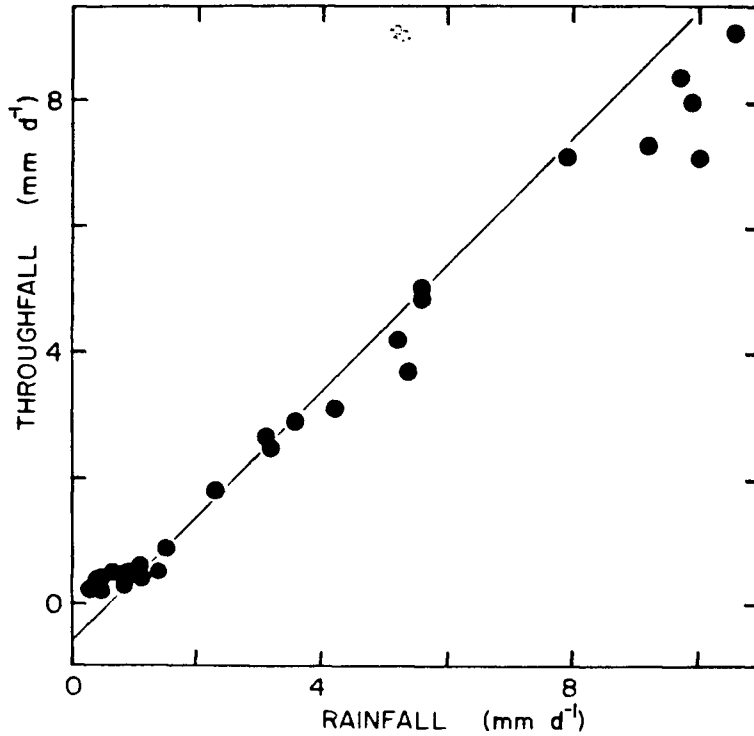


Figure 2.1 Relationship between daily throughfall (above the salal) and rainfall rates at the experimental site in 1978. A line of unit slope along the upper limit of the data is also shown. The negative intercept of this line (0.6 mm d^{-1}) gives the maximum water storage of the Douglas-fir subcanopy following Rutter et al. (1971).

4. Root Zone Water Balance Equation

The course of average root zone volumetric water content (θ) during two summer periods was calculated using the following water balance equation applied to the stand and its single-layer root zone

$$\theta_k = \theta_{k-1} + (P_k - E_k - F_k)\Delta t/\zeta \quad (8)$$

where P_k , E_k and F_k are the rates of rainfall, evapotranspiration and root zone drainage respectively, at time k , Δt is the time interval between k and $k-1$ (one hour except for when $W_1 > 0$ and then Δt is 15 minutes) and ζ is root zone depth. Evapotranspiration rates were calculated using (1) through (7) with the canopy divided into two layers (tree and understory subcanopies) and soil. Drainage from the root zone was calculated as a function of θ ($F \text{ (mm d}^{-1}\text{)} = 100 (\theta/0.3)^{1.7}$) (Spittlehouse and Black 1981). During most of the summer, drainage was a small term in the root zone water balance equation so that θ was largely determined by rainfall and evapotranspiration.

5. Testing the Evapotranspiration and Root Zone Water Balance Equations

During August 1981 and June 1982, θ was measured in one to two week intervals using the neutron moderation technique with a probe being lowered into access tubes placed in each subplot. Thermocouple psychrometers and tensiometers were used to measure Ψ_s every two to seven days in one of the plots. Measured values of θ and Ψ_s were compared during the two summer

periods with calculated values obtained using (8) and a field determined soil water retention characteristic (Ψ_s (MPa) = $-0.005 (\theta/0.3)^{-6.5}$) (see Appendix VIII).

Forest evapotranspiration was measured on four days in August 1982 using the Bowen ratio/energy balance technique. Half-hourly measurements of the Bowen ratio (β) were made using a D.C. powered rotating psychrometric apparatus described by Spittlehouse and Black (1980). The apparatus was located at the top of a 15 m tall tower adjacent to the four plots, with the vertical separation between the two psychrometers being 3 m. The lower psychrometer was about 1 m above the tops of the trees. Forest evapotranspiration was calculated using

$$E = (R_{na} - G - M)/(L(1 + \beta)) \quad (9)$$

where M is the rate of canopy heat storage estimated following Stewart and Thom (1973). This measurement of E was considered to include tree and understory transpiration and soil evaporation since the area where understory had been removed was small and 20 m from the tower in a direction at right angles to the prevailing wind direction. These measurements of E were compared to calculated values obtained using (1)-(6) ($W_i = 0$) applied to a two layer canopy (trees and understory) plus soil evaporation.

Stomatal resistance measurements were made on the two trees and salal understory in one plot using a ventilated diffusion porometer described by Tan et al. (1978). Hourly measurements were made from sunrise until late afternoon on August 12 and 20, 1981 and June 9, 17, 23 and 30, 1982 (trees

only). These measurements were used to test the r_s characteristic functions (Table 2.1) and the rates of tree and understory transpiration calculated using (1).

4. RESULTS AND DISCUSSION

1. Measured and Calculated Daytime Courses of E

There was generally good agreement between daily values of E measured during the 4-day test period using the energy balance/Bowen ratio and values calculated for the stand with understory present using (1) to (8) (Table 2.2) Agreement was not as good when comparing the daytime courses of measured and calculated E (Fig. 2.2). However, both measured and calculated E was highest for the period prior to noon on August 25, 1982. Calculated Douglas-fir r_s increased markedly after 1400 h ($> 6000 \text{ s m}^{-1}$) owing to the high values of D and salal E was highest for the period 1100-1400 h ($\approx 0.1 \text{ mm h}^{-1}$). Measurement error accounts for some of the disagreement since Bowen ratios were high (≥ 2) on August 24-26 and wet and dry bulb gradients small on August 27 (Spittlehouse and Black 1980).

2. Forest Floor Evaporation After Salal Removal

For θ less than 0.185, forest floor diffusive resistance was linearly related to θ ($r_{CO} \text{ (s m}^{-1}\text{)} = -83000 \theta + 16100$, $R^2 = 0.96$) (Fig. 2.3). On three days when $\theta > 0.185$, r_{CO} was 700 s m^{-1} ($\theta = 0.189$) and 900 s m^{-1} ($\theta = 0.200$ and 0.203). This meant that E_0 was limited by a dry surface layer whose thickness (l_d) can be related to r_{CO} using (Denmead 1984; Novak and Black 1985)

Table 2.2 Daily total net radiation flux density above the forest (R_{na}) ($\text{MJ m}^{-2} \text{d}^{-1}$) and daily measured and calculated values of evapotranspiration rate (E) (mm d^{-1}) following initialization of calculations on August 20, 1982 when measured θ was $0.16 \text{ m}^3 \text{ m}^{-3}$ ($\Psi_s = -0.3 \text{ MPa}$).

<u>Date (August, 1982)</u>	<u>24</u>	<u>25</u>	<u>26</u>	<u>27</u>
R_{na}	11.5	11.6	12.6	1.4
Measured E	1.8	2.2	1.8	0.2
Modelled E	1.9	2.0	2.0	0.3

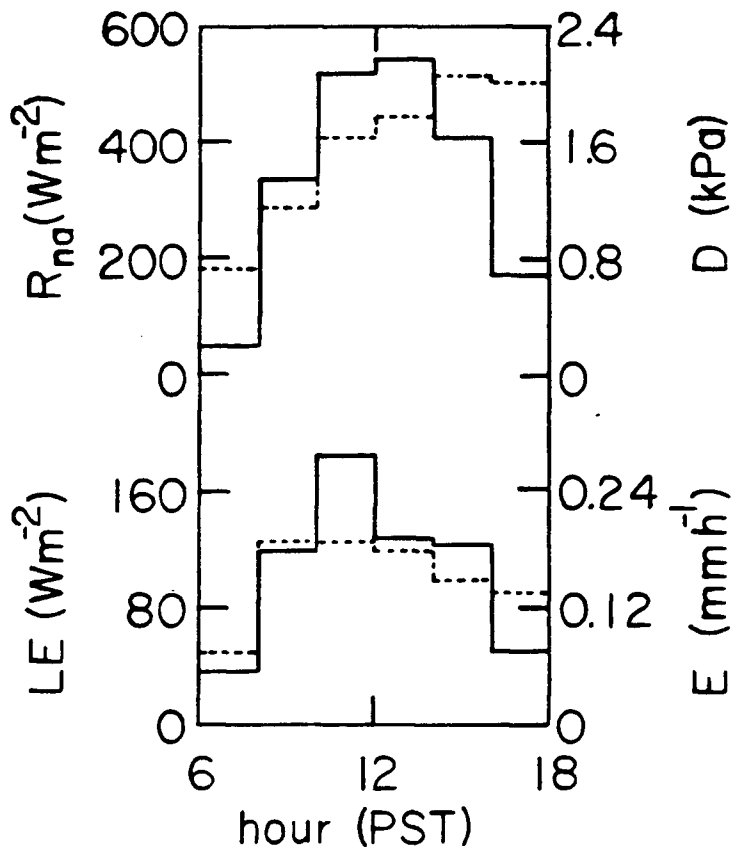


Figure 2.2

Courses of net radiation flux density and vapour pressure deficit above the forest (R_{na} (—) and D (- - -)) and measured (—) and calculated (- - -) forest evapotranspiration rate (E) (with understory) on August 25, 1982, a clear day when average root zone soil water potential (Ψ_s) was about -0.7 MPa. Errors in measured E were approximately $0.02-0.04$ $mm\ h^{-1}$ (Spittlehouse and Black 1980). Root mean square errors in calculated E were $0.04-0.06$ $mm\ h^{-1}$ as determined by differentiation of (1) applied to two layers and soil. A 10% error was assumed for D_i , a 20% error for $(R_{ni} - G)$ and a 30% error for the transfer resistances (r_{si} , r_{bi} and r_{ai}), LE_0 and R_{no} .

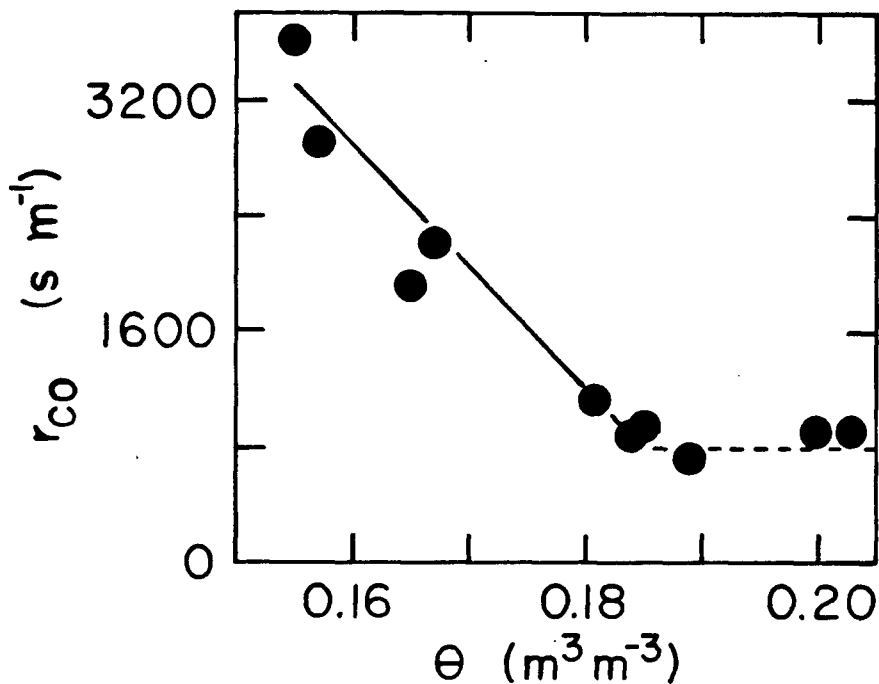


Figure 2.3 Relationship between forest floor diffusive resistance (r_{co}) and average root zone soil water content (θ) in the cut subplot of plot 2 for ten days in July and August 1981. For θ less than 0.185, r_{co} ($s\ m^{-1}$) = $-83000\ \theta + 16100$ ($R^2 = 0.96$) as shown by the solid line. For θ greater than 0.185, r_{co} was $800\ s\ m^{-1}$, on average, as shown by the dashed line.

$$\lambda_d = r_{co} \Omega_t (O_d - \theta_d) \kappa_d \quad (11)$$

where Ω_t is a "tortuosity" factor (0.66), O_d and θ_d are the porosity and volumetric water content of the dry layer and κ_d is the diffusivity for water vapour ($25.7 \times 10^{-6} \text{ m}^2 \text{ s}^{-1}$ at 20°C). For the forest floor, O_d and θ_d were taken from Plamondon (1972) as 0.88 (i.e. bulk density = 150 kg m^{-3} , organic matter density = 1300 kg m^{-3} (Van Wijk and De Vries 1963)) and 0.20 (i.e. matric potential = -1.5 MPa). Using these values and $r_{co} = 700 \text{ s m}^{-1}$ in (11) results in $\lambda_d = 8 \text{ mm}$. Field observations support this calculation. At about midday on the day following an evening irrigation equivalent to 100 mm of rain, the forest floor surface of a cut area (i.e. salal cut and removed) adjacent to the four plots was observed to be dry. The 8 mm value of λ_d for $r_{co} = 700 \text{ s m}^{-1}$ suggests that the top 8 mm of forest floor consisted of rapidly draining litter (i.e. undecomposed leaves and twigs) while the bottom 2-12 mm was humified with some water storage capacity. The soil surface was dry until r_{co} was 850 to 1500 s m^{-1} ($\theta = 0.184$ to 0.176). For $\theta = 0.125$ ($\Psi_s = -1.5 \text{ MPa}$), λ_d was 68 mm so that the top 48-58 mm of soil was dry.

For July 24-25, 1981, two consecutive clear days when Ψ_s was about -0.05 MPa , $r_{co} = 900 \text{ s m}^{-1}$ provided agreement between calculated and measured daily values of E_o (0.6 mm d^{-1}). Hourly values of calculated E_o generally agreed with lysimeter measurements in the cut subplot of plot 2 (Fig. 2.4). Aerodynamic resistances varied from 10 - 50 s m^{-1} and were highest for the period 0200-0600 on July 25. The high variability in the

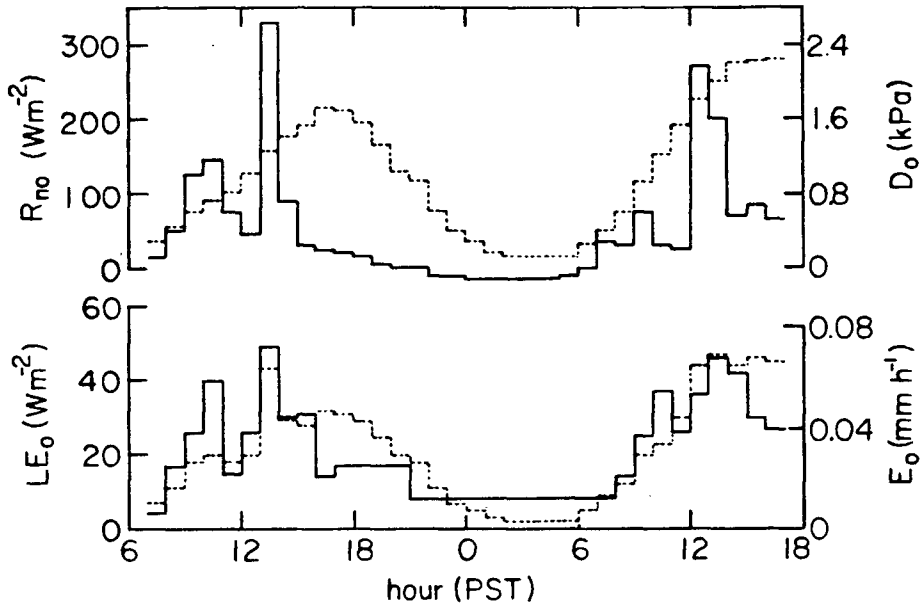


Figure 2.4

Courses of net radiation flux density and vapour pressure deficit above the forest floor (R_{no} (—) and D_o (- - -)) and measured (—) and calculated (- - -) forest floor evaporation rate (E_o) in the cut subplot of plot 2 on July 24-25, 1981, two clear days when average root zone soil water potential (ψ_s) was about -0.05 MPa. Standard deviations for measured E_o values were typically $0.004\ mm\ h^{-1}$ at night and $0.015\ mm\ h^{-1}$ during the daytime. Root mean square errors for calculated E_o values were similar. These errors were determined by differentiation of (1) with $\delta_o = 0$. A 20% error was assumed for ($R_{no} - G$) and r_{CO} , a 10% error for D_o and a 30% error for r_{Ao} .

measured values of R_{n0} and E_0 was due to sun flecks which were generally common to the net radiometer and lysimeters. About 16% of the daily measured E_0 occurred at night (2200-0600 h, Fig. 2.4) while for the calculations the value was 10%.

3. Measured and Calculated Courses of θ

1. Using Equations (1) to (4)

Calculations of courses of θ using the complete evapotranspiration theory and water balance equations were made for the eight subplots for the periods July 24-September 3, 1981 and May 27-July 1, 1982. There was good agreement between measured and calculated courses of θ in cut and uncut subplots (Figs. 2.5 and 2.6 and Table 2.3). In particular, there was excellent agreement in the measured and calculated differences between θ in paired subplots. Salal understory removal resulted in slightly higher values of θ and significantly higher values of Ψ_s (see Chapter 1). Owing to the steepness of the retention curve for this gravelly sandy loam soil at low values of θ , a small decrease in θ corresponded to a significant decrease in Ψ_s (Figs. 2.5 and 2.6).

2. Effect of Assuming $r_{A1} = 0$ in Equations (1) to (4)

Considerable simplification of the evapotranspiration theory is achieved when $W_1 = 0$ by using the limit $r_{A1} \rightarrow 0$ in (1) - (4) so that $E'_1 = \rho c_p D_1 / r_{ci}$ where $r_{ci} = r_{si} / a_1$. Working in the same stand as in this study, Tan et al. (1978) obtained good agreement between energy balance/Bowen ratio evapotranspiration measurements and values calculated using the above procedure in 1975 following heavy thinning of the stand.

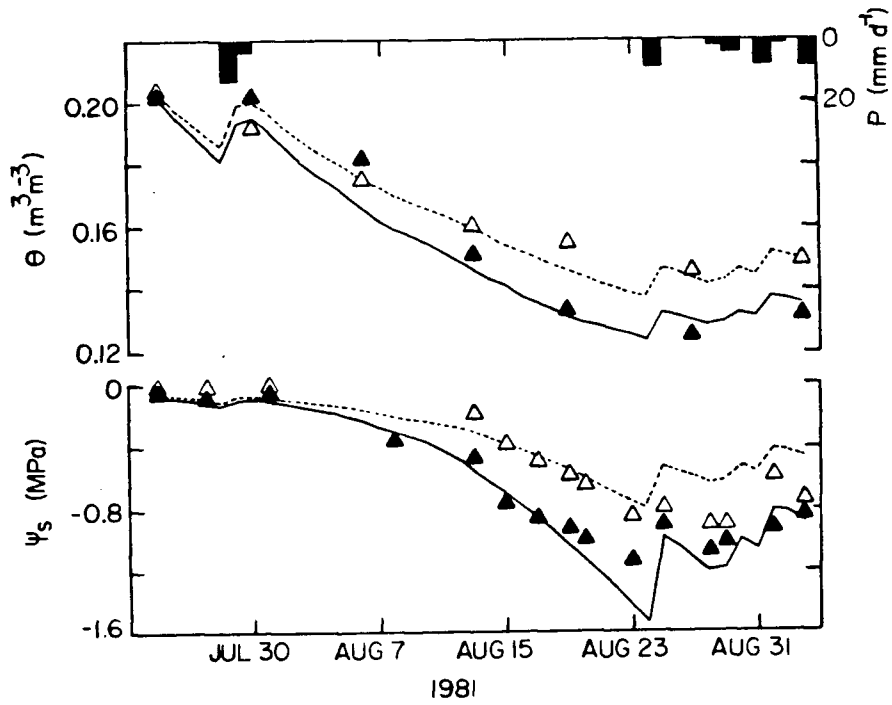


Figure 2.5 Courses of measured (symbols) and calculated (lines) average root zone soil water content (θ) and soil water potential (ψ_s) in the cut (Δ and - - -) and uncut (\blacktriangle and —) subplots of plot 2 for the period July 24 - September 3, 1981. Also shown is the daily rainfall rate (P).

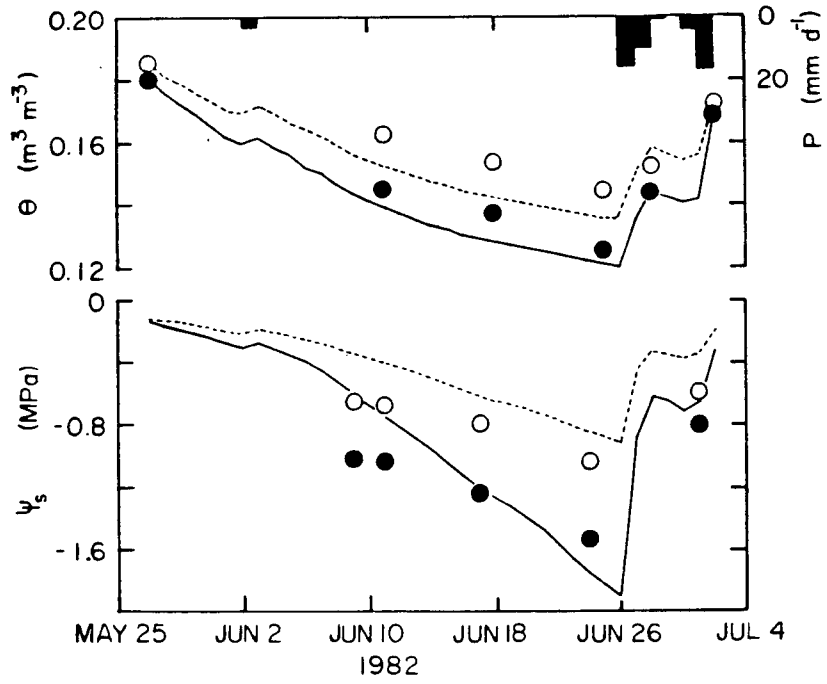


Figure 2.6 Same as for Fig. 2.5 except for May 27 - July 1, 1982 and \circ and \bullet .

Table 2.3 Average values of the minimum measured and calculated average root zone water content ($\text{m}^3 \text{m}^{-3}$) on the same day in the cut (C) and uncut (U) subplots.

	<u>August 27, 1981</u>		<u>June 25, 1982</u>	
	<u>Measured</u>	<u>Calculated</u>	<u>Measured</u>	<u>Calculated</u>
1U	0.14	0.14	0.14	0.12
1C	0.13	0.14	0.15	0.14
2U	0.13	0.13	0.12	0.12
2C	0.15	0.14	0.14	0.14
3U	0.14	0.13	0.14	0.12
3C	0.17	0.15	0.17	0.14
4U	0.16	0.14	0.16	0.13
4C	0.17	0.16	0.16	0.15
U	0.14	0.13	0.14	0.12
C	0.16	0.15	0.16	0.14

Use of this procedure in the cut subplot of plot 2 (salal understory cut and removed) for the rainless period July 30-August 18, 1981 resulted in only slightly higher calculated θ values than those obtained when r_{A1} was not assumed to be negligible (Fig. 2.7). This is to be expected since r_{A1} is much smaller than r_{s1} for Douglas-fir so that r_{s1}/a_1 is a good approximation of the Douglas-fir canopy resistance (Tan et al. 1978). The reason for the small difference between calculated θ values (with r_{A1} included) in Fig. 2.7 and those in Fig. 2.5 is due to the difference in the starting dates for calculations in the two figures.

For salal, $r_{A1} \approx r_{s1}$ so that neglecting r_{A1} for salal and Douglas-fir subcanopies in (1) - (4) resulted in lower calculated θ values in the uncut subplot of plot 2 for the same rainless period (Fig. 2.7). When r_{A1} for both subcanopies were included, calculated tree transpiration in the uncut subplot for this 20 day period was 29 mm. The corresponding value was 24 mm when r_{A1} for both subcanopies were neglected. The difference between these two values resulted from more salal understory transpiration being calculated using the latter procedure. Since salal stomatal resistance characteristics and leaf area index remained relatively constant from 1975-1981, it appears that the reduction in salal transpiration from 1975-1981 resulted from forest canopy closure leading to a reduction in the ratio of below to above tree canopy wind speed and an increase in r_{A1} for the salal subcanopy.

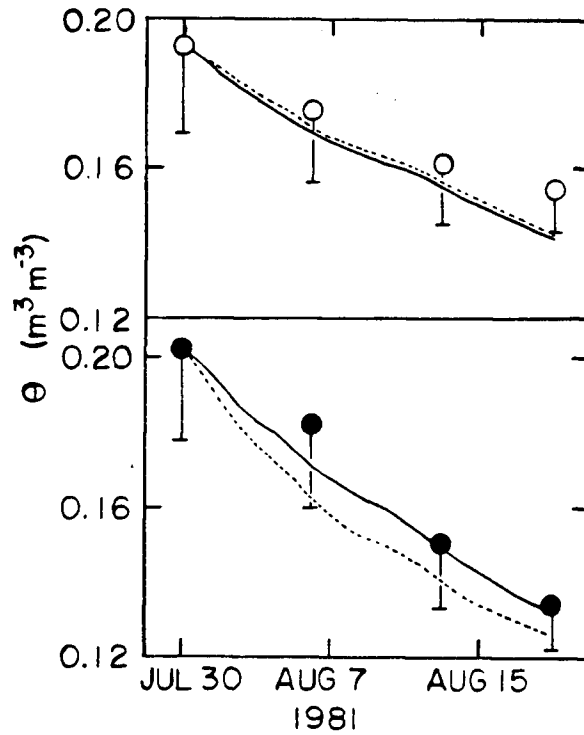


Figure 2.7 Courses of measured (symbols) and calculated (lines) average root zone soil water content (θ) in the cut (○) and uncut (●) subplots of plot 2 for the period July 30 - August 18, 1981. Calculated values with and without the aerodynamic and boundary-layer transfer resistances for the Douglas-fir and salal subcanopies are shown by the solid and dashed lines, respectively. Error bars are one standard deviation.

4. Partitioning of Evapotranspiration in Cut and Uncut Subplots

Table 2.4 gives the total calculated values of evapotranspiration, transpiration and interception of Douglas-fir and salal and forest floor evaporation for cut and uncut subplots for the 1981 and 1982 periods discussed in Section 3.1. Calculated total values of E for the uncut subplots were slightly larger than those for the cut subplots in both years. Throughout these periods, calculated values of E of the uncut subplots were also slightly higher than in the cut subplots. This was also found using water balance measurements in Chapter 1 except for plot 2 for August 6-19, 1981 when the measured average values of E were 2.4 and 1.1 mm d⁻¹ for the uncut and cut subplots respectively compared to calculated average values of 1.7 and 1.5 mm d⁻¹ respectively.

Calculated tree transpiration rates for the first 19 days of the 1981 period and 11 days of the 1982 period were slightly higher where salal had been removed but were considerably higher during the rest of the respective periods (Figs. 2.8 and 2.9). On August 12, 1981, calculated tree transpiration rates were 1.5 and 1.1 mm d⁻¹ in the cut and uncut subplots of plot 2 (leaf area index was 5 for both trees) respectively. The corresponding values on August 20 were 1.1 and 0.5 mm d⁻¹. Using (1) and r_g measurements made at about the midcrown height of the trees in plot 2, tree transpiration rates were estimated to be 1.4 and 1.1 mm d⁻¹ on August 12 and 0.8 and 0.6 on August 20, 1981. There was not as good agreement between calculated and estimated tree transpiration rates in plot 2 for June 9, 17 and 23, 1982; however the differences between the cut and uncut subplots were in good agreement (see Table 1.7 in Chapter 1).

Table 2.4 Average calculated values (mm) of total evapotranspiration (E), transpiration (E_T'), evaporation of intercepted water (E_I') and forest floor evaporation (E_O) in the cut (C) and uncut (U) subplots for the periods July 24-September 3, 1981 and May 27-July 1, 1982.

	E	E_T'		E_I'		E_O
		<u>Fir</u>	<u>Salal</u>	<u>Fir</u>	<u>Salal</u>	
<u>1981</u>						
1U	92	47	25	15	2	3
1C	84	57	--	15	-	12
2U	88	39	28	15	3	3
2C	79	51	--	15	-	13
3U	83	32	31	14	3	3
3C	84	53	--	14	-	17
4U	84	38	27	14	2	3
4C	75	43	--	14	-	18
U	88	39	28	15	3	3
C	81	51	--	15	-	15
<u>1982</u>						
1U	61	23	17	17	1	3
1C	64	39	--	17	-	8
2U	66	23	21	17	2	3
2C	58	33	--	17	-	8
3U	60	17	21	17	2	3
3C	60	32	--	17	-	11
4U	64	22	21	17	1	3
4C	55	26	--	17	-	12
U	63	21	20	17	2	3
C	59	32	--	17	-	10

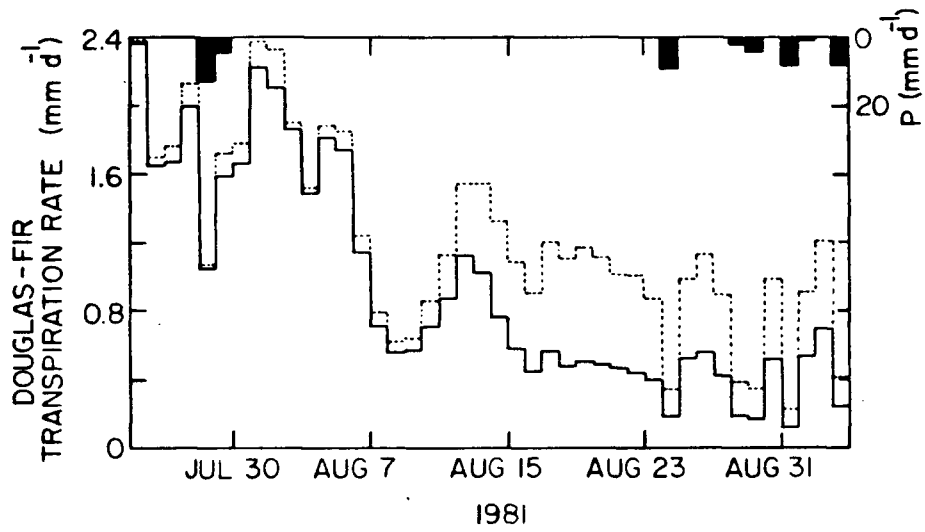


Figure 2.8 Courses of calculated tree transpiration rates in the cut (---) and uncut (—) subplots of plot 2 for the period July 24 - September 3, 1981. Also shown is the daily rainfall rate (P).

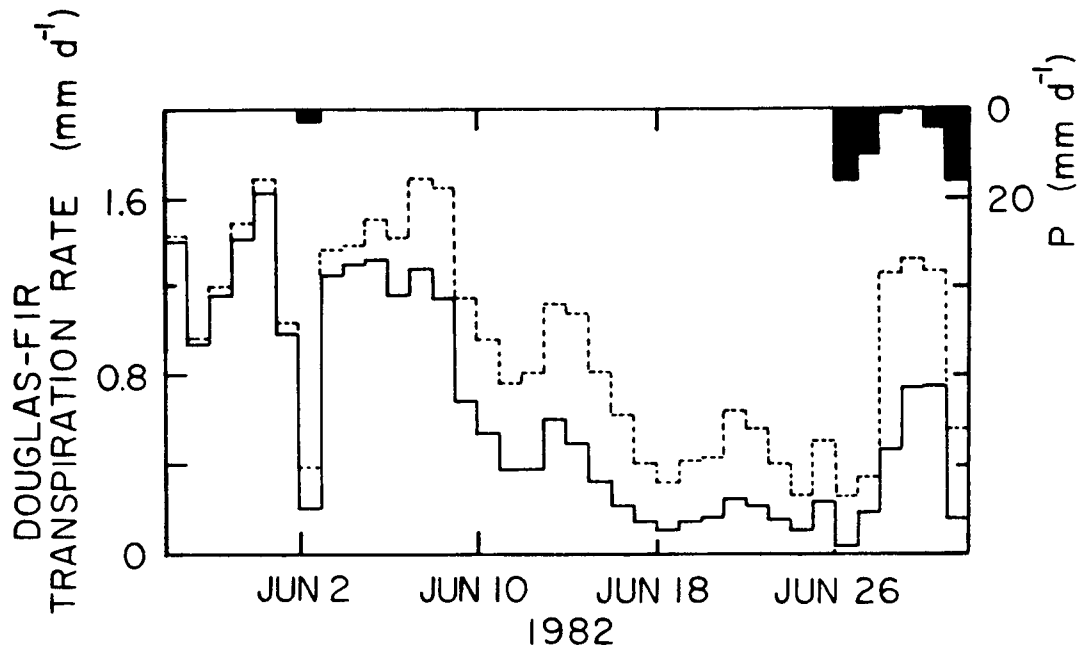


Figure 2.9 Same as for Fig. 2.8 except for May 27 - July 1, 1982.

During the 1981 and 1982 periods, salal removal resulted in an average increase in tree transpiration rate of 31 and 52% respectively in the four plots. These results agree with the conclusion in Chapter 1 that salal removal resulted in an average increase in tree transpiration rate of 30 and 58% in 1981 and 1982 based on r_s measurements. Calculations indicate that the increase in tree transpiration rate was greatest in plot 3 where salal leaf area index (3 and 2.4 in 1981 and 1982 respectively) was highest and was least in plot 4 where salal leaf area index was lowest (2.1 and 1.7 in 1981 and 1982). Although salal leaf area index values in plot 1 were similar to those in plot 4, the larger tree in plot 1 (Douglas-fir leaf area index was 6 and 3.1 in plots 1 and 4 in 1981 (less by 10% in 1982)) responded more to salal removal than the small tree in plot 4.

Total calculated values of salal transpiration (plus forest floor evaporation below the salal) were about twice those of forest floor evaporation after salal removal in the 1981 and 1982 periods. The above difference largely accounts for the increased tree transpiration following salal removal since Douglas-fir interception in adjacent subplots was identical and salal interception was a small term in the water balance.

5. CONCLUSIONS

Shuttleworth's evapotranspiration theory with canopy and root zone water balance models proved to be practical in calculating the courses of θ , ψ_s and tree transpiration during extended periods in the growing season. The difficulty in using the theory is in estimating the transfer resistances

(r_{si} , r_{bi} , r_{ai} and forest floor diffusive resistance) although r_{si} is often available from physiological studies. Simplifying the evapotranspiration theory when $W_i = 0$ by using the limit $r_{Ai} \rightarrow 0$ in (1) - (6) resulted in more understory transpiration being calculated because of the relatively closed forest canopy and an underestimation of the courses of θ , Ψ_s and tree transpiration in uncut subplots. This simplification resulted in little change in cut subplots since r_{Ai} is much smaller than r_{si} for Douglas-fir.

Calculations showed that the slightly higher values of θ as a result of understory removal corresponded to significantly higher tree transpiration rates. During early (June 1982) and late (August 1981) growing season drying periods, most of difference in tree transpiration occurred during the latter one-half of the period owing to the steepness of the soil water retention curve for low values of θ and stomatal closure by Douglas-fir where salal remained. Increase in tree transpiration as a result of understory removal was greatest where understory leaf area index was highest and trees were largest.

6. REFERENCES

- Black, T.A., C.B. Tanner and W.R. Gardner. 1970. Evapotranspiration from a snap bean crop. *Agron. J.* 62: 66-69.
- Denmead, O.T. 1984. Plant physiological methods for studying evapotranspiration: Problems of telling the forest from the trees. *Agric. Wat. Mgt.* 8: 167-189.
- Finnegan, J.J. 1985. Turbulent transport in flexible plant canopies. pp. 443-480. In: B.A. Hutchison and B.B. Hicks (eds.) *The Forest-Atmosphere Interaction*. D. Reidel Publ. Co., Boston.
- Fuchs, M. and C.B. Tanner. 1968. Calibration and field test of heat flux plates. *Soil Sci. Soc. Am. Proc.* 32: 326-328.

- Garratt, J.R. and B.B. Hicks. 1973. Momentum, heat and water vapour transfer to and from natural and artificial surfaces. *Quart. J. R. Met. Soc.* 99: 680-687.
- Gates, D.M. 1980. *Biophysical Ecology*. Springer-Verlag, New York.
- Jarvis, P.G., G.B. James and J.J. Landsberg. 1976. Coniferous forest. pp. 171-240. In: J.L. Monteith (ed.) *Vegetation and the Atmosphere*. Vol. 2, Case Studies, Academic Press, New York.
- Landsberg, J.J. and D.B.B. Powell. 1973. Surface exchange characteristics of leaves subject to mutual interference. *Agric. Met.* 12: 169-184.
- Lindroth, A. 1984. Seasonal variation in pine forest evaporation and canopy conductance. Ph.D. thesis, Univ. of Uppsala, Uppsala, Sweden.
- Monteith, J.L. 1965. Evaporation and environment. *Symp. Soc. Exp. Biol.* XIX: 205-234.
- Novak, M.D. and T.A. Black. 1985. Theoretical determination of the surface energy balance and thermal regime of bare soils. *Boundary-Layer Met.* (in press).
- Plamondon, A.P. 1972. Hydrologic properties and water balance of the forest floor of a Canadian west coast watershed. Ph.D. thesis, Univ. of B.C., Vancouver, B.C.
- Raupach, M.R. and A.S. Thom. 1981. Turbulence in and above plant canopies. *Ann. Rev. of Fluid Mech.* 13: 97-129.
- Roberts, J. C.F. Pymar, J.S. Wallace and R.M. Pitman. 1980. Seasonal changes in leaf area, stomatal conductance and transpiration from bracken below a forest canopy. *J. Appl Ecol.* 17: 409-422.
- Rutter, A.J., K.A. Kershaw, P.C. Robins and A.J. Morton. 1971. A predictive model of rainfall interception in forests, 1. Derivation of the model from observations in a plantation of Corsican pine. *Agric. Met.* 9: 367-384.
- Santantonio, D., R.K. Herman and W.S. Overton. 1977. Root biomass studies in forest ecosystems. *Pedobiol.* 17: 1-31.
- Shuttleworth, W.J. 1978. A simplified one-dimensional theoretical description of the vegetation-atmosphere interaction. *Boundary-Layer Met.* 14: 3-27.
- Shuttleworth, W.J. 1979. Below-canopy fluxes in a simplified one-dimensional theoretical description of the vegetation-atmosphere interaction. *Boundary-Layer Met.* 17: 315-331.
- Spittlehouse, D.L. 1981. Measuring and modelling forest evapotranspiration. Ph.D. thesis, Univ. of B.C., Vancouver, B.C.

- Spittlehouse, D.L. and T.A. Black. 1980. Evaluation of the Bowen ratio/energy balance method for determining forest evapotranspiration. *Atmos-Ocean* 18: 98-116.
- Spittlehouse, D.L. and T.A. Black. 1981. A growing season water balance model applied to two Douglas-fir stands. *Water Resour. Res.* 17: 1651-1656.
- Spittlehouse, D.L. and T.A. Black. 1982. A growing season water balance model used to partition water use between trees and understory. pp. 195-214. In: *Proc. Can. Hydrol. Symp. 82, Hydrol. processes in for. areas.* June 14-15, 1982, Fredericton, N.B.
- Stanhill, G. 1969. A simple instrument for the field measurement of turbulent diffusion flux. *J. Appl. Met.* 8: 509-513.
- Stewart, J.B. and A.S. Thom. 1973. Energy budgets in a pine forest. *Quart. J. R. Met. Soc.* 99: 154-170.
- Szeicz, G., G. Endrodi and S. Tajchman. 1969. Aerodynamic and surface factors in evaporation. *Water Resour. Res.* 5: 380-394.
- Tan, C.S. and T.A. Black. 1976. Factors affecting the canopy resistance of a Douglas-fir forest. *Boundary-Layer Met.* 10: 475-488.
- Tan, C.S., T.A. Black and J.U. Nnyamah. 1977. Characteristics of stomatal diffusion resistance in a Douglas-fir forest exposed to soil water deficits. *Can. J. For. Res.* 7: 595-604.
- Tan, C.S., T.A. Black and J.U. Nnyamah. 1978. A simple diffusion model of transpiration applied to a thinned Douglas-fir stand. *Ecol.* 59: 1221-1229.
- Thom, A.S. 1972. Momentum, mass and heat exchange of vegetation. *Quart. J. R. Met. Soc.* 98: 124-134.
- Thom, A.S. 1975. Momentum, mass and heat exchange of plant communities. pp. 57-109. In: J.L. Monteith (ed.) *Vegetation and atmosphere. Vol.1, Principles*, Academic Press, New York.
- Van Wijk, W.R. and D.A. De Vries. 1963. Periodic temperature variation. pp. 102-143. In: W.R. Van Wijk (ed.) *Physics of Plant Environment*. North Holland Publishing Co., Amsterdam.

CONCLUSIONS

Salal understory removal resulted in little change in the growing season course of θ because E was only slightly higher where salal was present than where it had been removed. The slight increase in θ where salal had been removed corresponded to significantly higher Ψ_s at low values of θ owing to the steepness of the soil water retention curve. This resulted in significantly greater tree water use and diameter growth where salal had been removed than where it remained.

Shuttleworth's evapotranspiration theory when modified for use in hypostomatous canopies and combined with canopy and root zone water balance equations proved to be practical in calculating the courses of θ , Ψ_s and tree transpiration over extended growing season periods. The difficulty in using the theory is in estimating the transfer resistances (r_{si} , r_{bi} , r_{ai} , and forest floor diffusive resistance). Simplifying the theory when $W_1 = 0$ by using the limit $r_{Ai} \rightarrow 0$ resulted in an overestimate of understory transpiration and an underestimate of θ , Ψ_s and tree transpiration in uncut subplots. This simplification resulted in little change in the calculations for cut subplots. Calculations showed that most of the salal removal effect to increase tree transpiration occurred during the final one-half of drying periods owing to the steepness of the retention curve at low values of θ leading to stomatal closure and a reduction in tree transpiration where salal remained. Increases in tree transpiration rates as a result of salal removal were calculated to be greatest where salal leaf area index was highest and trees were largest.

The evapotranspiration theory was developed for extensive homogeneous surfaces so that its use in the cut subplots included employment of below-tree-canopy values of D and T_{air} largely determined by the presence of salal in the surrounding forest. Values of below-tree-canopy D and T_{air} would be expected to be higher following extensive salal removal; however, it is difficult to estimate the magnitude of the increase. McNaughton and Jarvis (1983) show that the D above a conifer forest canopy is likely to be well coupled to the outer mixed portion of the planetary boundary layer. Consequently, they argue that a 50% reduction in forest leaf area index would not result in an increase in above-forest D and therefore would result in a significant reduction in forest E . Since D below the tree canopy in this study was well correlated to that above (in agreement with the results reported by Stewart (1984) for Thetford forest), it is probable that only a slight increase in below-tree-canopy D would result from extensive salal removal. The mechanism for this below to above-tree-canopy D coupling may be attributed to the gust penetration phenomenon observed in the Uriarra forest by Bradley et al. (1985). Recent experimental evidence from 30 m by 40 m plots in a similar Douglas-fir forest about 130 km south of the experimental site also showed little change in the growing season course of θ and that E was only slightly higher where salal was present than where it had been removed (Black et al. 1985).

Operational removal of salal understory would likely require the use of herbicides as regrowth could be considerable. At the end of the first and second year following salal understory removal in a 50 m² area adjacent to the four plots, salal leaf area index was 1.0 and 1.6 (originally, it was 3.7). Alternatively, Black and Spittlehouse (1981) suggested that, for dry sites with salal understory, the ratio of Douglas-fir to stand transpiration

(including salal understory) may be increased by increasing stocking density. In young Douglas-fir stands close to and including the one used in this study, increased stand basal area corresponded to decreased salal understory leaf area index (Fig. C.1) and increased salal leaf size (Fig. C.2). The former result would directly decrease the amount of salal transpiration while the latter, when combined with the likely decreased below-tree-canopy wind speeds in the denser tree stands, would tend to increase salal r_{bi} and thus decrease salal transpiration. The results of this study indicate that on dry, salal-dominated sites where salal control is not feasible, tree water use and wood production may be jeopardized in low density stands.

REFERENCES

- Black, T.A. and D.L. Spittlehouse. 1981. Modeling the water balance for watershed management. pp. 117-129. In: D.M. Baumgartner (ed.) Proc. symp. interior west watershed mgt. Apr. 8-10, 1980, Spokane, WA, U.S.A.
- Black, T.A., D.T. Price, P.M. Osberg and D.G. Giles. 1985. Effect of reduction of salal competition on evapotranspiration and growth of early stage Douglas-fir plantations. Contract Research Report to Research Branch, British Columbia Min. of For., Victoria, B.C.
- Bradley, E.F., O.T. Denmead and G.W. Thurtell. 1985. Measurements of turbulence and heat and moisture transport in a forest canopy. Quart. J. Roy. Met. Soc. (in preparation).
- McNaughton, K.G. and P.G. Jarvis. 1982. pp. 1-47. In: T.T. Kozlowski (ed.). Water Deficits and Plant Growth, Vol. VII. Academic Press, New York.
- Stewart, J.B. 1984. Measurement and prediction of evaporation from forested and agricultural catchments. Agric. Water Mgt. 8: 1-28.

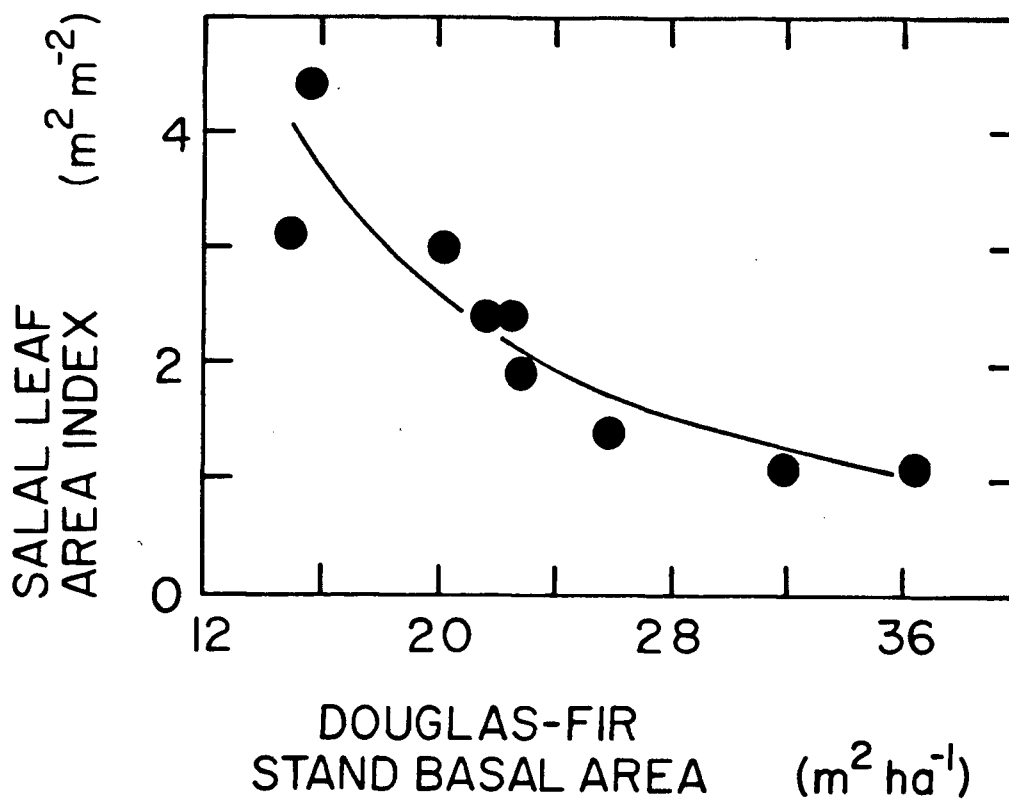


Figure C.1

Relationship between salal leaf area index and Douglas-fir stand basal area in 31-36 year old stands close to and including the one at the experimental site. The curve indicates salal leaf area index = $288 (\text{Douglas-fir stand basal area } (\text{m}^2 \text{ ha}^{-1}))^{-1.57}$ ($R^2 = 0.89$).

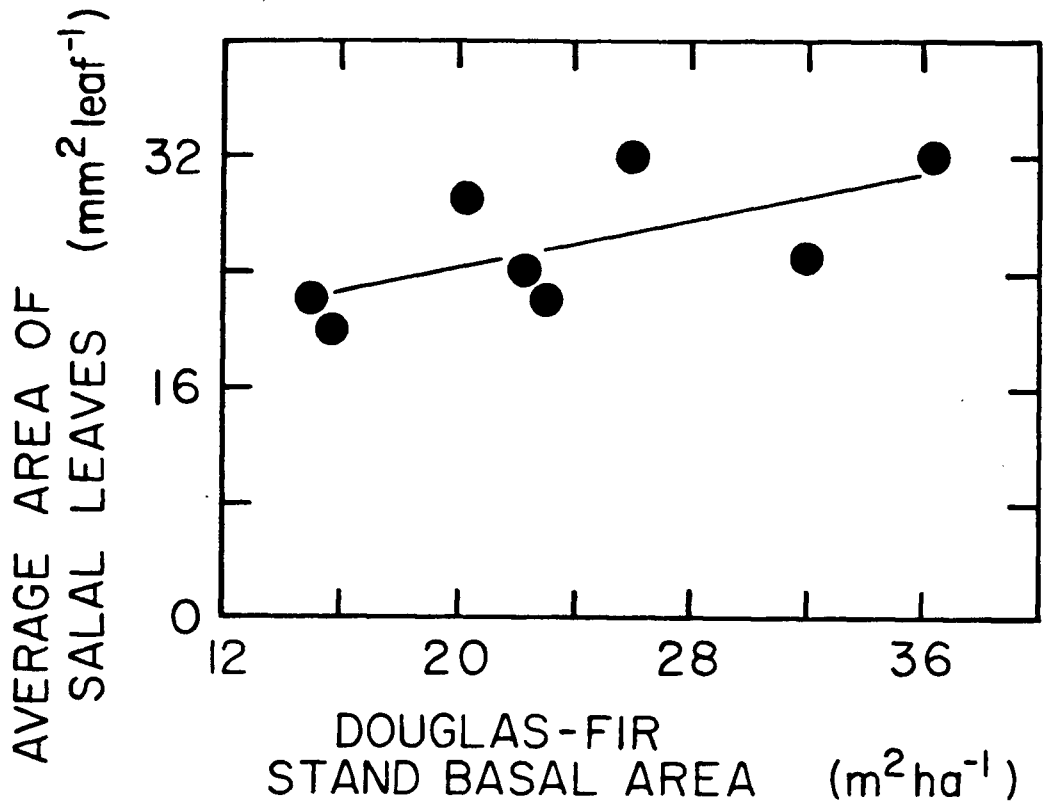


Figure C.2

Relationship between the average area of salal leaves and Douglas-fir stand basal area in 31-36 year old stands close to and including the one at the experimental site. The line indicates average area of salal leaves (mm² leaf⁻¹) = 0.41 (Douglas-fir stand basal area (m² ha⁻¹)) + 16 (R² = 0.41).

APPENDIX I

DERIVATION OF EQUATION (1) IN CHAPTER 2

Appendix I

DERIVATION OF EQUATION (1) IN CHAPTER 2

The derivation is essentially the same as that given in Shuttleworth (1979) (p. 321). Applying Ohm's Law to the electrical analog of the model for canopy layer i shown in Fig. AI.1, the relationships between fluxes and resistances can be written as

$$T_i - T_{i-1} = -Hr_{aHi}/\rho c_p \quad (\text{AI.1})$$

$$T_{i-1} - T_{Si}^e = -(H_i - H_{i-1})(r_{H1}/2a_i)/\rho c_p \quad (\text{AI.2})$$

$$e_i - e^*(T_{Si}^e) = -(LE_i r_{aVi} \gamma / \rho c_p) - (LE_i - LE_{i-1}) (r_{ci} + (r_{Vi}/2a_i)) \gamma / \rho c_p \quad (\text{AI.3})$$

where T_{Si}^e , the effective temperature of the leaves in layer i , can be calculated by substituting (AII.1), (AII.20) (see Appendix II) and the sensible heat transfer equation into the energy balance equation for the layer.

Using the Penman transformation, we have

$$e_i - e^*(T_{Si}^e) = D_i + s(T_i - T_{i-1}) + s(T_{i-1} - T_{Si}^e) \quad (\text{AI.4})$$

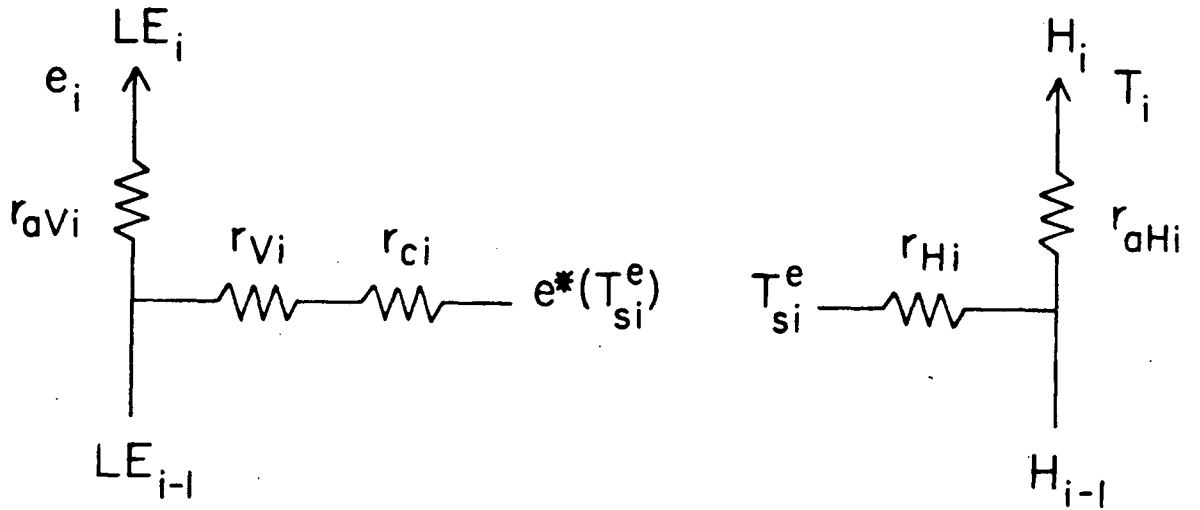


Figure AI.1 Electrical analog depicting the transfer of latent and sensible heat fluxes for a single canopy layer i (LE_i and H_i) where T_{si}^e is the "effective" surface temperature of the layer (i.e. wet and dry portions) and other symbols have been previously defined. The depiction shows the identical leaf, single source limit of the Penman-Monteith equation described by Shuttleworth (1979).

where, since $T_{S1}^e - T_1$ is not large, the same value of s is used for both temperature differences. The energy balance equation for all layers 1 to i (neglecting energy storage) is

$$R_{ni} - G = H_i + LE_i \quad (\text{AI.5})$$

Substituting (AI.1), (AI.2) and (AI.3) into (AI.4), using (AI.5) and dividing by L , we have

$$E_i = \frac{s(R_{ni} - G) + \rho c_p (D_i + \delta'_i) / r_{AHi}}{L(s + \gamma(r_{AVi} / r_{AHi})(1 + (r_{ci} / r_{AVi})))} \quad (\text{AI.6})$$

where

$$\delta'_i = [LE_{i-1}[(r_{ci} + (r_{Vi} / 2a_i))\gamma + (r_{Hi} / 2a_i)s] - s(R_{ni-1} - G)(r_{Hi} / 2a_i)] / \rho c_p, \quad (\text{AI.7})$$

$$r_{AHi} = r_{Hi} / 2a_i + r_{aHi}$$

and

$$r_{AVi} = r_{Vi} / 2a_i + r_{aVi}$$

Equation (AI.6) is the same as (9) in Shuttleworth (1979) . Subtracting E_{i-1} from (AI.6) and assuming similarity (i.e. $r_{Hi} = r_{Vi}$ and $r_{aHi} = r_{aVi}$) gives (1).

APPENDIX II

DERIVATION OF THE EQUATION FOR r_c SHOWING DEPENDENCE
ON THE FRACTION OF WET LEAF AREA

APPENDIX II

DERIVATION OF THE EQUATION FOR r_c SHOWING DEPENDENCE

ON THE FRACTION OF WET LEAF AREA

The Penman-Monteith equation for a canopy is

$$LE = \frac{s(R_n - G) + \rho c_p D_o / r_{Ha}}{s + \gamma r_{Va} / r_{Ha} (1 + (r_c / r_{Va}))} \quad (\text{AII.1})$$

This is the combination equation for the latent heat flux from an extended isothermal flat leaf with one side having boundary layer resistances r_{Ha} and r_{Va} to sensible heat and vapour transfer respectively and a canopy or surface resistance r_c to vapour transfer. If $r_{Ha} = r_{Va}$

$$LE = \frac{s(R_n - G) + \rho c_p D_o / r_{Ha}}{s + \gamma (1 + (r_c / r_{Ha}))} \quad (\text{AII.2})$$

The latent heat flux on a ground area basis from a canopy with a projected leaf area index (a) and a fraction of the leaf area wet (W) can be written as

$$LE = Wa \left[\frac{s(R_n - G)/a + \rho c_p D_o / r_{HTOT}}{s + \gamma r_{VTOT} / r_{HTOT}} \right] + (1-W) a \left[\frac{s(R_n - G)/a + \rho c_p D_o / r_{HTOT}}{s + \gamma r_{VTOT} / r_{HTOT}} \right] \quad (\text{AII.3})$$

The first bracketed term of (AII.3) is the evaporation rate from the average wet leaf on a projected leaf area basis, the second bracketed term is the transpiration rate from the average dry leaf on a projected leaf area basis. The resistances are defined as

$$r_{HTOT}^{-1} = r_{HTOP}^{-1} + r_{HBTOT}^{-1} = 2/r_H, \quad (\text{AII.4})$$

$$r'_{VTOT}^{-1} = r_{VTOP}^{-1} + r_{VBTOT}^{-1} = 2/r_V, \quad (\text{AII.5})$$

$$r_{VTOT}^{-1} = (r_{VTOP} + r_{STOP})^{-1} + (r_{VBTOT} + r_{SBOT})^{-1}, \quad (\text{AII.6})$$

where TOP, BOT and TOT refer to top, bottom and total respectively.

Equation (AII.3) can be rewritten as

$$\begin{aligned} LE = W & \left[\frac{s(R_n - G) + \rho c_p D_o / (r_{HTOT}/a)}{s + \gamma r'_{VTOT} / r_{HTOT}} \right] \\ + (1-W) & \left[\frac{s(R_n - G) + \rho c_p D_o / (r_{HTOT}/a)}{s + \gamma r_{VTOT} / r_{HTOT}} \right] \end{aligned} \quad (\text{AII.7})$$

In order that (AII.3) can be rewritten in the form of (AII.1) by making r_c a function of W , we require

$$r_{Ha} = r_{HTOT}/a = r_H/(2a) \quad (\text{AII.8})$$

and

$$\frac{1}{s + \gamma r_{Va}/r_{Ha}(1 + (r_c/r_{Va}))} = \frac{W}{s + \gamma r'_{VTOT}/r_{HTOT}} + \frac{1-W}{s + \gamma r_{VTOT}/r_{HTOT}} \quad (\text{AII.9})$$

Solving for r_c we have

$$r_c = \left[\frac{W}{(s/\gamma)r_{Ha} + r'_{VTOT}/a} + \frac{1-W}{(s/\gamma)r_{Ha} + r_{Vsa}} \right]^{-1} - (s/\gamma)r_{Ha} - r_{Va} \quad (\text{AII.10})$$

where

$$r_{Vsa} = r_{VTOT}/a \quad (\text{AII.11})$$

In order that $r_c = 0$, when $W = 1$, r_{Va} must be

$$r_{Va} = r'_{VTOT}/a = r_v/(2a) \quad (\text{AII.12})$$

Substituting (AII.12) into (AII.10) we have

$$r_c = \left[\frac{W}{(s/\gamma)r_{Ha} + r_{Va}} + \frac{1-W}{(s/\gamma)r_{Ha} + r_{Vsa}} \right]^{-1} - (s/\gamma)r_{Ha} - r_{Va} \quad (\text{AII.13})$$

with the resistances given by (AII.8), (AII.11) and (AII.12).

For amphistomatous leaves, r_{VTOT} is given by (AII.6), but if $r_{sTOP} =$

$r_{sBOT} = r_s$ and $r_{VTOP} = r_{VBOT} = r_v$, so that

$$r_{VTOT} = (r_v + r_s)/2 \quad (AII.14)$$

then

$$r_{Vsa} = (r_v + r_s)/(2a) \quad (AII.15)$$

For hypostomatous leaves with, say, $r_{sTOP} = \infty$ and $r_{sBOT} = r_s$, then from (AII.6)

$$r_{VTOT} = r_v + r_s \quad (AII.16)$$

so that

$$r_{Vsa} = (r_v + r_s)/a \quad (AII.17)$$

When $W = 1$, $r_c = 0$ for both leaf types. When $W = 0$, r_c for the amphistomatous leaf is

$$r_c = r_s/2a \quad (AII.18)$$

while for the hypostomatous leaf it is

$$r_c = r_s/a + r_v/2a \quad (AII.19)$$

which is the sum of the average stomatal resistance and average boundary layer resistance of the canopy. Equation (AII.19) is correct since without the boundary layer resistance term, halving r_s of the hypostomatous leaf would result in the same transpiration as that of an amphistomatous leaf

with the same initial r_s (see Appendix III). In the hypostomatous leaf all vapour has to go through a single r_v (one side) rather than two r_v 's in parallel as in the amphistomatous case. In summary, r_c , as defined by (AII.1), for the hypostomatous Douglas-fir canopy of this study can be written as follows (after substituting (AII.8), (AII.12) and (AII.17) into (AII.10))

$$r_c = \left[\frac{W}{(s/\gamma)r_H/(2a) + r_v/(2a)} + \frac{1 - W}{(s/\gamma)r_H/(2a) + (r_v + r_s)/a} \right]^{-1} - (s/\gamma)r_H/(2a) - r_v/(2a) \quad (\text{AII.20})$$

where r_H , r_v and r_s are the one-sided resistances of the leaf. Note we have made the reasonable assumption that the bottom and top boundary layer resistances are equal in (AII.4) and (AII.5).

APPENDIX III

RELATIONSHIP BETWEEN STOMATAL RESISTANCES OF
AMPHISTOMATOUS AND HYPOSTOMATOUS LEAVES THAT
RESULTS IN EQUAL TRANSPIRATION RATES

APPENDIX III

RELATIONSHIP BETWEEN STOMATAL RESISTANCES OF AMPHISTOMATOUS AND
HYPOSTOMATOUS LEAVES THAT RESULTS IN EQUAL TRANSPIRATION RATES

This appendix derives the expression for the stomatal resistance of an amphistomatous leaf in terms of that of a hypostomatous leaf which would result in equal transpiration rates for the two leaves. Following Monteith (1973), LE from an isothermal leaf can be estimated from the Penman-Monteith equation written as

$$LE = \frac{s(R_n - G) + \rho c_p D / (r_H / 2)}{s + n\gamma r_V / r_H (1 + r_s / r_V)} \quad (\text{AIII.1})$$

where $n = 1$ or 2 for amphistomatous ($r_{sTOP} = r_{sBOT} = r_s$) or hypostomatous leaves, respectively. Assuming $r_V = r_H$, (AIII.1) can be written for amphistomatous leaves as

$$LE = \frac{s(R_n - G) + \rho c_p D / (r_H / 2)}{s + \gamma(1 + (r_{sa} / 2) / (r_H / 2))} \quad (\text{AIII.2})$$

and for hypostomatous leaves as

$$LE = \frac{s(R_n - G) + \rho c_p D / (r_H / 2)}{s + \gamma(1 + (r_{sh} + r_H / 2)) / (r_H / 2)} \quad (\text{AIII.3})$$

where r_{sa} and r_{sh} are the stomatal resistances of amphistomatous and hypostomatous leaves respectively. Comparing (AIII.2) and (AIII.3), we see that for transpiration rates for the two leaves to be equal

$$r_{sa}/2 = r_{sh} + r_H/2 \quad (\text{AIII.4})$$

or

$$r_{sa} = 2r_{sh} + r_H. \quad (\text{AIII.5})$$

If the amphistomatous leaf equation is used to calculate LE from a hypostomatous leaf, the stomatal resistance of this "equivalent" amphistomatous leaf must be calculated using (AIII.5).

REFERENCES

Monteith, J.L. 1973. Principles of environmental physics. American Elsevier Publ. Co., Inc., New York.

APPENDIX IV

DERIVATION OF EQUATION (5) IN CHAPTER 2

APPENDIX IV

DERIVATION OF EQUATION (5) IN CHAPTER 2

The water vapour flux density from layer i (E'_i) with leaf area (one side) index (a_i) within a multilayer forest canopy of hypostomatous leaves is given by

$$E'_i = \frac{s(R_{ni} - R_{ni-1}) + \rho c_p D_{i-1}/(r_{Hi}/2a_i)}{L(s + \gamma(r_{Vi}/r_{Hi})(1 + r_{ci}/(r_{Vi}/2a_i))} \quad (\text{AIV.1})$$

where D_{i-1} is the vapour pressure deficit within the layer (i.e. at the effective "source" height). This can be obtained by setting $r_{ai} = 0$ (e.g. $r_{aHi} = r_{aVi} = 0$) in (1), (2) and (3) of Chapter 2. The rate of evaporation of intercepted water from layer i (E'_{Ii}) is obtained by multiplying the fraction of leaf area (one side) that is completely wet (W_i) by (AIV.1) with $r_{ci} = 0$ which gives

$$E'_{Ii} = \frac{W_i[s(R_{ni} - R_{ni-1}) + \rho c_p D_{i-1}/(r_{Hi}/2a_i)]}{L(s + \gamma(r_{Vi}/r_{Hi}))} \quad (\text{AIV.2})$$

Dividing (AIV.2) by (AIV.1), assuming similarity (i.e. $r_{Hi} = r_{Vi} = r_{bi}$), making use of (4) and rearranging gives (5).

APPENDIX V

ELECTRICAL ANALOGS OF THE LATENT AND SENSIBLE HEAT FLUXES
IN UNCUT AND CUT SUBPLOTS

APPENDIX V

ELECTRICAL ANALOGS OF THE LATENT AND SENSIBLE HEAT FLUXES

IN UNCUT AND CUT SUBPLOTS

The purpose of this appendix is to present electrical analogs depicting the transfer of latent and sensible heat fluxes for uncut and cut subplots (Figs. AV.1 and AV.2). The forest canopy was divided into two layers ($n = 2$) where the Douglas-fir subcanopy was designated as layer 2 and the salal subcanopy as layer 1 (the forest floor was layer 0). Individual leaves were considered either completely wet or completely dry so that wet and dry leaves had different surface temperatures (T_{S1}^w and T_{S1}^d). For cut subplots, forest floor aerodynamic resistances were estimated by r_{aV1} and r_{aH1} .

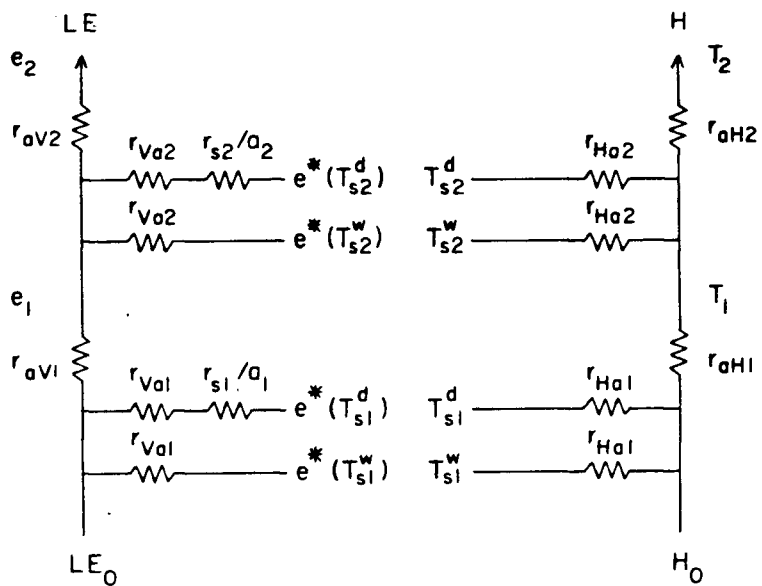


Figure AV.1 Electrical analog depicting the transfer of latent and sensible heat fluxes in an uncut subplot.

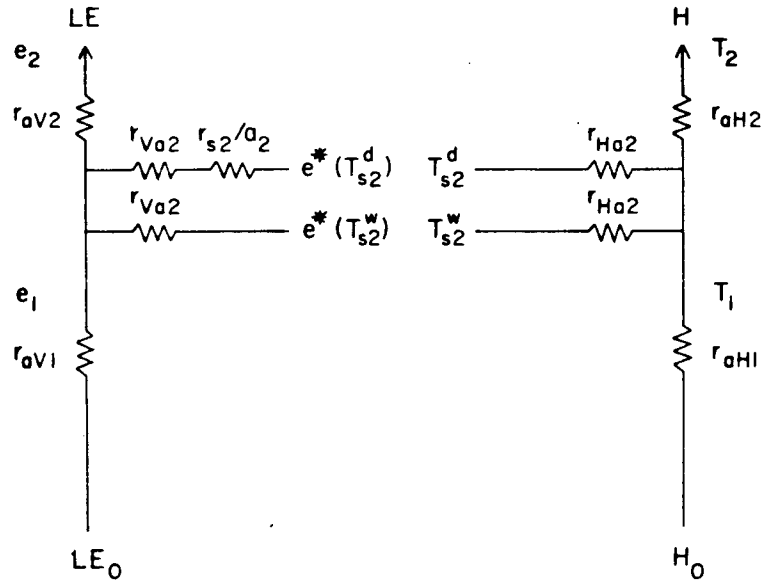


Figure AV.2 Same as for Fig. AV.1 except for cut subplot.

APPENDIX VI

UNDERSTORY REMOVAL EFFECTS ON THE BELOW-TREE-CANOPY RADIATION REGIME

APPENDIX VI

UNDERSTORY REMOVAL EFFECTS ON THE BELOW-TREE-CANOPY RADIATION REGIME

1. INTRODUCTION

The radiation balance below the tree canopy is important in determining the rate of soil evaporation and the transpiration rate of understory vegetation. In this appendix, below-tree-canopy radiation data collected as part of the salal understory removal experiment from July 24-September 1, 1981 and July 30-September 1, 1982 are presented. Sky view factors determined from photographs taken with a fish eye lens are also presented.

2. METHODS

1. Radiation Measurements

Net radiation and solar irradiance above the forest (R_{na} and $K\downarrow_a$) were measured using a Swissteco S-1 net radiometer and Kipp and Zonen pyranometer located on top of a 15 m tall tower. In 1981, hourly average values of net radiation below the tree canopy (R_{nb}) were measured in one of the four plots (plot 2) using one net radiometer above the salal canopy and another above the forest floor surface, where salal had been removed. Measurements of solar irradiance below the tree canopy ($K\downarrow_b$) were also made in 1981 with a pyranometer located next to the net radiometer over the forest floor surface.

In 1982, R_{nb} and $K\uparrow_b$ were measured using a net radiometer and pyranometer mounted on a tram travelling at a rate of about 0.5 m min^{-1} at the 1 m height along a 10 m path where salal along a portion of the path had been removed. Measurements of R_{na} , R_{nb} , $K\uparrow_a$ and $K\uparrow_b$ were made every 2 seconds and 10 second average values were recorded using a Campbell Scientific CR-21 data logger.

A control circuit for the tram provided a positive or negative voltage indicating the direction of travel by the tram. This voltage was also recorded every 10 seconds using the data logger. A negative voltage indicated that the tram was traversing to the west (i.e. to the cut (salal cut and removed) portion of the path) while a positive voltage indicated the reverse (i.e. to the uncut portion of the path). A change in the sign of the voltage indicated that the tram had just passed one end of the path and had reversed its direction toward the other end. Using the rate and direction of travel and the time when the tram passed the end of the path, periods were designated when the tram passed over the cut and uncut portions of the path. This was the period when the tram was located between a 1 m buffer east (uncut) or west (cut) of the cut/uncut border and the end of the path. The tram travelled over the cut or uncut portion of the path twice during the period, going to and from the end of the path. The period was about 13 minutes for the cut portion (distance from west end of path to cut/uncut border was 4.2 m) and about 19 minutes for the uncut portion (distance from east end of path to the cut/uncut border was 5.8 m).

On September 1, 1982, the tram was run in conjunction with a net radiometer next to the tram path in the cut portion. All radiation measurements on this day were made every two seconds and recorded by the data logger as 10 second average values.

2. Determination of Sky View Factors

The view factor V_{12} is defined as follows:

$$q_{12} = V_{12}A_1\epsilon_1 \quad (\text{AVI.1})$$

where q_{12} is the flux emitted by area A_1 toward area A_2 , and ϵ_1 is the emittance of A_1 and V_{12} is the fraction of $A_1\epsilon_1$ that is intercepted by A_2 or the fraction of the view by A_1 that is occupied by A_2 . The general expression for V_{12} can be obtained as follows:

$$dq_{12} = I_1 dA_1 \cos \phi d\omega \quad (\text{AVI.2})$$

where ϕ is the angle between the normal to dA_1 and the straight line connecting dA_1 and dA_2 , $d\omega$ is the small solid angle given by dA_2 divided by the square of the distance between dA_1 and dA_2 , and I_1 is the radiance from A_1 which is related to ϵ_1 by (Reifsnyder 1967):

$$I_1 = \epsilon_1/\pi \quad (\text{AVI.3})$$

so that

$$dq_{12} = (\epsilon_1/\pi)dA_1 \cos \phi d\omega \quad (\text{AVI.4})$$

Integrating over A_1 and A_2 we have

$$q_{12} = (\epsilon_1/\pi) \int_{A_1} \int_{A_2} dA_1 \cos \phi d\omega \quad (\text{AVI.5})$$

Assuming A_1 is small,

$$q_{12} = A_1 \epsilon_1 \int_{A_2} \cos \phi d\omega/\pi \quad (\text{AVI.6})$$

From (AVI.1) we see that

$$V_{12} = \int_{A_2} \cos \phi d\omega/\pi \quad (\text{AVI.7})$$

as given in (6) of Reifsnnyder (1967).

A hemisphere of radius r_0 can be constructed over a small area on the forest floor (dA_1) (Fig. AVI.1) to give the forest floor-sky view factor (V_{fs})

$$V_{fs} = \int_{\phi=0}^{\pi/2} \int_{\alpha=0}^{2\pi} \cos \phi f(\phi, \alpha) r_0 \sin \phi d\alpha r_0 d\phi / (\pi r_0^2) \quad (\text{AVI.8})$$

where α is the azimuthal angle, $f(\phi, \alpha)$ is the fraction of dA_2 not obscured by the forest canopy and $d\omega$ is replaced by dA_2/r_0^2 . Taking $\bar{f}(\phi)$ to be an average non-obscuration fraction for an entire annulus ($0 < \alpha < 2\pi$), (AVI.8) can be rewritten as:

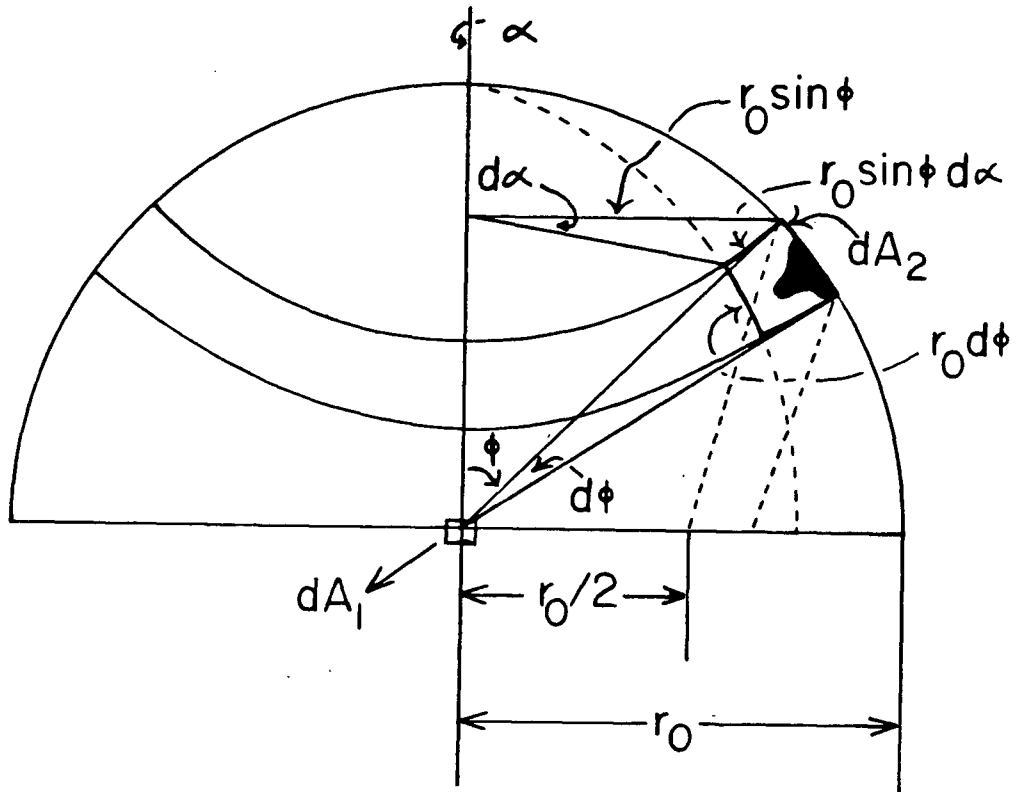


Figure AVI.1 Construction of a hemisphere of radius r_0 over a small area of forest floor (dA_1). The angle ϕ between the normal to dA_1 and the straight line connecting dA_1 and a small area on the hemisphere (dA_2) is $\pi/4$ radians. Using the azimuthal angle α and the derived geometric relationships shown in this figure, $dA_2 = r_0 \sin \phi \, d\alpha \, r_0 \, d\phi$. The partial obscuration of dA_2 indicates the forest canopy.

$$V_{fs} = 2 \int_{\phi=0}^{\pi/2} \bar{f}(\phi) \cos \phi \sin \phi \, d\phi \quad (\text{AVI.9})$$

An equiangular fish-eye lens projection results in an image of an object at an angle ϕ from the normal being located at a distance from the centre of the projection (r) defined by

$$r = 2\phi \, r_0 / \pi \quad (\text{AVI.10})$$

which indicates the proportionality between radial distance on the projection (photograph) and ϕ . Consequently,

$$d\phi = [\pi / (2r_0)] dr. \quad (\text{AVI.11})$$

Expressing (AVI.9) as a sum of n annuli (Steyn 1980) and using (AVI.10) and the finite difference form of (AVI.11) gives

$$V_{fs} = (\pi/r_0) \sum_{i=1}^n \bar{f}'(r_i) \cos(\pi/2(r_i/r_0)) \sin(\pi/2(r_i/r_0)) \Delta r_i \quad (\text{AVI.12})$$

where $\bar{f}'(r_i)$ ($\approx \bar{f}(\phi_i)$) is the average non-obscuration fraction for the annulus r_i , of width Δr_i , on the projection (eg. photograph). Using constant width annuli $\Delta r_i = \Delta r_0$, (AVI.12) becomes

$$V_{fs} = (\pi/\eta) \sum_{i=1}^n \bar{f}'(r_i) \cos(\pi/2(r_i/r_o)) \sin(\pi/2(r_i/r_o)) \quad (\text{AVI.13})$$

where $\eta = r_o/\Delta r_o$. The forest floor-canopy view factor (V_{fc}) is equal to $1 - V_{fs}$.

Photographs taken using an equiangular fish-eye lens were divided into three annuli $0-r_o/3$, $r_o/3-2/3r_o$ and $2/3r_o-r_o$ which correspond to the $0-30^\circ$, $30-60^\circ$ and $60-90^\circ$ zenith angles respectively. The midpoint of each range was taken as r for the annulus (i.e. $r_o/6$, $r_o/2$ and $5r_o/6$). The $0-r_o/3$ annulus was divided into nine equal size sectors while the $r_o/3-2/3r_o$ and $2/3r_o-r_o$ annuli were each divided into eighteen equal size sectors. Using a clear plastic sheet with the annuli and sectors marked on it (Fig. AVI.2) over the photograph (eg. Fig. AVI.3), the fraction of sky visible in each sector of the photograph was estimated by eye to 0.05 and the average value of all sectors in each annulus was taken as $\bar{f}'(r_i)$. The forest floor sky view factor was determined using (AVI.13).

Ten black and white photographs were taken with a fish eye lens (using Kodak PX-135 panchromatic film, 125 ASA) in the stand on November 23, 1983. Photographs were taken from about a 300 mm lens height at the locations of the 1981 R_{nb} measurements in plot 2 (i.e. two photographs), the centres of the three other plots and from about the 1 m height along the tram path (five photographs). Prints with a 78 mm diameter circular field were used in the analysis (Fig. AVI.3).

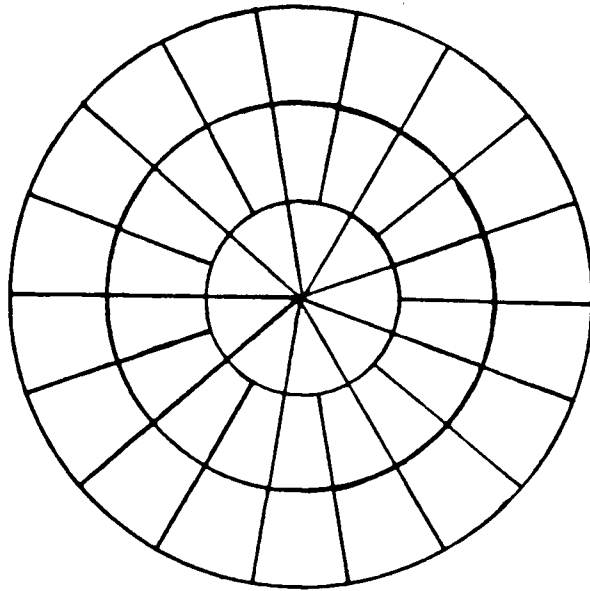


Figure AVI.2 Grid used for analyses of fish eye lens photographs of radius r_0 . The $0-r_0/3$ annulus of the grid was divided into nine equal size sectors while the $r_0/3 - 2r_0/3$ and $2r_0/3 - r_0$ annuli were each divided into eighteen equal size sectors.

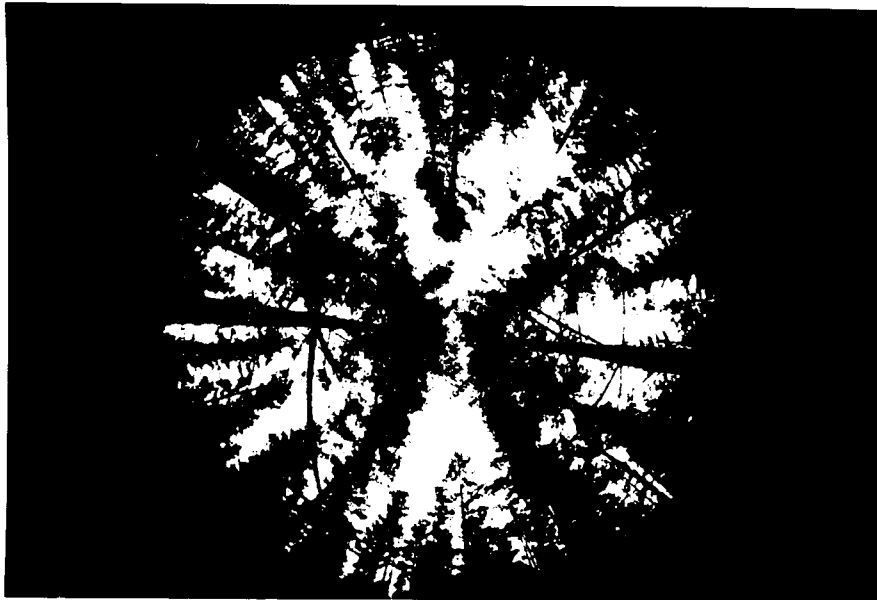


Figure AVI.3 Fish eye lens photograph taken at about the 300 mm height from the 1981 location of the net radiometer (below the tree canopy) in the cut subplot of plot 2 on November 23, 1983. The forest floor-sky view factor for this location was 0.28.

3. RESULTS

In August 1981, daily total R_{nb} in plot 2 was generally similar for the salal canopy (uncut subplot) and forest floor (cut subplot) except near the end of the month when it was very cloudy (Fig. AVI.4). The ratio R_{nb}/R_{na} was fairly constant during this period with the average values being 0.15 and 0.13 for the salal canopy and forest floor respectively. The sky view factor for the net radiometer over the salal canopy was slightly greater than that for the net radiometer over the forest floor (Table AVI.1). For the forest floor, there was little difference between values of R_{nb}/R_{na} and $K_{\downarrow b}/K_{\downarrow a}$ (Fig. AVI.4).

In 1982, daily total values of R_{nb} for the uncut portion of the tram path were usually slightly higher than for the cut portion (Table AVI.2). The sky view factor and values of $K_{\downarrow b}/K_{\downarrow a}$ for the uncut portion of the tram path were also higher than for the cut portion (Tables AVI.1 and AVI.2). On two clear days (August 7 and 18), R_{nb}/R_{na} and $K_{\downarrow b}/K_{\downarrow a}$ were significantly higher in the uncut portion. Average values of the ratio $K_{\downarrow b}/K_{\downarrow a}$ (i.e. below-tree-canopy albedo) for August 10-19 were 0.28 and 0.19 for the salal canopy and forest floor respectively. There was a downward trend in the values of R_{nb}/R_{na} and $K_{\downarrow b}/K_{\downarrow a}$ from July 30-September 1. The zenith angle of the sun at noon decreased from 31° on July 30 to 42° on September 1 (List 1971). However, the average values of R_{nb}/R_{na} for the uncut and cut portions of the tram path (0.16 and 0.14, respectively) were very similar to those values obtained in 1981 using stationary net radiometers.

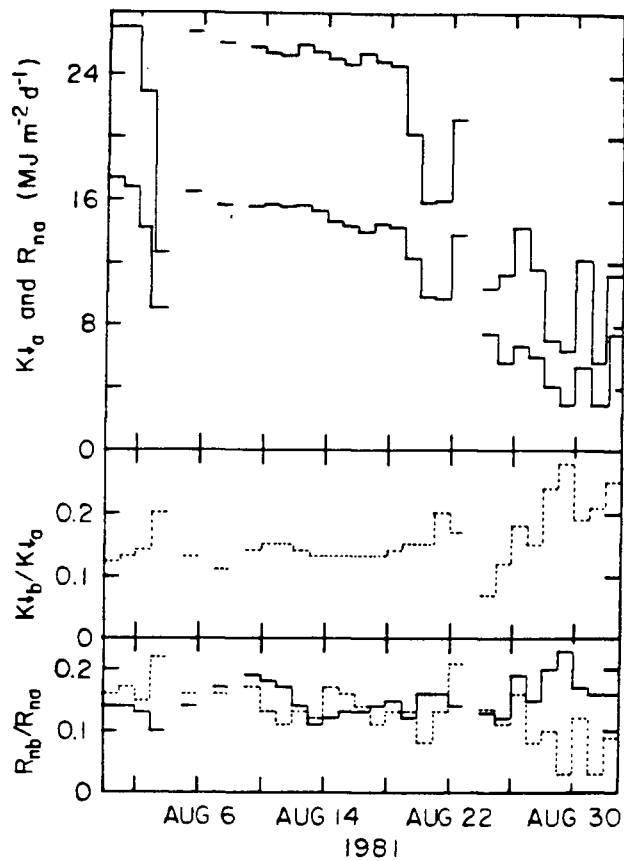


Figure AVI.4 Courses of solar irradiance (top line) and net radiation flux density above the forest ($K+a$ and $R+na$) for the period July 31 - September 1, 1981. Also shown are the courses of the ratio of below to above tree canopy solar irradiance ($K+b/K+a$) for the cut subplot of plot 2 and the ratio of below to above tree canopy net radiation flux density ($R+nb/R+na$) for the cut (---) and uncut (—) subplots of plot 2 during the same period.

Table AVI. 1. Sky view factors (S.V.F.) determined from photographs taken with a fish eye lens in each of the four plots and along the path traversed by the tram.

LOCATION	S.V.F.
Centre of plot 1	0.22
Centre of plot 3	0.24
Centre of plot 4	0.26
Net radiometer in subplot 2 uncut (1981)	0.30
Net radiometer in subplot 2 cut (1981)	0.28
West end of tram path	0.25
1 m west of tram path's cut/uncut border	0.21
1 m east of tram path's cut/uncut border	0.19
East end of tram path	0.25
Net radiometer adjacent to tram path in the cut portion on September 1, 1982	0.23

Table AVI.2. Daily total values of the ratio of below to above tree canopy net radiation flux density (R_{nb}/R_{na}) and solar irradiance ($K_{\downarrow b}/K_{\downarrow a}$) for the cut and uncut portions of the tram's path for seven days in 1982. Also shown is the solar irradiance and net radiation flux density above the forest ($K_{\downarrow a}$ and R_{na}) for the same days.

1982	R_{nb}/R_{na}		$K_{\downarrow b}/K_{\downarrow a}$		$K_{\downarrow a}$	R_{na}
	Uncut	Cut	Uncut	Cut	(MJ m ⁻² d ⁻¹)	
<u>Jul.</u> 30	0.21	0.19	0.17	0.16	8.6	5.7
<u>Aug.</u> 4	0.18	0.17	0.14	0.13	15.8	8.9
7	0.18	0.10	0.17	0.11	26.2	15.4
17	0.15	0.15	0.13	0.12	19.5	10.5
18	0.14	0.10	0.12	0.09	24.4	13.5
25	0.14	0.13	0.11	0.11	21.5	11.6
<u>Sept.</u> 1	0.13	0.14	0.09	0.09	17.6	11.4

During a cloudy day, July 30, 1982, R_{nb}/R_{na} was generally constant (Fig. AVI.5) while on a clear day, August 18, 1982, R_{nb}/R_{na} was quite variable (Fig. AVI.6). There was no apparent pattern in the variation of R_{nb}/R_{na} on this clear day, reflecting the complex canopy geometry of the forest. On September 1, 1982, values of R_{nb}/R_{na} were similar for most of the day for the tram net radiometer along the cut portion and an adjacent stationary net radiometer in the cut portion of the tram path (Fig. AVI.7). The daily total values of R_{nb}/R_{na} on this day were 0.14 and 0.12 for the tram and stationary net radiometers.

4. CONCLUSIONS

Measurements of daily total R_{nb} were similar using tram and adjacent stationary net radiometers. The sky view factor was similar for all four plots and the tram path. In the absence of R_{nb} measurements or a major below-tree-canopy net radiation modelling effort, the best estimates of R_{nb}/R_{na} for uncut and cut areas in the forest would be 0.16 and 0.14, respectively.

5. REFERENCES

- List, R.J. 1971. Smithsonian meteorological tables (6th ed.). Smithsonian Miscellaneous Collections Vol. 114. Smithsonian Institution Press, Washington, D.C.
- Reifsnyder, W.E. 1967. Radiation geometry in the measurement and interpretation of radiation balance. *Agr. Meteorol.* 4: 255-265.
- Steyn, D.G. 1980. The calculation of view factors from fisheye-lens photographs. *Atmos.-Ocean* 18: 254-258.

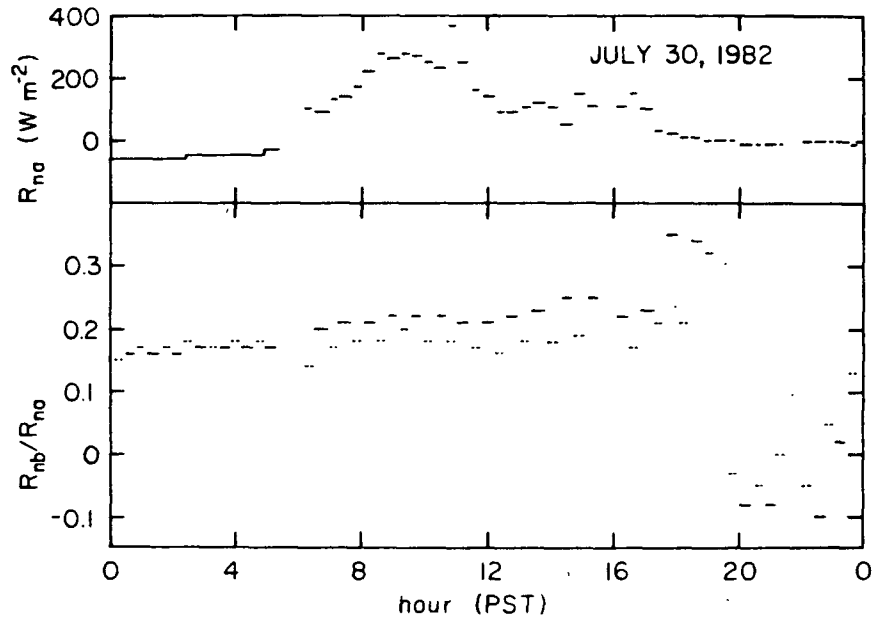


Figure AVI.5 Courses of net radiation flux density above the forest (R_{na}) and the ratio of below to above tree canopy net radiation flux density (R_{nb}/R_{na}) for the cut (- - -) and uncut (—) portions of the tram path on July 30, 1982.

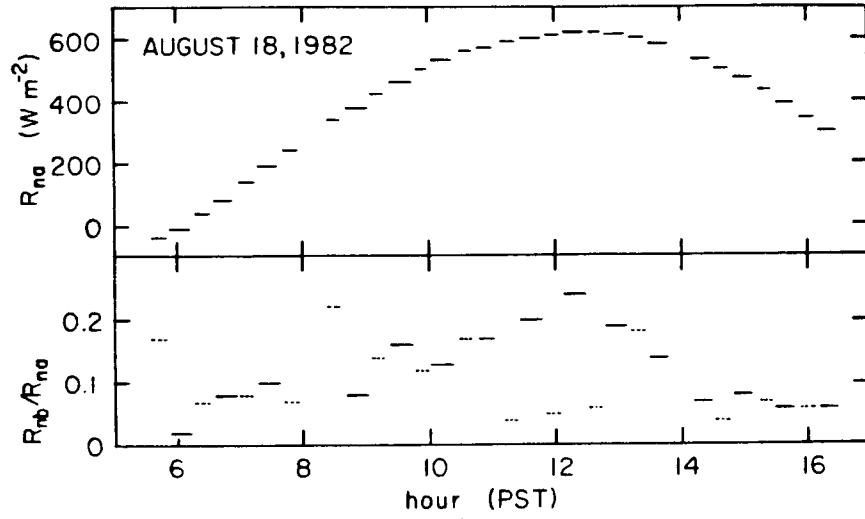


Figure AVI.6 Same as for AVI.5 except for August 18, 1982.

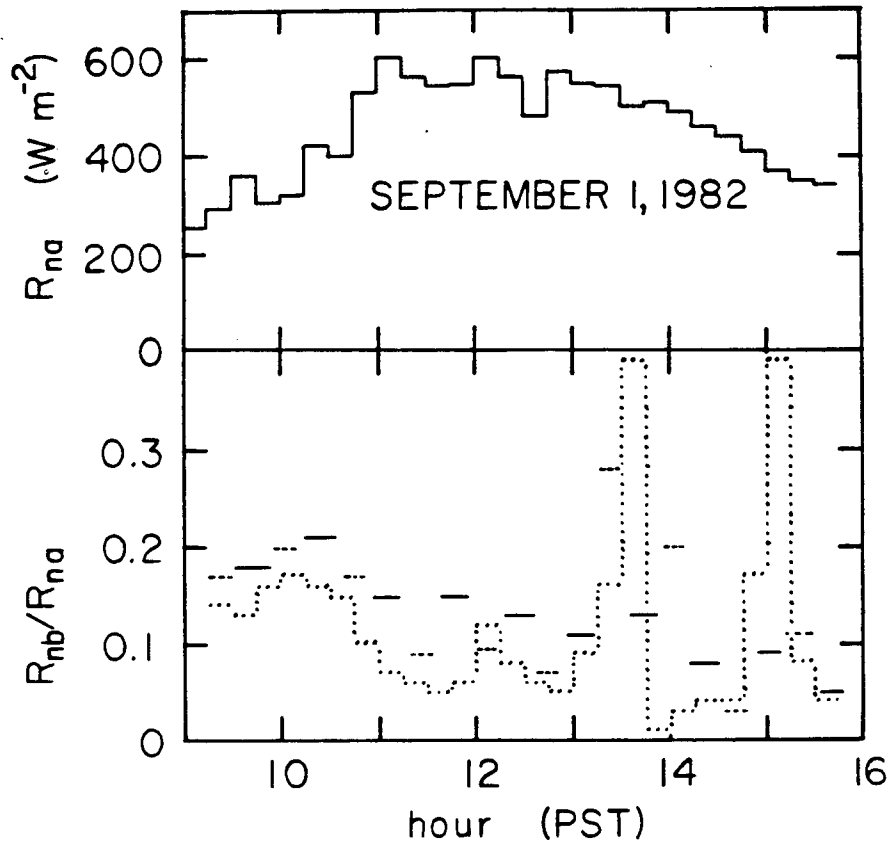


Figure AVI.7 Same as for AVI.5 except for September 1, 1982 and R_{nb}/R_{na} for the cut portion of the tram path measured using a single stationary net radiometer (• • •).

APPENDIX VII

MEASUREMENTS OF r_s IN DOUGLAS-FIR AND SALAL

APPENDIX VII

MEASUREMENTS OF r_s IN DOUGLAS-FIR AND SALAL

The purpose of this appendix is to report r_s measurements made, following the procedure of Kelliher et al. (1984), in 1980 and 1981 adjacent to the four plots at the experimental site. In 1980, measurements were made on June 18, 19 and 30, July 17, 18 and 22 and August 7, 8 and 20. In 1981, measurements were made on July 3 and August 5. On August 20, 1980, ψ_s was -0.3 MPa and for other days (1980 and 1981) $\psi_s > -0.3$ MPa.

Salal r_s was far less responsive to increasing D than Douglas-fir r_s in agreement with the results of Tan et al. (1978) for r_s measurements made at the same site in 1975 (Fig. AVII.1). However, Douglas-fir r_s in 1980 and 1981 increased somewhat more in response to increasing D than in 1975 (the value of ξ in Table 2.1 was 0.27 in 1975 (Tan et al. (1978), equation (7a)) and 0.38 in 1980 and 1981). The r_s characteristic functions for ψ_s of -0.01 and -0.30 MPa (lower and upper curves in Fig. AVII.1) describe the range of the 1980 and 1981 r_s measurements fairly well although there was considerable variation in r_s for Douglas-fir when D was about 1-1.5 kPa.

REFERENCES

- Kelliher, F.M., T.A. Black and A.G. Barr. 1984. Estimation of twig xylem water potential in young Douglas-fir trees. Can. J. For. Res. 14: 481-487.
- Tan, C.S., T.A. Black and J.U. Nnyamah. 1978. A simple diffusion model of transpiration applied to a thinned Douglas-fir stand. Ecol. 59: 1221-1229.

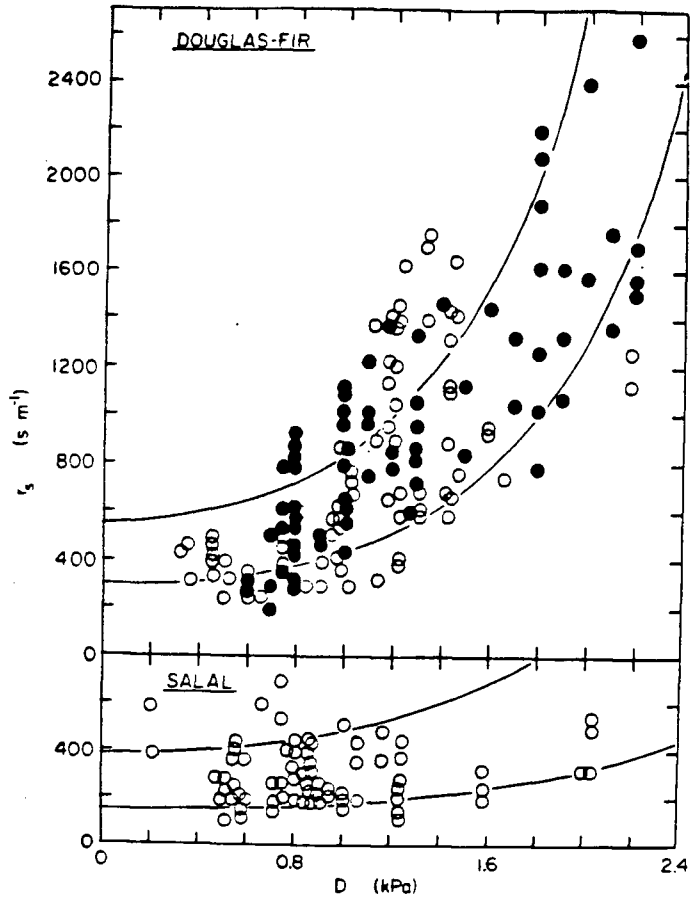


Figure AVII.1 Relationship between stomatal resistance (r_s) and vapour pressure deficit (D) in Douglas-fir and salal adjacent to the four plots at the experimental site for June-August 1980 (O) and 1981 (●) when average root zone soil water potential (Ψ_s) was greater than -0.3 MPa and photon flux density was greater than 2.5 and 1.0 $m\ mol\ m^{-2}\ s^{-1}$ for Douglas-fir and salal respectively. Curves show characteristic r_s values for $\Psi_s = -0.01$ (lower curve) and -0.3 MPa (upper curve) (see Table 2.1).

APPENDIX VIII

SOIL WATER RETENTION CURVE

APPENDIX VIII

SOIL WATER RETENTION CURVE

The purpose of this appendix is to report θ and Ψ_s measurements used to determine the soil water retention curve at the experimental site. Measurements were made in plot 2 as described in Chapter 1. An equation of the form proposed by Campbell (1974) was fitted to average root zone values of θ and Ψ_s (Ψ_s (MPa) = $-0.005 (\theta/0.3)^{-6.5}$) (Fig. AVIII.1).

REFERENCES

Campbell, G. 1974. A simple method of determining unsaturated conductivity from moisture retention data. Soil Sci. 117: 311-314.

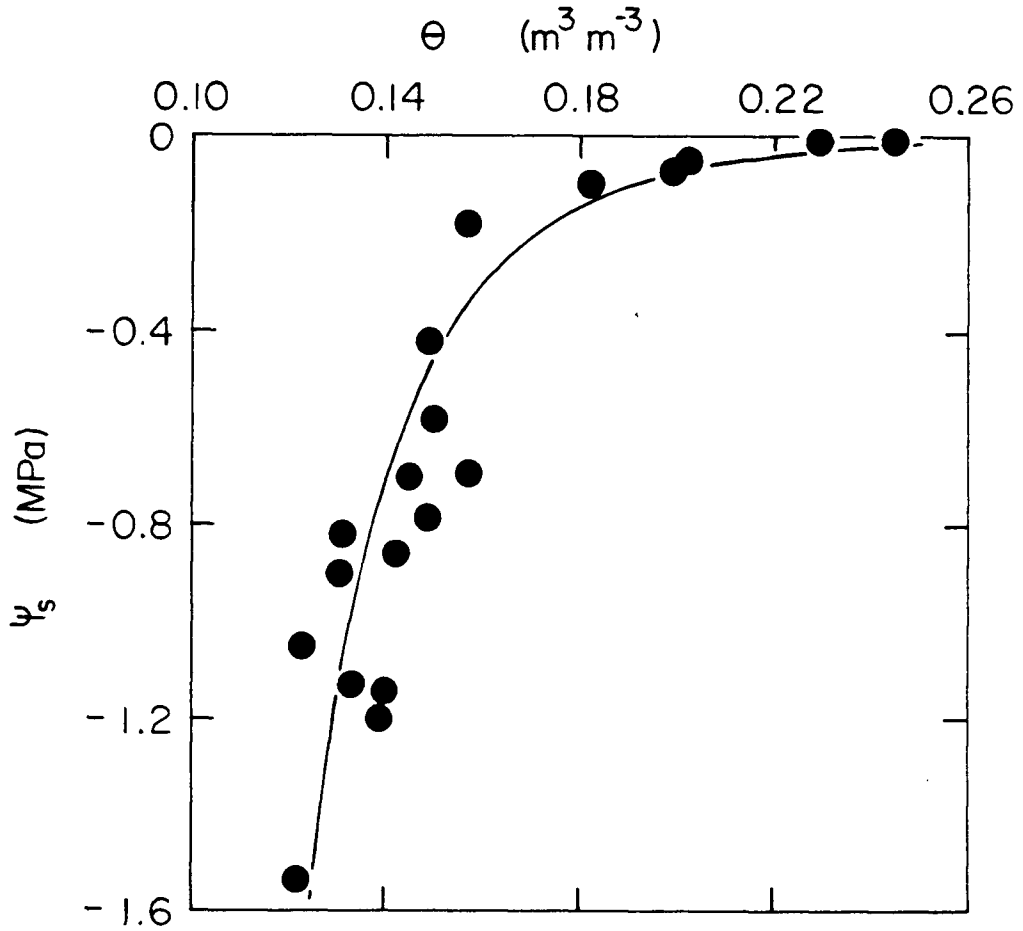


Figure AVIII.1 Relationship between average root zone soil water potential (Ψ_s) and water content (θ) in plot 2. The soil water retention curve shown is Ψ_s (MPa) = $-0.005 (\theta/0.3)^{-6.5}$.